TEHNOLOGIA INOVATIVĂ

REVISTA CONSTRUCŢIA DE MAŞINI

Anul 59, Nr. 2/ 2007

ISSN 0573 – 7419

EDITOR: ICTCM – CITAf - OID.ICM

041303 Bucuresti
Şos. Olteniţei nr. 103, sector 4, O.P. 8
Tel: **332.37.70/234**
Fax: **332.07.75; sau 332.31.95**
E-mail: ictcm@ictcm.ro, oid@ictcm.ro

Redactor: Elena Baican

Responsabil editor: Irina Rădulescu

Responsabil marketing: Eugenia Gheorghicescu

Tehnoredactor: Mihaela Neagu

Coperta: arh. Adriana Ciocan

INFORMAŢII, ABONAMENTE:
Abonamentele se fac direct, prin dispoziţie de plată sau mandat poştal, trimis pe adresa revistei.

CONT – ICTCM:
nr. RO14 RNCB 5040 0000 0031 0001;
BCR sector 4
TIPAR: OID.ICM

DIN SUMAR

ANUL 59 / 2007 – NR. 2

TEHNOLOGIA INOVATIVĂ

REVISTA CONSTRUCȚIA DE MAȘINI

COMITET ȘTIINȚIFIC

COMITET ONORIFIC

EDITOR
Oficiul de Informare Documentară pentru Industrie, Cercetare, Management
din cadrul
Centrului Incubator Tehnologic de Afaceri
S.C. ICTCM S.A. BUCUREŞTI

RESPONSABIL EDITOR
ing. Irina Rădulescu

REDACTOR
Elena Baican

TEHNOREDACTOR
Mihaela Neagu

GRAFICA
Arh. Adriana Ciocan

CUPRINS

TEHNOLOGII

MECANISME

ORGANE DE MAŞINI

TRIBOLOGIE

MANAGEMENT. ECONOMIE INDUSTRIALĂ

TEHNOLOGII INOVATIVE

CHIMIE INDUSTRIALĂ

DETERMINAREA RANDAMENTELOR CENTRALELOR TERMICE DE ÎNCĂLZIRE LOCALĂ, PRIN METODE DIRECTE ŞI INDIRECTE

Constantin Neaga

Universitatea POLITEHNICA din Bucureşti, constantin_neaga@yahoo.com

ABSTRACT

This paper present the calculation methods of the design and operating efficiency of local heating plants (LHP). This intervention by the author was necessary, because, in the environment, affirmation was made by "experts" such as, these local heating plants, operating with the condensation of the vapours from flue gases, would achieve efficiencies of 107- 109%, opinions which contradict the fundamental thermodynamic laws. Actually, some elements related to this issue were related briefly in [1]. Besides heating, these plants provides to the cohabitants domestic hot water. These category includes the mural plants (installed inside every appartment), staircase plants and building plants; the plants which provides heat and domestic hot water to a large number of buildings are not considered, in order to eliminate the inevitable energy and hot water losses with the transport system between the provider and the costumer. Actually this is the reason why these plants are built, because the transport networks, wrong mounted and with a large amount of heat and hot water losses made that the central heating system be ignored by the costumers. More, the local heat supply provides convenience and rapid conformation to the thermal environment conditions; because of its great inertia, the central system controls very hard the operation transient regimes – start-up shut down – with negative consequences on the costs supported by the costumers. The author is convinced that, central generation of heat and hot water, necessary to the costumers , is more cheaper then the local generation of the same utilities (not considering the transport systems and distribution). This is the start point of the urban and industrial central heating idea and the construction of central heating power plants. If the installed power of the system is greater, the specific consumption and costs are smaller.

KEYWORDS: Local heating plant; LHP efficiencies; LHP with the condensation of the vapours from flue gases.

Descriptori: centrală termică de încălzire locală (CTIL); randamente; CTIL cu condensarea vaporilor de apă din gazele de ardere.

Notaţii:

$\sum C_m H_n^{um} + H_2^{um} + O_2^{um} + N_2^{um} + H_2O^{um} + CO_2^{um} = 100,\%$

– compoziţia combustibilului gazos umed (procente de volum); se admite că CTIL foloseşte energie primară, energia chimică a unui combustibil gazos;

Q_i^{um}; Q_s^{um} – puterea calorifică inferioară, respectiv, superioară a combustibilului gazos umed, kJ/m$^{3(*)}$;

d – conţinutul de umiditate a combustibilului gazos anhidru, g/m^3;

x – conţinutul de umiditate a aerului de ardere anhidru, g/kg;

B_i; B_s – debitul de combustibil gazos umed consumat calculat în raport cu puterea calorifică inferioară, respectiv, superioară, m^3/s;

(*) mărimile sunt exprimate în condiţii normale: 273,15 K; 0,1013 MPa.

D_i; D_a – debitul de apă pentru încălzire, respectiv, de apă caldă menajeră, kg/s;

V_a^0, V_{aum}^0 – volumul teoretic de aer anhidru, respectiv, umed necesar arderii unui m^3 de combustibil, m^3/m^3;

V_{gu}^0; V_g^0 – volumul teoretic de gaze de ardere uscate, respectiv, umede rezultate din arderea unui m^3 de combustibil, m^3/m^3;

$V_{H_2O}^0$ – volumul teoretic de vapori de apă rezultați din arderea unui m^3 de combustibil, m^3/m^3;

Q_{ev}; Q_{ch}; Q_{ex} – pierderile de căldură cu gazele de ardere umede evacuate (dar şi cu condensatul), respectiv, prin ardere chimic incompletă şi în exterior, kJ/m^3; (indice *i* – pentru inferior, indice *s* – pentru superior);

q_{ev}; q_{ch}; q_{ex} – idem, dar exprimate procentual, %;

$I_{aum}^0(t_0)$ – entalpia aerului umed teoretic la temperatura mediului ambiant, t_0, kJ/m^3;

$I_g(\lambda,t)$ – entalpia gazelor de ardere pentru coeficientul de exces de aer λ şi de temperatura variabilă *t*, kJ/m^3;

i_{it}; i_{ir} – entalpia specifică a apei de încălzire tur, respectiv, retur, kJ/kg (t_{it}; t_{ir} – idem, temperaturile, ^0C);

i_{ac}; i_{ar} – entalpia specifică a apei calde menajere, respectiv, rece la intrarea în CTIL, kJ/kg (t_{ac}; t_{ar} – idem, temperaturile, ^0C);

$i_{co} = c_c^{um} t_0$ – entalpia specifică a combustibilului gazos, kJ/m^3;

c_c^{um} – căldura specifică a combustibilului gazos umed, $kJ/(m^3 \cdot K)$;

t_0 – temperatura mediului ambiant, ^0C;

t_{ev} – temperatura gazelor de ardere evacuate (dar şi a condensatului), ^0C;

c_{gu}; c_{va} – căldura specifică a gazelor de ardere uscate, respectiv, a vaporilor de apă, $kJ/(m^3 \cdot K)$;

c_{aum} – căldura specifică a aerului umed, $kJ/(m^3 \cdot K)$;

$c_{\text{apă}}$ – căldura specifică a apei (condensatului), $kJ/(kg \cdot K)$;

i_{cd} – entalpia specifică a condensatului care iese din SCC, kJ/kg (t_{cd} – temperatura condensatului, ^0C);

γ – fracția volumică a debitului de vapori de apă din gazele de ardere, care au condensat.

Contribuții

În lucrările străine consacrate centralelor termice de încălzire locală din motive uşor de înțeles, nu se prezintă expresii de calcul al randamentului acestora, sau date privind proiectarea, construcția şi exploatarea lor; rezultă din cele afirmate încă un motiv de ce autorul şi-a propus să abordeze acest subiect.

În dezvoltarea ulterioară a temei s-a admis model fizic schema prezentată în figura 1.

În regimul de vară centrala serveşte numai pentru pregătirea apei calde menajere.

Din schimbătorul de căldură principal 1, ventilul cu trei căi 2 dirijează apa fierbinte numai spre schimbătorul de căldură 3 (schimbător de suprafață apă-apă); apa caldă pregătită în 3, intră în circuitul de consum al acesteia 5, iar apa încălzitoare, care s-a răcit este preluată de pompa de circulație 6 şi introdusă în schimbătorul 1 (ventilele 7 sunt închise).

În regimul de iarnă – numai încălzirea locuințelor – ventilul cu trei căi 2 dirijează apa fierbinte în circuitul închis de încălzire 4; punctul de funcționare a sistemului centrală – consumator se determină din intersecția caracteristicilor hidraulice ale pompei 6 (caracteristica internă) cu caracteristica externă a rețelei de încălzire (conducte, calorifere etc.).

Dacă e nevoie şi de apă caldă menajeră – regim complet de iarnă –, ventilul 2 distribuie apă fierbinte şi spre schimbător de căldură 3 (a se vedea. mai sus).

1. DEZVOLTAREA MODELULUI

Pentru determinarea randamentului CTIL, obiectivul principal propus al lucrării, se apelează la două tipuri de ecuații, ecuația generală de bilanț energetic, redusă numai la bilanțul debitelor calorice (suma debitelor calorice care intră în sistem trebuie să fie egală cu suma debitelor calorice care ies din sistem) şi la ecuația conservării debitelor materiale, scrise special pentru modelul fizic adoptat (fig. 1). Aceste ecuații se scriu pentru regimul stabilizat de funcționarea centralei. De remarcat că aceste instalații funcționează real în regimuri extrem de variabile; analiza lor din acest unghi de vedere, constituie însă o altă problemă.

Scrierea ecuațiilor de conservare impune: alegerea unei suprafețe de referință care delimitează sistemul S (fig. 1); temperatura de referință 273,15 K şi presiunea de referință 0,1013 MPa.

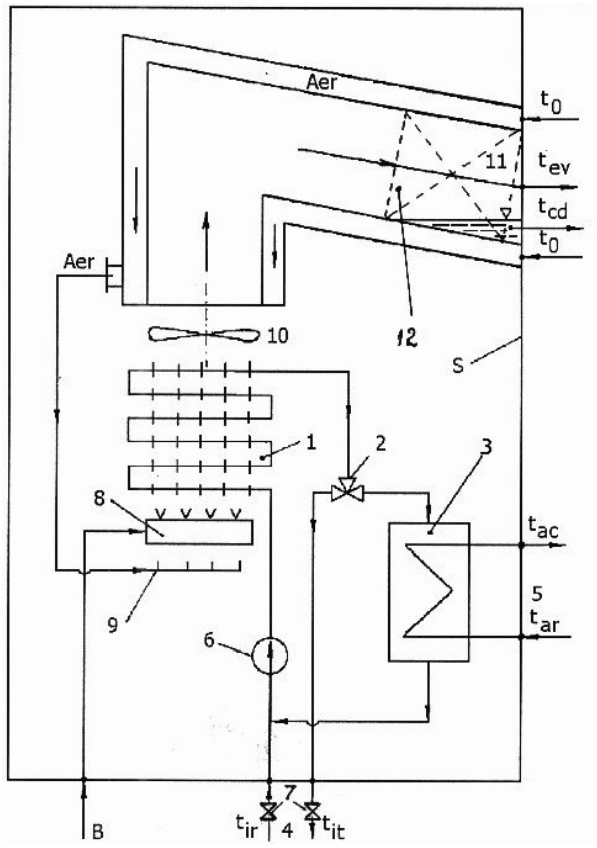

Figura 1. *Schema unei centrale termice de încălzire locală cu tiraj forţat:*

1– schimbător principal de căldură;
2– ventil cu trei căi;
3– schimbător de căldură pentru pregătirea apei calde menajere;
4– circuitul de încălzire a apartamentelor;
5– circuitul apei calde menajere;
6– pompa de circulaţie;
7– ventile de blocare a circuitului de încălzire;
8– arzător bloc;
9– distribuitor de aer de ardere;
10– ventilator de gaze de ardere;
11– coş de evacuare a gazelor de ardere;
12– schimbător de căldură gaze-aer, cu condensarea vaporilor de apă din gazele de ardere (SCC);
B – intrarea combustibilului;
S – suprafaţa de referinţă a sistemului.

1.1. Calculul randamentelor centralei în cazul în care vaporii de apă din gazele de ardere nu ajung la temperatura de condensaţie (de rouă), sau altfel spus, centrala nu funcţionează în regim de condensaţie

Ţinând seama de definiţiile puterilor calorifice ale combustibilului (aici, combustibilul gazos), în această situaţie se foloseşte puterea calorifică inferioară Q_i^{um} (În procesul arderii, umiditatea din combustibil şi cea rezultată din reacţiile de oxidare a componentelor combustibile cu hidrogen în compoziţia lor chimică, vaporizează consumând căldura de vaporizare – căldura latentă – la presiunea de referinţă; căldura de vaporizare este preluată din căldura rezultată din arderea combustibilului. Deoarece la ieşirea din centrală gazele de ardere anhidre, plus umiditatea, nu ajung la temperatura de rouă şi deci vaporii de apă (sau o parte a lor) nu condensează, căldura fizică a amestecului în care se găseşte şi căldura latentă a vaporilor de apă necondensaţi este pierdută pentru sistem):

$$B_i(Q_i^{um}+i_{co})+B_i\,\lambda\, I^0_{aum}(t_0)=D_i(i_{it}-i_{ir})+D_a(i_{ac}-i_{ar})+$$
$$+B_i\,I_g(\lambda,t_{ev})+B_i(Q_{chi}+Q_{exi}),\quad \text{kW},\qquad (1)$$

unde indicele *i* arată că mărimile respective se calculează folosind puterea calorifică inferioară.

Se fac notaţiile:

- debitul caloric util transmis de centrală:

$$Q_u=D_i(i_{it}-i_{ir})+D_a(i_{ac}-i_{ar}),\quad \text{kW};\qquad (2)$$

- pierderea de căldură cu gazele de ardere umede evacuate:

$$Q_{evi}=I_g(\lambda,t_{ev})-\lambda\, I^0_{aum}(t_0)-i_{co},\quad \text{kJ/m}^3.\qquad (3)$$

Cu acestea,ecuaţia de bilanţ termic (1) devine:

$$B_iQ_i^{um}=Q_u+B_i(Q_{evi}+Q_{chi}+Q_{exi}),\ \text{kW},\qquad (4)$$

expresie care permite calculul randamentelor CTIL prin ambele metode (evident, valoarea lor trebuie să fie aceeaşi):

- prin metoda directă (se foloseşte definiţia clasică a randamentului):

$$\eta_i=\frac{Q_u}{B_i\,Q_i^{um}}100,\ \%;\qquad (5)$$

- prin metoda indirectă (se calculează prin evaluarea pierderilor de căldură; ambii membri ai ecuaţiei (4) se înmulţesc cu $100/(B_iQ_i^{um})$ şi se foloseşte (5)):

$$\eta_i=100-(q_{evi}+q_{chi}+q_{exi}),\%,\qquad (6)$$

unde pierderile procentuale de căldură se calculează cu formulele

$$q_{evi}=100\,Q_{evi}/Q_i^{um};$$
$$q_{chi}=100\,Q_{chi}/Q_i^{um};$$
$$q_{ex}=100\,Q_{exi}/Q_i^{um};$$

în cazul în care componenta combustibilă măsurată din gazele evacuate este numai monoxidul de carbon, atunci pierderea de căldură prin ardere chimic incompletă se calculează cu formula

$$Q_{chi} = 10^{-2}\, CO\, V_{gu}\, Q_{ico}\ , \text{kJ/m}^3,$$

unde *CO* este valoarea procentuală a monoxidului de carbon din gazele uscate evacuate, iar Q_{ico} – puterea calorifică inferioară a lui, kJ/m^3 (se găseşte în tabele).

[

$$B_s(Q_s^{um} + i_{co}) + B_s\,\lambda\, I^0_{aum}(t_0) = Q_u + B_s\, V_{gu}\, c_{gu}\, t_{ev} + (1-\gamma)\, B_s\, \rho_{H_2O}\, V_{H_2O}\, i(p_s^{''}) +$$

$$+\gamma\, B_s\, \rho_{H_2O}\, V_{H_2O}\, i_{cd} + B_s(Q_{chs} + Q_{exs}),$$

kW, (7)

Expresia randamentului determinată pe cale directă (5) serveşte la analiza condiţiilor de funcţionare a centralei (în exploatare), caz în care cu ajutorul aparatelor de măsură se determină valorile efective ale parametrilor implicaţi în formule (debite, temperaturi etc.).

Metoda de calcul indirectă (6) se foloseşte la proiectarea centralei, situaţie în care unele pierderi de căldură se calculează, altele se admit ($q_{exi} = f(Q_u)$); de asemenea ea poate fi folosită cu succes şi în analiza funcţionării centralei, în vederea verificării şi creşterii performanţelor ei.

1.2. Calculul randamentelor în cazul în care centrala funcţionează în regim de condensaţie

În această situaţie, gazele de ardere, în evoluţia lor spre evacuare ajung la un moment dat la temperatura de saturaţie corespunzătoare presiunii parţiale a vaporilor de apă din amestec; se mai numeşte şi temperatura de rouă t_r, ^{0}C.

Geometric, valoarea abscisei (sensul de curgere a produselor de ardere) se plasează în schimbătorul final de căldură, un subansamblu special cu schimbare de fază a vaporilor de apă din agentul termic cald. Acesta poate fi un schimbător gaze-aer, sau gaze-apă. Din acest moment, pe măsură ce vaporii de apă condensează presiunea lor parţială scade, în sensul de curgere a lor. Dacă se neglijează pierderile de presiune la curgerea amestecului gazos peste schimbător, presiunea gazelor necondensabile creşte în acelaşi sens. Prin condensarea vaporilor de apă căldura lor latentă eliberată se transmite prin filmul de apă care se formează pe suprafaţa ţevilor schimbătorului, agentului rece; în acest fel căldura de condensaţie (egală cu căldura de vaporizare, deoarece se admite p = const în circuitul gazelor de ardere), rămâne în interiorul sistemului. În final rezultă că temperatura gazelor evacuate se micşorează în strânsă dependenţă cu gradul de condensare şi că pierderea de căldură cu gazele evacuate scade (trebuie însă ţinut seama şi de căldura fizică a condensatului care iese din sistem şi care constituie o pierdere pentru centrală) şi astfel randamentul global creşte, cu consecinţa imediată, scăderea debitului de combustibil consumat.

Ecuaţia generală de bilanţ termic devine:

unde

$$V_{gu} = V^0_{gu} + (\lambda - 1)V^0_a\ ,$$

$$V_{H_2O} = V^0_{H_2O} + 0,00161\, x\, (\lambda - 1)V^0_a, \quad \text{m}^3/\text{m}^3$$

sunt volumele reale de gaze de ardere uscate şi de vapori de apă; volumul gazelor de ardere umede rezultă din însumarea

$$V_g(\lambda) = V_{gu} + V_{H_2O};$$

$p_s^{'}$, $p_s^{''}$ – presiunea parţială a vaporilor de apă la intrarea în schimbătorul final al centralei, pentru $\gamma = 0$, respectiv la ieşire, MPa;

$i(p_s^{''})$ – entalpia vaporilor de apă la ieşire, kJ/kg;

i_{cd} – entalpia condensatului evacuat, kJ/kg (nu se ia în consideraţie eventuala subrăcire a acestuia, procesul fiind astfel coordonat încât asemenea fenomen să nu aibă loc); temperatura gazelor evacuate $t_{ev} = t_s(p_s^{''})$, este mult mai mică faţă de t_{ev} din cazul 1.1.

Presiunile parţiale ale vaporilor de apă şi gazelor de ardere uscate (necondensabile) la intrarea şi ieşirea din schimbător se calculează cu expresiile:

$$p_s^{'} = p^{'}_{H_2O} = \frac{V_{H_2O}}{V_g}\, p\ ;$$

$$p^{'}_{gu} = \frac{V_{gu}}{V_g}\, p\ ;$$

$$p_s^{''} = p^{''}_{H_2O} = \frac{(1-\gamma)\, V_{H_2O}}{V_g - \gamma\, V_{H_2O}}\, p\ ;$$

$$p''_{gu} = \frac{V_{gu}}{V_g - \gamma V_{H_2O}} p \; ; \; p'_{H_2O} + p'_{gu} = p \; ;$$

$$p''_{H_2O} + p''_{gu} = p \; , \qquad (8)$$

unde *p* este presiunea totală a amestecului (s-a admis 0,103 MPa).

Corespunzător presiunilor parțiale ale vaporilor de apă la intrarea și ieșirea din schimbătorul SCC se citesc din tabele sau se calculează cu ajutorul formulelor semiempirice [5], temperaturile de saturație, entalpiile etc.,

$$t'_r = t_s(p'_{H_2O}) \; ;$$

$$t''_r = t_s(p''_{H_2O}) \; , \; ^0\text{C}.$$

Se notează expresia căldurii pierdute cu amestecul gazos umed ($\gamma > 0$) și cu condensatul evacuat, în cazul folosirii puterii calorifice superioare:

$$Q_{evs} = V_{gu}\, c_{gu} t_{ev} + (1 - \gamma)\rho_{H_2O} V_{H_2O}\, i(t''_s) + \gamma \rho_{H_2O} V_{H_2O}\, i_{cd} - \lambda\, I^0_{aum}(t_0) - i_{co},$$

kJ/m^3, (9)

cu care ecuația de bilanț termic (7) devine:

$$B_s Q^{um}_s = Q_u + B_s (Q_{evs} + Q_{chs} + Q_{exs}) \; , \text{ kW.} \qquad (10)$$

picăturile de condensat care se formează și se depun pe pereții țevilor la intrarea în schimbătorul de căldură, au temperatura de saturație t'_r. În continuare temperatura de rouă scade, grosimea peliculei de condensat crește, căldura latentă de condensare crește, debitul de condensat crește; pelicula de condensat primește căldură de la curentul de amestec gazos cu care este în contact, dar și cedează, prin peretele metalic, agentului rece. Pentru evaluarea i_{cd} este, deci, necesar un bilanț termic al debitului de condensat, lucru necesar în calculul termic al SCC, aspect care iese din obiectivele lucrării de față.

În zona temperaturilor coborâte ale gazelor de ardere evacuate (0…60^{0}C) pentru căldura latentă de condensare a vaporilor de apă se poate folosi dependența liniară:

$$r(t) = 2501 - 2,3767\, t \; , \text{ kJ/kg.} \qquad (13)$$

Debitul de condensat evacuat din schimbător se poate determina cu expresia (14):

$$D_{cd} = \rho_{H_2O} B_s (V_{H_2O} - V''_{H_2O}) = \gamma\, \rho_{H_2O} B_s V_{H_2O},$$

kg/s. (14)

$$Q_{scc} = \varphi B_s \left[I_g(\lambda, t'_r) - V_{gu}\, c_{gu}\, t_{ev} - (1-\gamma)\rho_{H_2O} V_{H_2O}\, i(t''_s) - \gamma \rho_{H_2O} V_{H_2O}\, i_{cd} \right],$$

kW, (15)

Formulele de calcul al randamentului sunt:

– prin metoda directă:

$$\eta_s = \frac{Q_u}{B_s Q^{um}_s} 100, \% \; , : \qquad (11)$$

– prin metoda indirectă:

$$\eta_s = 100 - (q_{evs} - q_{chs} - q_{exs}), \; \% \; , \qquad (12)$$

unde pierderile procentuale de căldură se calculează cu expresii similare celor din subcap. 1.1.

Relațiile (5) și (11) duc la egalitatea ($Q_u \approx \text{const}$) ,

$$\eta_i B_i Q^{um}_i = \eta_s B_s Q^{um}_s \; .$$

Dacă în (9) se admite $\gamma = 0$ (vaporii de apă din gazele de ardere evacuate nu condensează), atunci $Q_{evs} = Q_{evi}$ (relația 3), egalitate care se verifică ușor.

Asupra valorii entalpiei condensatului, evacuat din SCC, i_{cd} se pot face următoarele observații:

În analiza precedentă apare coeficientul de exces de aer λ, care se admite constant, atât pentru circuitul de aer, cât și pentru circuitul gazelor de ardere. Valoarea lui se deduce impunând mărimea temperaturii teoretice de ardere a gazului natural, mărime care să evite arderea aripioarelor țevilor schimbătorului principal (poz. 1 din fig. 1), dacă acesta este astfel realizat, dar mai ales să nu ducă la formarea oxizilor de azot termici; conform teoriei Zeldovici, privind formare oxizilor de azot termici, temperatura teoretică de ardere nu trebuie să depășească cca 1600 K, pentru ca $NO^a_x \sim 0$.

Temperatura teoretică de ardere a gazelor naturale se deduce din ecuația de bilanț termic al sistemului format din distribuitorul de aer 9 și

arzătorul bloc 8 (fig. 1), adică focarul propriu-zis al centralei:

$$Q_i^{um} + i_{co} + \lambda I^0_{aum}(t_{ap}) = I_g(\lambda, t_t) + Q_{chi},$$

kJ/m^3, (16)

unde t_{ap} este temperatura aerului preîncălzit, la intrarea în focar, ^{0}C; t_t – temperatura teoretică de ardere, a cărei valoare se impune, ^{0}C.

2. ANALIZĂ DE CAZ

O centrală termică de încălzire locală asigură încălzirea şi apa caldă menajeră pentru o scară de bloc cu cca 40 apartamente convenționale: $Q_u = 1000$ kW.

Caracteristicile chimice şi termice ale combustibilului gazos, exprimate la stările anhidră şi umedă ale acestuia sunt date în Tabelul 1.

Tabelul 2

t [C]	$I^0_g(t)$	$I^0_{aum}(t)$	$I_g(\lambda,t) = I^0_g(t) + (\lambda-1) I^0_{aum}(t)$			
			$\lambda = 1{,}8$	$\lambda = 1{,}9$	$\lambda = 2$	$\lambda = 3$
1	2	3	4	5	6	7
0	0	0	0	0	0	0
100	1363	1172	2301	2418	2535	3707
200	2750	2359	4637	4873	5109	7468
400	5624	4800	9464	9944	10424	15224
600	8672	7352	14554	15289	16024	23376
800	11849	10016	19862	20863	21865	31881
1000	15168	12724	25347	26620	27892	40616
1200	18585	15543	31020	32574	34128	49671
1400	22090	18400	36810	38650	40490	58890
1600	25663	21293	42697	44827	46956	68249
1800	29278	24187	48628	51046	53465	77652
2000	32953	27154	54680	57392	60107	87261

Pentru calculul coeficientului de exces de aer se foloseşte relația (16) care, în vederea utilizării valorilor din tabelul 2, se scrie sub forma:

$$Q_i^{um} + i_{co} + \lambda I^0_{aum}(t_{ap}) = I^0_g(t_t) + (\lambda - 1) I^0_{aum}(t_t) + 10^{-2} CO\left[V^0_{gu} + (\lambda - 1) V^0_a\right] Q_{ico}$$

Pentru combustibilul gazos umed s-au calculat [2]:

$V^0_a = 8{,}7226$ m^3/m^3;

$V^0_{aum} = 8{,}863$ (conținutul de umiditate a aerului anhidru $x = 10$ g/kg);

$V_{CO_2} = 0{,}9544$; $V^0_{N_2} = 6{,}9246$;

$V^0_{gu} = 7{,}879$; $V^0_{H_2O} = 1{,}9792$;

$V^0_g = 9{,}8582$.

Cu aceste mărimi se întocmeşte Tabelul 2 şi se trasează diagrama specială $I_g(\lambda, t)$, pentru combustibilul gazos umed, figura 2.

Tabelul 1

Mărimea	U.M.	Starea	
		Anhidră	Umedă
CH_4	%	89	85,803
C_2H_2	"	3	2,892
C_2H_6	"	2	1,928
O_2	"	2,5	2,410
N_2	"	3,5	3,374
H_2O	"	-	3,592
d	g/m^3	30	-
Q_i	kJ/m^3	34855	33530

Se admit: $t_{ap} = 50^0$C; $t_t = 1300^0$C;

$CO_{\text{măsurat}} = 20$ ppm; $Q_{ico} = 12644$ kJ/m^3;

rezultă $\lambda = 1{,}842$.

Dacă se prezintă complet analiza gazelor de ardere anhidre evacuate, atunci λ se poate calcula pe baza acestei analize, cu ajutorul expresiilor cunoscute [2].

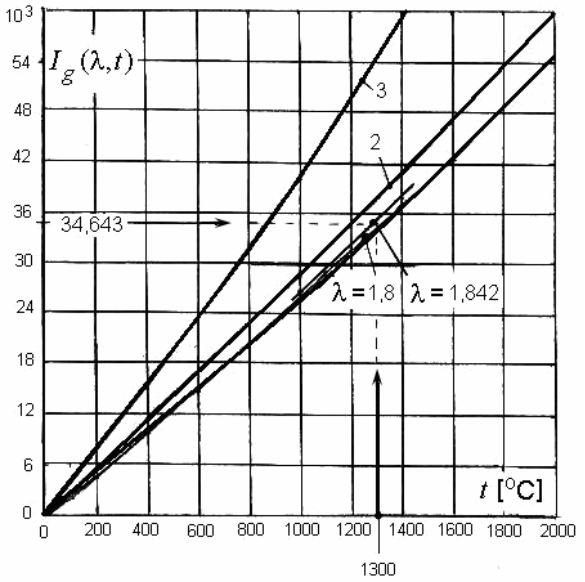

Figura 2. *Diagrama specială* $I_g(\lambda, t)$ *pentru gazul natural umed*

2.1. Centrala nu funcţionează în regim cu condensarea vaporilor de apă

Se admit: $t_{ev} = 120^0$C; $t_0 = 25^0$C; rezultă: $Q_{evi} = 2249$ kJ/m^3; $q_{evi} = 6,7\%$; $q_{chi} = 0,0115\%$; $q_{exi} = 1\%$; $\eta_i = 92,29\%$; $B_i = 0,0323155$ m^3/s=116,336 m^3/h.

Se admit: $t_{ev} = 120^0$C; $t_0 = 5^0$C; $q_{evi} = 8,085\%$; $\eta_i = 90,9\%$; $B_i = 118,11$ m^3/h.

Dacă temperatura mediului t_0 scade de la 25 la 5^{0}C, consumul de combustibil creşte cu 1,774 m^3/h.

2.2. Centrala funcţionează în regim cu condensarea vaporilor de apă

Se presupune că schimbătorul de căldură cu condensaţia vaporilor de apă este scăldat de aer, pe partea rece a acestuia.

Volumele reale ale componentelor gazelor de ardere (se ţine seama de excesul de aer) au valori: $V_{gu} = 15,233$ m^3/m^3; $V_{H_2O} = 2,097$; $V_g = 17,32$ m^3/m^3.

Presiunea parţială a vaporilor de apă la intrarea în SCC este $p_s' = 0,1247$ bar, căreia îi corespunde temperatura de rouă (de saturaţie) $t_s' = t_r' = 50,22^0$C.

În domeniul temperaturilor coborâte (0…100^{0}C), relaţia între presiunea la saturaţie şi temperatura la saturaţie poate fi exprimată prin dependenţa [5] (eroarea, faţă de valorile din tabele este de ± 0,5%):

$$p_s = \exp\,[9,77 - 4054/(236 + t_s)],\ \text{MPa}.$$

Se impune temperatura de evacuare a gazelor din SCC, $t_{ev} = 18,4^0$C ($t_0 = 5^0$C); presiunea de saturaţie corespunzătoare acestei temperaturi, din tabele este $p_s'' = 0,0208518$ bar; din expresiile (8) se găseşte gradul de condensare a vaporilor de apă $\gamma = 0,85$. Căldura pierdută cu gazele umede evacuate (nu a condensat întregul volum al vaporilor de apă) – expresia 9 – are valoarea de 369,68 kJ/m^3; $q_{evs} = 0,985\%$; $q_{chs} = 0,01\%$; $q_{exs} = 0,89$; $\eta_s = 98,115\%$; (temperatura mediului ambiant este $t_0 = 5^0$C); $B_s = 97,77$ m^3/h; economia de combustibil gazos,centrala funcţionând în condensaţie este $\Delta B = B_i - B_s = 118,11 - 97,77 = 20,34$ m^3/h, sau, procentual, 17,22%.

Din egalitatea $Q_{scc} = \lambda B_s c_{aum} V^0_{aum} (t_{a2} - t_0)$, se obţine temperatura de ieşire a aerului din SCC, $t_{a2} = 36,9^0$C.

Valoarea randamentului centralelor de încălzire locală cu condensaţie, care apare în unele prospecte rezultă din (11) în care Q_s^{um} se înlocuieşt cu Q_i^{um}; în aceste condiţii $\eta_s = 109,8\%$.

După cum s-a spus acest mod de calcul este incorect.

Relaţia (14) duce la aflarea debitului de condensat evacuat, $D_{cd} = 140$ kg/h, apă care poate fi folosită în diverse scopuri.

Dacă agentul rece al schimbătorului de căldură cu condensaţia vaporilor de apă din gazele de ardere este apa, atunci aceasta va circula prin interiorul ţevilor, iar posibilităţile de coordonare a proceselor din SCC sunt mult mai uşor de realizat.

În figura 3 [6] se arată dependenţa randamentului CTIL de temperatura apei la intrarea în schimbător t_{e1}, ^{0}C, atât în regim fără condensaţie, dar şi cu condensaţie; se constată creşterea apreciabilă a randamentului la funcţionarea centralei în regim cu condensaţia vaporilor de apă (temperaturi coborâte ale apei la intrarea în centrală).

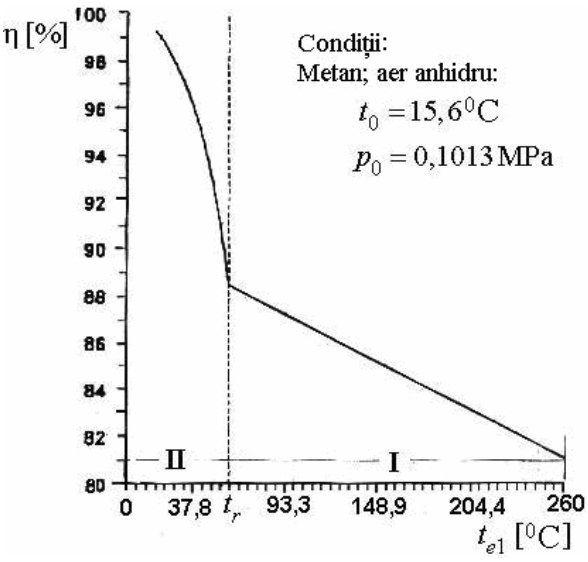

Figura 3. *Variaţia randamentului centralei cu temperatura apei de alimentare:* $\eta = f(t_{e1})$*:*

I – regim obişnuit de funcţionare (fără condensarea vaporilor de apă):
II – cu condensarea vaporilor de apă.

3. CONCLUZII

- s-au demonstrat expresiile de calcul al randamentelor (pe cale directă şi prin metoda indirectă) ale unei centrale termice de încălzire locală, în cele două situaţii posibile de funcţionare a acesteia: fără condensarea vaporilor de apă din gazele de ardere şi cu condensarea acestora;

- din analiza de caz, rezultă superioritatea centralelor de încălzire la funcţionarea în regim cu condensaţie: randamentul creşte, consumul de combustibil scade şi deci cheltuielile de exploatare scad;

- s-a justificat valoarea mare, faţă de instalaţiile termice clasice, a coeficientului de exces de aer (evitarea formării oxidului de azot termic);

- s-a evidenţiat rolul şi importanţa analizei termice a schimbătorului de căldură cu condensaţia vaporilor de apă;

- expresiile găsite servesc specialiştilor din proiectarea, realizarea şi exploatarea unor asemenea sisteme termice de alimentare cu căldură şi apă caldă menajeră;

- lucrarea deschide direcţii pentru diverse analize ale acestor centrale, cum ar fi regimurile tranzitorii, optimizarea constructivă şi funcţională a lor etc.

BIBLIOGRAFIE

[1]. **Neaga, C.**, *Metode de calcul al randamentului unor centrale termice murale*. Conf. Nat. de Echipament Termomecanic Clasic şi Nuclear şi Energetică urbană, UPB, Bucureşti, 12-13 iunie 2003, pg. 93-96.

[2]. **Neaga, C.**, *Tratat de Generatoare de Abur*, *vol. I*, Ed. AGIR – 2001, 544 pg., cap. 3 şi 4.

[3]. **Isacienko, V.P. i dr**., *Teploperedacia.* Izd. "Energhiia", Moskva – 1975, 488 st., subcap. 14.6.

[4]. **Buharkin, E.N.,** *K metodike rascieta teploobmennikov s condensaţiei para iz nasâsciennoi parogazovoi smesi.* Izv. VUZ "Energhetika", 7/1980, st. 110-113.

[5]. **Bezliudnâi, P.P. i dr.**, *Opredelenie temperaturî tociki rosî productov sgoraniia prirodnogo gaza*. Izv VUZ "Energhetika", 12/1986, st. 89-91.

[6]. * * * , *Modulating / Condensing Fuel – Fired Water Heater and Hydronic Boiler*. Contract DOE /EE - 0171, 32 pg.

[7]. * * * , Prospecte ale firmelor.

Recenzie

Neaga,C.Constantin,
Universitatea **„Politehnica"**,Bucureşti.

TRATAT DE GENERATOARE DE ABUR

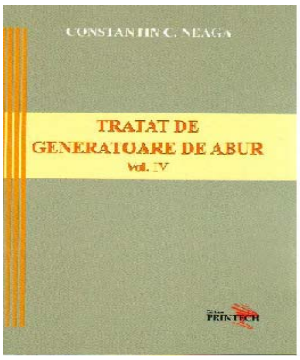

-vol.I, Ed.AGIR, Bucureşti-2001, 544 pg.
Cap1. Introducere în ingineria generatoarelor de abur;
Cap.2.Combustbilii energetici organici;
Cap.3.Bilanţuri materiale ale arderii combustibililor organici;
Cap.4. Bilanţuri termice ale generatoarelor de abur. Randamentul şi consumul de combustibil;
Cap.5. Focare şi arzătoare pentru combustibili organici.
-vol.II, Ed.MATRIX ROM, Bucureşti-2002, 348 pg.
Cap.6.Calculul şi construcţia sistemelor de pregătire pentru ardere a combustibililor organici.
-vol III, Ed.PRINTECH, Bucureşti-2005, 394 pg.
Cap.7.Tipuri constructive şi funcţionale de generatoare de abur;
Cap.8. Supraîncălzitoare de abur.
-vol IV, Ed.PRINTECH, Bucureşti-2006, 430 pg.
Cap.9. Preîncălzitoare de apă de alimentare ale generatoarelor de abur. Economizoare;
Cap.10. Preîncălzitoare de aer de ardere ale generatoarelor de abur.

Ţinând seama de materialul acumulat în ţară,cât şi în lume,legat de cercetarea ştiinţifică, experimentarea, construcţia şi exploatarea acestor echipamente vitale în producerea energiei electrice şi a căldurii, lucrarea prof.dr.ing. C. Neaga reprezintă o necesitate.

Cu toată amploarea care se acordă expunerii problemelor specifice generatoarelor de abur,cartea se adresează,în primul rând,studenţilor din universităţile de profil; ea este însă utilă şi specialiştilor care frecventează masteratul, doctoranzilor, cercetătorilor ştiinţifici, inginerilor implicaţi în proiectarea, realizarea şi exploatarea acestui tip de echipament termomecanic.

Recitind capitolele din cuprinsul tratatului se constată că pentru acoperirea obiectivelor propuse autorul mai are de scris.

Îl aşteptăm.

Revista „Tehnologia Inovativă"
– serie nouă a Revistei „Construcţia de Maşini"

PRODUCTION OF COLD PRESSED PPO AND ITS USE IN COMBUSTION ENGINES

D. Merckx, K. Deprez, B. Goris, V. Lesourt

Department of mechanical engineering, KaHo Sint-Lieven, Gent, Belgium, dirk.merckx@kahosl.be

ABSTRACT

Paper presents some aspects concerning the production of cold pressed PPO and its use in combustion engines.
It is important to know the difference PPO vs. Bio Diesel and how to use the pure plant oil in combustion engines, some aspects concerning the emissions, about the PPO production. Conclusions present further actions within the project.

KEYWORDS: production of cold pressed PPO, combustion engines, pure plant oil, emissions

1. INTRODUCTION

Today our entire economy is based on the petroleum industry. Just as fuel for vehicles, practically all fuels have fossil origin. Unless the world appeals to renewable and sustainable energy sources, our dependence on petroleum based fuels will continue to increase. Therefore, Europe wants to encourage the use of renewable fuels by lowering or removing their taxes. With this measure they hope to have 5.75% of the consumed energy coming from renewable sources by 2010.

Another issue is the release of a considerable amount of CO_2 when burning fossil fuels. In the treaty of Kyoto in 1997, was agreed to reduce the emission of CO_2 by 8.1% by 2010 compared to 1990. The search for fuels with a reduced CO_2 emission is open. Hydrogen, PPO, bio diesel, alcohols (mainly methanol and ethanol) are all new energy sources.

With respect to a reduced CO_2 emission, the use of pure plant oil (PPO) is an ideal solution. Rapeseed as fuel is CO_2 neutral. This means that the rapeseed plant consumes as much CO_2 as there is emitted by producing and burning the rapeseed oil.

Rising fuel prices and environmental problems have stimulated the interest in the use of PPO as a substitute for traditional diesel in engines. It's possible that in the future, plant oil will be an important alternative for petroleum.

2. DIFFERENCE PPO VS. BIO DIESEL

Very often, the expressions pure plant oil and bio diesel are confused or used in a wrong way. What follows is the difference between these two expressions.

The use of vegetable oils in combustion engines is possible but one of the major differences between traditional diesel fuel and plant oil is the viscosity of these fluids.

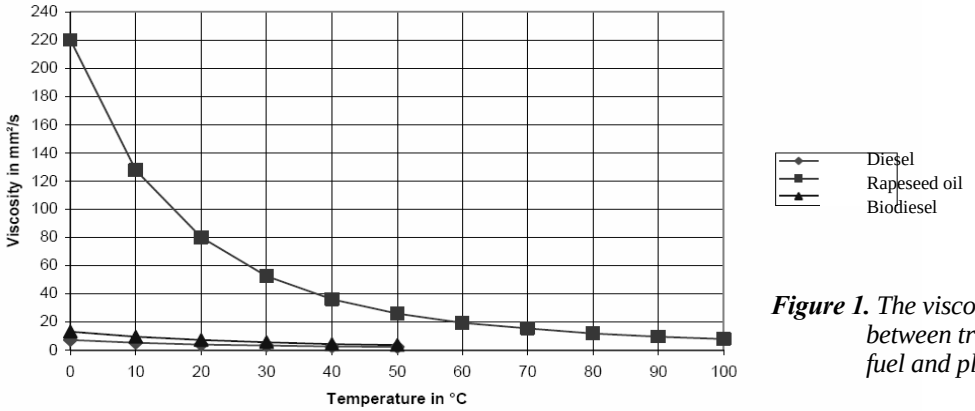

Figure 1. *The viscosity differences between traditional diesel fuel and plant oil*

Traditional engines are designed for the viscosity of diesel. Either the engine has to be adapted to a more viscous fluid; or the viscosity of the fluid has to be reduced in a chemical way to fit the engine. The chemical process to lower the viscosity of plant oil is called a transesterification. Adding an alcohol to plant oil leads to a reaction. The end products of this reaction are glycerol and an alcylester (the so called bio diesel) Often a catalyst is added to accelerate the reaction. The viscosity of bio diesel is comparable to traditional diesel.

One of the major disadvantages of the bio diesel process is that energy has to be added to make the reaction happen. Where PPO is a CO_2 neutral fuel, bio diesel isn't.

Because of the chemical transesterification process, bio diesel is not 100% biodegradable. In case of leakage or spill, the soil needs cleaning up.

Apart from its non-toxicity, another advantage is that PPO is not volatile. This has as consequence that there is no danger for explosion by transportation and storage. The flash point of plant oil is at 220°C where it is at ±150°C for bio diesel and at ±70°C for traditional diesel.

3. USE OF PURE PLANT OIL IN COMBUSTION ENGINES

The energy content of rapeseed oil is 94% of the energy content of traditional diesel fuel. Where PPO contains 32,6MJ/l, diesel contains 34,6MJ/l.

The fuel consumption is slightly higher when engines are running on PPO.

When using pure plant oil as fuel for an engine, there are two possibilities:

- a special designed engine or
- a converted engine.

When Rudolf Diesel (1858-1913) invented his first engine, it wasn't designed for running on petroleum. He used peanut oil, rapeseed oil and sunflower oil as fuel. In 1977, the German company Elsbett started the development of the so called "Elsbett engine".
This type of engine had a special piston shape and an adapted injection system.
These modifications made this engine optimised for running on plant oil.

Another possibility is the use of plant oil in a converted engine. There is a single tank system and a two tank system.

With a single tank system, the tank can be filled up with PPO as well as with diesel.
A vehicle equipped with a single tank system, needs to be equipped with a pre-heating device in order to improve the liquidity of the oil in cold conditions.

The engine management also needs to be adapted to change the injection-timing.
Since the source code of the engine management is mostly a secret of the manufacturer, the single tank system isn't used very often.

With a two tank system, the engine is always started on normal diesel.
The PPO is warmed up in a separate fuel circuit by a heat exchanger to a temperature of ±60°C.
When this temperature is reached (after approx 10-15 minutes) a small on board computer switches the fuelling system of the engine from diesel to PPO.

The system is completely automated, with a small display on the dashboard.
Before the end of the ride, the driver manually needs to change to normal diesel fuel again, so no PPO remains in the fuel pipes.
This is to prevent starting problems and plugging of pipes and filters.

When a standard vehicle is converted, very often the injectors are changed, bigger fuel pipes, a heat exchanger, valves to change between PPO/diesel and an extra fuel filter are added.

The two tank system is more expensive than the single tank system but nevertheless preferable because it has proven it's functioning.

During the last decade many researchers have investigated the use of vegetable oils in compression ignition engines.

Direct use of vegetable oils and/or the use of blends of the oils has generally been considered to be not satisfactory and problematic for both direct (DI) and indirect (IDI) injection diesel engines.

The high viscosity, acid composition, free fatty acid content, as well as gum formation due to oxidation and polymerisation during storage and combustion, carbon deposits and lubricating oil thickening are obvious problems.

The probable reasons for the problems and the potential solutions were proposed and are shown in the next table (Table 1).

Another considerable problem is the guarantee. Once an engine is converted to a single or a two tank PPO system, all factory guarantee expires.

Up to now, no converter replaces the guarantee of the engine manufacturers.

Table 1. *Probable reasons for the problems and the potential solutions*

Problem	Probable cause	Potential solution
Short-term 1. Cold weather starting	High viscosity, low cetane, and low flash point of vegetable oils.	Preheat fuel prior to injection.
2. Plugging and gumming of filters, lines and injectors	Natural gums (phosphatides) in vegetable oil. Other ash.	Partially refine the oil to remove gums. Filter to 4-Microns.
3. Engine knocking	Very low cetane of some oils. Improper injection timing.	Adjust injection timing. Use higher compression engines. Preheat fuel prior to injection.
Long-term 4. Coking of injectors on piston and head of engine	High viscosity of vegetable oil, incomplete combustion of fuel. Poor combustion at partial load with vegetable oils.	Heat fuel prior to injection. Switch engine to diesel fuel when operation at partial load.
5. Carbon deposits on piston and head of engine	High viscosity of vegetable oil, incomplete combustion of fuel. Poor combustion at partial load with vegetable oils.	Heat fuel prior to injection. Switch engine to diesel fuel When operation at part loads.
6. Excessive engine wear	High viscosity of vegetable oil, incomplete combustion of fuel. Poor combustion at partial load with vegetable oils. Possibly free fatty acids in vegetable oil. Dilution of engine lubricating oil due to blow-by of vegetable oil.	Heat fuel prior to injection. Switch engine to diesel fuel when operation at partial load. Motor oil additives to inhibit oxidation. Use lubrication oil based on vegetable oil.
7. Failure of engine lubricating oil due to polymerisation	Collection of polyunsaturated vegetable oil blow-by in crankcase to the point where polymerisation occurs.	Heat fuel prior to injection. Switch engine to diesel fuel when operating at partial load. Motor oil additives to inhibit oxidation. Use lubrication oil based on vegetable oil.

(source: Elsbett)

4. EMISSIONS

The exhaust emissions of PPO are generally better than the traditional diesel emission. A study showed the following results:

Carbon monoxide (CO): minus 50%
Carbon dioxide (CO2): neutral (see earlier)
Hydrocarbons (HC): minus 40%
Nitrogen oxides (NOx): equivalent
Soot particles: equivalent to diesel
(source: solaroilsystems)

In Germany, 100 tractors were converted for the use of PPO. This gave the following emission results.

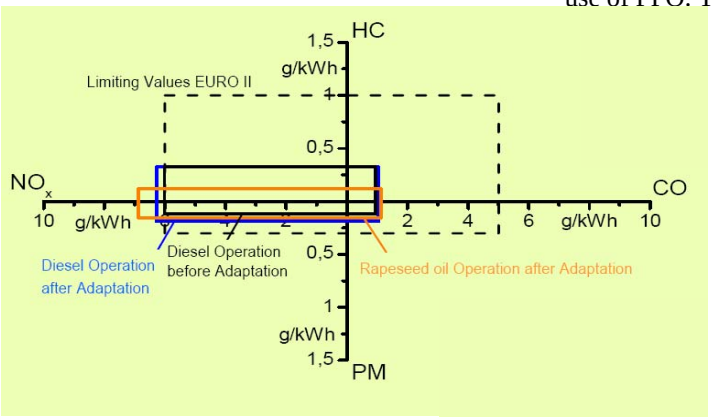

Figure 2. *The limiting values of CO-, HC- and particulate matter of EURO II for rapeseed oil and diesel fuel*

(Source: Technologie- und Förderzentrum, Straubing)

In this study, the limiting values of CO-, HC- and particulate matter of EURO II for rapeseed oil and diesel fuel are met. Emission of NOx with rapeseed oil fuel is up to 14 % higher than limiting value.

It has to be noticed that these emissions are found on a properly converted engines. When using plant oil as fuel in an unconverted vehicle, the emissions are worse than running on conventional diesel!

5. PRODUCTION OF PPO

The most common oilseed is winter rapeseed. *(Brassica napus*) The plant grows from August to July and can be cultivated every four years on the same soil. The harvest yield differs strongly and is located between 3 and 4 tons/hectare. The oil content in the seeds is around 40-45%.

After harvesting, the seeds need to be sieved to separate them from contaminants and foreign seeds. The moistness of the seeds measures then 14-18%. For storage, it has to be dried to 7-9%. The ideal humidity for pressing the rapeseed is 6-7%

Once harvested, sieved and dried, the seeds can be pressed by an oil press. With a procedure of cold pressing, 75% of the oil in the seeds can be extracted. To achieve a higher yield, the seeds need chemical extraction. This technique requires special equipment and knowledge and is not applied in decentralised oil production.

The oil press at KaHo Sint-Lieven is a rotary screw press with cylindrical arranged knives. Between the knives there is a small opening for the oil to escape when the seeds are pressed.

The pressing happens by a decrease of the pitch of the screw and an increase of the core diameter of the screw. The cage around the screw, composed by the knives, is cylindrical. This results in a decreased volume for the seeds, so the oil is pressed out of the seeds.

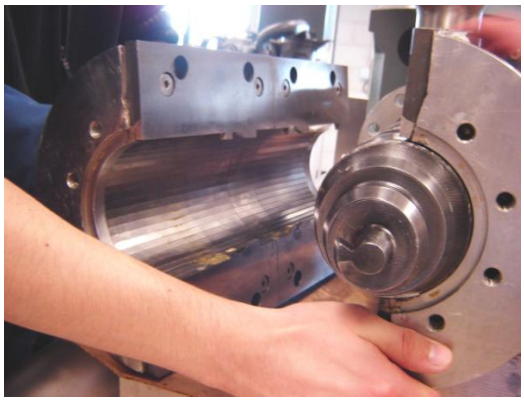

Figure 3. *Cylindrical cage of knives around the screw*

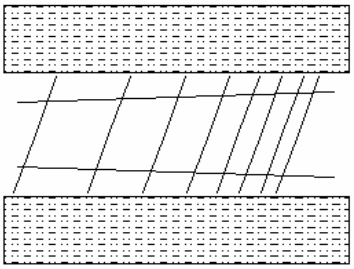

Figure 4. *Decreasing pitch and increasing core diameter*

In order to be able to produce oils, suitable for the use in engines and to compare different vegetable oils, in Germany, a standard has been formulated.

The RK-qualitätstandard (Rapsöl als Kraftstof) The same values as in this standards are used in the formulation of the pre-norm Din 51605.

The standard is divided in two parts.

The first part are properties, typical for rapeseed oil, the second part are properties that depend on the production of the oil. Quality standard for rapeseed oil is shown below (Table 2).

Table 2*. Quality standard for rapeseed oil*

Quality standard for rapeseed oil as a fuel (RK-quality standard, 05/2000)				
characteristics/ substances	**units**	**limiting values**		**test procedure**
		min.	**max.**	
characteristic properties				
density (15°)	kg/m³	900	930	DIN EN ISO 3675 DIN EN ISO 12185
PM flash point	° C	220		DIN EN ISO 22719
calorific value	kJ/kg	35,000		DIN 51900-3
kinematic viscosity (40 °C)	Mm²/s		38	DIN EN ISO 3104
behaviour at low temperatures				rotation viscosimetry
cetane number (ignition quality)				process is being evaluated
coke residues	% by mass		0.40	DIN EN ISO 10370
iodine number	G/100g	100	120	DIN 53241-1
sulphur content	mg/kg		20	ASTM D 5453-93
variable characteristics				
total contamination	mg/kg		25	DIN EN 12662
neutralisation value	Mg KOH/g		2.0	DIN EN ISO 660
oxidation stability	h	5.0		ISO 6886
phosphor content	mg/kg		15	ASTM D3231-99
ash content	% by mass		0.01	DIN EN ISO 6245
water content	% by mass		0.075	pr EN ISO 12937

One of the major issues is the value of the total contamination.

When the crude oil comes out of the oil press, the total contamination can be up to 35000mg/kg and even more. Filters that get out all contamination up to 25mg/kg are very expensive and/or require a lot of maintenance.

When the production doesn't exceed 50kg/hour of rapeseed, sedimentation can be used to eliminate the majority of the contamination.

After sedimentation of four days, values around 300mg/kg can be reached.

Disadvantages of this method are that it's a long method and the layer of dirt that is evacuated still contains a lot of oil.

Further research to efficient and reasonably priced filter methods needs to be done.

6. CONCLUSIONS. FURTHER ACTIONS WITHIN THIS PROJECT

Temperature and pressure sensors are being built in the press.

This is in order to understand what happens inside. Different oilseeds will be pressed, different degrees of dehulled rapeseed, combinations of rapeseed and press cake and all of this with different speeds.

During this operation, temperature and pressure at four different places in the press will be monitored and the quality of the produced oils will be verified.

Different filtering methods and filter tissues will be tested. Not only the total contamination, but also the particle size distribution will be measured with a laser particle counter.

REFERENCES

[1]. http://www.tfz.bayern.de/
[2]. http://www.elsbett.com/engl/hist.htm
[3]. http://www.energie51.nl/laatste-nieuws/solaroil-systems-wint-eerste-prijs-mkb-energie-idee.html

Quick Info

Beswick Engineering announces the release of an ultra-miniature Pressure Compensated Flow Control Valve with low friction diaphragm – PCFCD-1N1. The PCFCD-1N1 is designed to maintain a constant flow rate, which the customer can adjust, regardless of upstream or downstream pressure variations. It works with both liquids (incompressible fluids) and gasses (compressible fluids) but is primarily intended for the control of liquids.

The pressure regulation is accomplished with a low friction diaphragm mechanism. Beswick has applied for patent protection on this unique valve.

The PCFCD-1N1 sets an industry standard for miniaturization. It is lightweight….tipping the scales at only 48 grams. Customers will find it particularly useful when space, weight, and precise liquid flow control are critical.

The PCFCD-1N1 controls flow rates of 0 to 4.2 gallons per hour of Water (0 to 20 cubic feet/hour of Air). It is especially suited for the control of low flow rates. The maximum rated inlet supply pressure is 500 psig. Both the inlet and outlet ports are tapped 10-32. The valve body is both small and lightweight allowing for convenient in-line mounting without the need for a panel mount thread. The PCFCD-1N1 is currently available in brass. Buna-N is the standard seal material. Fluorocarbon (Vitonâ) is optional.

The PCFCD-1N1 controls flow rates of 0 to 4.2 gallons per hour of Water (0 to 20 cubic feet/hour of Air). It is especially suited for the control of low flow rates. The maximum rated inlet supply pressure is 500 psig. Both the inlet and outlet ports are tapped 10-32. The valve body is both small and lightweight allowing for convenient in-line mounting without the need for a panel mount thread. The PCFCD-1N1 is currently available in brass. Buna-N is the standard seal material. Fluorocarbon (Vitonâ) is optional.

(www.beswick.com)

Quick Info

Worlds Smallest Servo Drive From AllMotion Inc.

EZSV10 Servo Motor Controller + Driver Description

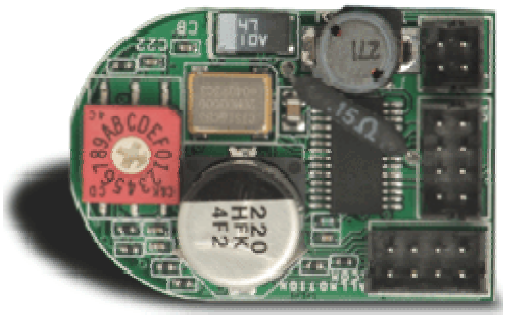

The EZ Servo was designed to allow the **rapid** implementation of DC Brush motor solutions in products requiring automation.
The fully intelligent controllers, measuring just 0.95" x 1.4", require little or no tuning when used with most motors measuring less than 1.5" in diameter.(Default PID Values are robust and are stable with most motors). A single 4 wire bus, containing 2 power wires and two communications wires, links up to 16 such DC motors in a daisy chain. Commands can be issued from any serial terminal program (such as HyperTerminal) or from the EZ Servo/Stepper Windows application.
The Commands are intuitive and simple. For example the command **A10000** will move the Servo motor to **A**bsolute position **10000**. (This communications protocol is compatible with devices that use the Cavro DT or OEM protocol.).
The EZ Servo is also capable of stand alone operation with no connection to a PC. It can be set to execute a preset string of commands upon power up (i.e. Only power is required in this mode). The Commands include nested loops and execution halt pending a switch closure, which is useful in stand alone applications.
Using our Starter Kits, a first time user is able to make a DC Brush Servo Motor move intelligently in less than half an hour.

Features:
· Single 4 wire bus linking up to 16 Stepper/Servo motors.
· 2Amp Peak, 1.5Amp Continuous DC Brush Motor Driver.
· 4 Quadrant Operation.
· Operates from 12V-40V.
· RS232, RS485 or USB Based Communications.
· On Board EEPROM For User Program storage.
· Stand alone operation with no connection to a PC.
· Position Velocity and Torque modes.
· Industry standard communications protocol.
· Homes to an Opto or Encoder Index with a single command.
· Fully programmable ramps and speeds.
· Quadrature encoder based feedback.
· Switch selectable device address.
· Software selectable max currents.
· 4MHz max encoder frequency.
· Optional PWM or On/Off Output.
· Optional ADC Inputs Halt / Branch On ADC Value.

(www.allmotion.com)

Innovate & Win!

The 2007 Create the Future Design Contest, presented by SolidWorks Corp. and NASA Tech Briefs, is now open for entries in these categories: Machinery, Equipment, and Component Technology; Consumer Products; Medical; Safety and Security; Transportation; and Sustainable Technologies.

The sixth annual Create the Future design contest recognizes outstanding innovations in product design, awarding a Grand Prize of $20,000, and six First Prizes (one from each category) of Hewlett-Packard engineering workstations. Entrants may elect to have their entry posted on the contest Web site, and the 10 most-visited entries will each be awarded $250. All qualified entrants will receive a Create the Future Design Contest T-shirt.

The contest is co-sponsored by COMSOL Inc., Hewlett-Packard Co. and the Hong Kong Polytechnic University. So, exercise your imagination and submit your innovative design ideas today.
All entries must be received by October 15, 2007.

(http://www.createthefuturecontest.com/)

BASICS OF COMMERCIAL AVAILABLE CORRELATION MEASUREMENT SYSTEMS

S. Cooreman, S. Coppieters*, F. De Bal*, V. Danel ***

*Katholieke Hogeschool (KaHo) SintLieven, Association KULeuven, Ghent, Belgium,
** EIGSI, La Rochelle, France

ABSTRACT: *In European Industrial production, mechanical testing is becoming more and more important. In order to make production economically profitable, warranty complaints have to be avoided by using material in the most efficient way.*
In the quest for nonintrusive high accuracy measurements, Electronic Speckle Pattern Interferometry (ESPI) and Digital Image Correlation (DIC) have been commercially developed in practical equipment. Both systems provide considerable advantages towards conventional experiments.
The Digital Image correlation is an optical–numerical measurement technique, based on the comparison between pictures taken during the deformation of the object.

KEYWORDS: testing equipment, measurement technique, Digital Image Correlation

1. INTRODUCTION. ABOUT TESTING EQUIPMENT

In European Industrial production, mechanical testing is becoming more and more important.

In order to make production economically profitable, warranty complaints have to be avoided by using material in the most efficient way.

For these reasons testing equipment is commonly used in three fields.

First of all, testing equipment is used in quality control.

One can only produce good quality products, if the quality of the ingredients or raw materials is guaranteed.

Similarly, one can only sell higher quality products if one can confirm this with the necessary tests.

A second application is the characterization of the materials. Especially determining the mechanical properties of composite materials, such as woven structures, sandwich materials, tripand multiplex steel, foam and others, is a more complex matter.

Thirdly, prototype and product evaluation are used to optimize Finite Element Models. If this is not the case, the FE Model is improved by data supplied by real experiments. The parameters for the material model are commonly given by the practical results obtained from the Inverse Method.

Conventional techniques have the advantage of being well known in industry and have been standardized. One measures deformations and calculates technical or true strain, etc.

The most common systems are crosshead displacement, extensometers and strain gauges.

In the same order, they gain in precision, but are more expensive and complex in usage. By their contact, they also affect the measurement in a mechanical way.

For modern, anisotropic and, or heterogeneous materials, these methods are also often insufficient as material characterization technique.

Until a few years ago, noncontact extensometers failed in accuracy for mechanical tests to determine elastic properties of rigid materials.

2. THE DIC TECHNIQUE

In the quest for nonintrusive high accuracy measurements, Electronic Speckle Pattern Interferometry (ESPI) and Digital Image Correlation (DIC) have been commercially developed in practical equipment. Both systems provide considerable advantages towards conventional experiments.

One of the major advantages derives from the fact that they are fullfield measurements. Displacements and deformations are calculated out of images, recorded during the test. Due to number of economical reasons, DIC came as first in reach of the SME's.

In 2003 a consortium of eleven organizations began a EUfunded research project to develop

reference tests for inplane measurements by optical techniques (SPOTS – Standardization Project for Optical Techniques of Strain Measurement).

In proXpert, a national funded project, the DIC technique is evaluated as a valuable displacement measurement system in traditional standardized mechanical tests.

Most standardized methods for the determination of constitutive material parameters are based on the use of test specimens with a welldefined standardized geometry, and are submitted to well known boundary conditions.

Classic examples are uniaxial tensile tests and bending tests.

The DIC technique can solve the problem of the position of the necking towards the position of the extensometer. There are the advantages of having a noncontact measurement in general. One could also obtain more information for heterogeneous and/or anisotropic materials, out of the same test.

An important goal of proXpert is to obtain experience with modern mechanical testing equipment and share this knowledge with SME's.

The Digital Image correlation is an optical–numerical measurement technique, based on the comparison between pictures taken during the deformation of the object. This technique was principally developed by M.A. Sutton, Department of Mechanical Engineering of the University of South Carolina.

It offers the possibility to determine displacement fields at the surface of objects under any kind of loading. For an optimized use, the object of interest has to be covered with random painted speckles. The image of the test specimen is represented by a discrete function. Values between 0 and 255 represent its grey levels. The correlation calculation is done for a group of pixels called subset. The displacement field is supposed homogeneous inside the pattern.

The initial image representing the specimen before distortion is a discrete function noted f(x,y). This one will be transformed in another discrete function noted f*(x*, y*) after displacement or distortion.

The theoretical relation between the two discrete functions could be written as:

$$f^*(x^*, y^*) = f(x + u(x,y), y + v(x,y)) \qquad (1)$$

u(x,y) and v(x,y) represent the displacement field for a pattern as shown in the next figure (Figure 1).

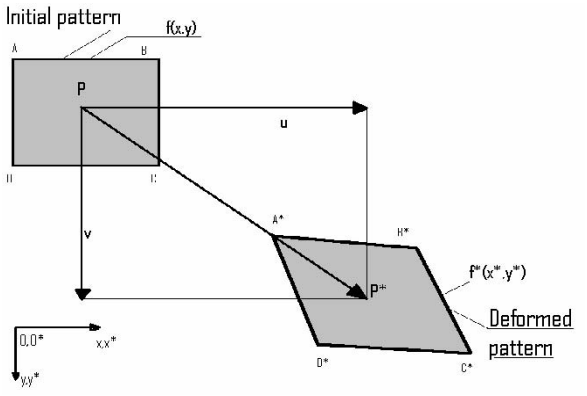

Figure 1. *The displacement field for a pattern*

Notations NB: Both images are represented in the same coordinate system.

The four elements required for a correlation technique are:

- Firstly, the mathematical definition for the displacement strain term and the term of rigid body displacement have to be taken in account at the same time.
- Secondly, a mathematical correlation criterion (coefficient) functions f and f* has to be defined.
- Thirdly, an interpolation method for the grey level is needed in order to reach a subpixel precision.
- And fourthly, the mathematical solution for determination of elongation and the strain term for a pattern.

This theory can immediately been applied to the 2Dimension image analysis with only one camera and a predefinition of the subset of each pixel.

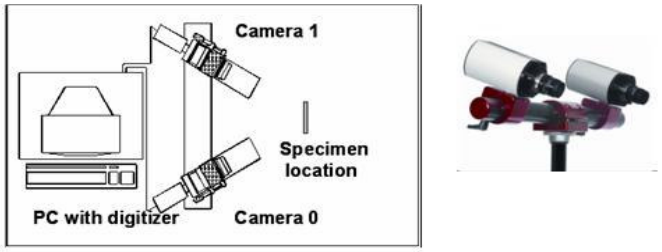

Figure 2. *3D setup.*

Furthermore, with two camera's, data in 3D can be obtained. The correlation method is based on the same principle even though reckonings are more consequent. This correlation method is used for different optical systems on the market.

3. ASPECTS CONCERNING DIC TECHNIQUE. LIMESS SYSTEM TESTS.

Among the commercial systems available, KaHo decided in favor of Limess (www.limess.com) .

The choice for the Limess deformation measurement system was made due it's modular and

open structure. The purchase at the University of Brussels (VUB) and the KULeuven of the same system confirmed our decision. In the meantime one more system at University of Liege (with 6 cameras for round view) is installed.

The lack of popularity of the DIC technique is due to the little knowledge on the reliability and repeatability. The technique has a very large number of difficulties to quantify influences on its accuracy.

Firstly there are the environmental influences. Since the DIC technique is an optical technique, based on grey patterns, lightning and especially shadows are very important. A moving cloud, reflection in the window, interference of light waves or a cooperator watching to close can interfere with the measurement. One should illuminate with strong, diffused light, and avoid reflection. Since the measurement system is no longer attached to the test specimen, environmental vibrations have a larger influence then with contact systems. A rigid connection between the cameras and the testing machine is preferable, but not required. A solid, rigid camera support is necessary. The Limess system is flexible enough, so cameras can be positioned in any possible way.

If the cameras are further away from each other, depth resolution improves. Once the positions are chosen, the complete setup needs to stay in the same position and has to be calibrated. Stereo pictures of the calibration target are used to determine calibration parameters for the two cameras as well as the cameras interrelation. The calibration process involves the acquisition of a series of images of the calibration target in different orientations (rotations around all three axes). During this process, the standard deviation of the calibration parameters is shown as an indication of the quality of the process.

Figure 3. *Calibration targets*

Secondly there are also the influences of the specimen. The quality of the speckle pattern is of great importance. Several studies have been devoted to different aspects, like contrast, pattern spreading, randomness, adhesion and others. Tests with computer generated patterns, applied by silkscreen printing give better results, but are not always applicable. The heat of the light and possible chemical reaction between specimen and coating are also often forgotten, nevertheless they are very meaningful.

A third factor to take into account is the evaluation settings. The user has to define an area of interest, a subsetsize with start position and a stepsize. The magnification should be chosen in order to fill the view with the test object. The speckle size should be at least 3x3 pixels. The largest speckle determines the subsetsize. There should be at least 3x3 speckles per subset. The start position should be the pixel with the slightest movement in the area of interest.

In order to obtain a global idea about feasible accuracies several basic setups were optimized and compared with traditional methods. Because the ranges of application, important for the proXpert project, are basic mechanical tests, examples were taken out of this field.

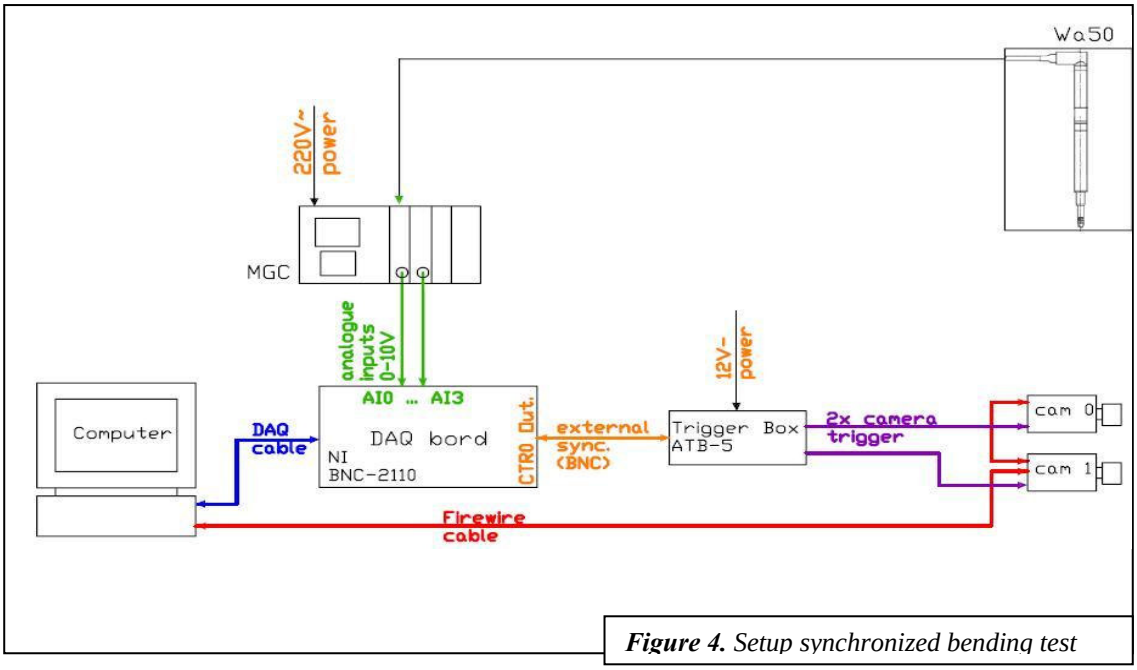

Figure 4. *Setup synchronized bending test*

The basis of the calculation of most of the results of the mechanical tests are displacements. Therefore, displacements and/or elongations are compared. The first tests were 3 point bending tests on profiles, made out of different materials. The bend curve of a copper bar, a steel bar and a polypropylene beam was measured by an electronic clock gauge and the Limess DIC system, simultaneously.
The synchronized measurements prevented the environmental properties of changing.

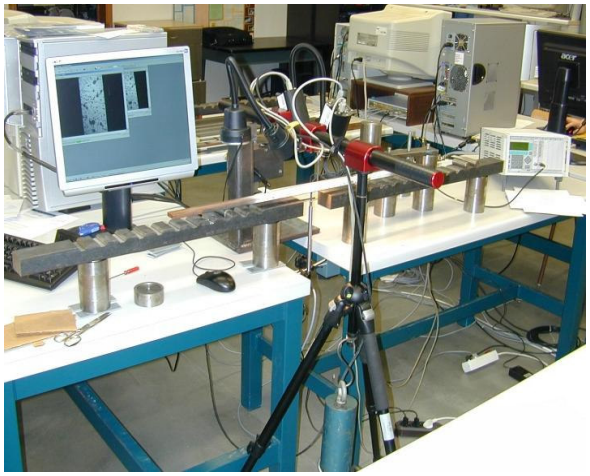

Figure 5. *Stabilized setup*

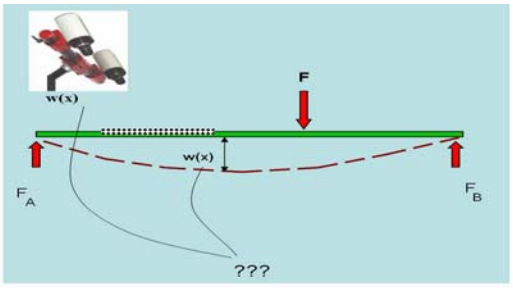

Test results copper bar:

calculated		systems results	
m [kg]	w(x) self calc. [mm]	w(x) WA50 [mm]	w(x) Vic3D [mm]
0	0	0	0
10	2,30	2,23	2,19
12	2,76	2,67	2,63
14	3,22	3,19	3,14
16	3,68	3,67	3,60
18	4,14	4,16	4,08

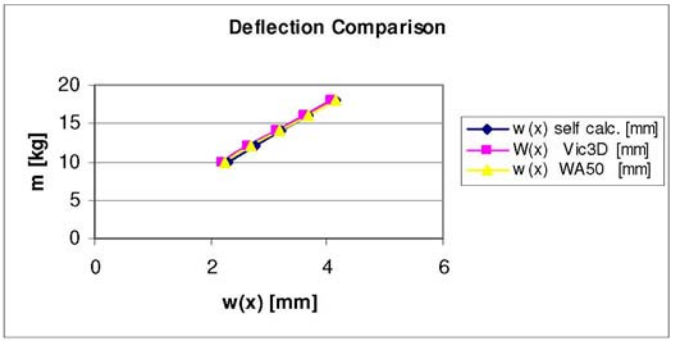

Figure 6. *Test results copper bar*

Test results steel bar:

calculated		systems results	
m [kg]	w(x) self calc. [mm]	w(x) WA50 [mm]	W(x) Vic3D [mm]
0	0,00	0,00	0,00
14	1,59	1,70	1,67
18	2,04	2,19	2,06
22	2,50	2,70	2,52
26	2,95	3,16	2,98

Test results polypropylene profile:

calculated		systems results	
m [kg]	w(x) self calc. [mm]	w(x) WA50 [mm]	W(x) Vic3D [mm]
0	0,00	0,00	0,00
14	0,58	0,60	0,65
18	0,75	0,78	0,86
22	0,91	0,99	1,07
26	1,08	1,19	1,28
30	1,24	1,39	1,50

For evaluation of these results, one has to take into account that the result from the DIC measurement is an average of an area of interest, and the gauge was placed on a point. The gauge was also placed below the specimen, while the cameras were focused on thetop of the profile. Tiling and/or narrowing of the specimen are also not taken into account. In all these cases, the speckle pattern was applied manually with a spray can.

An important application of the DIC system in the frame of proXpert is a tensile test. For this application the input of the DAQcard of the Limess system was connected to an analog output of a Zwick tensile machine.

A standard flat sheet metal tensile probe was tested. Expertise out of previous tests helped to improve the setup. The speckle pattern was now computer generated. To compare the results, some conversions were necessary. Displacements out of the DIC system are related to the initial reference picture.

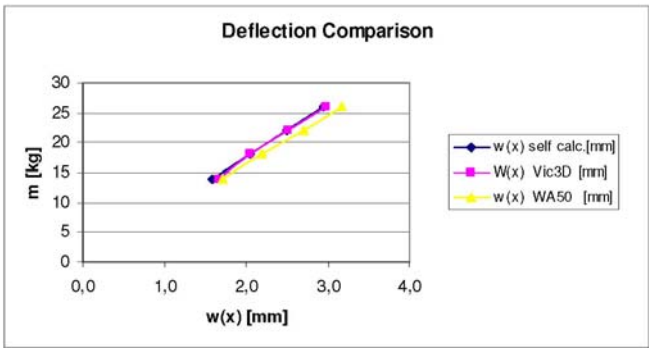

Figure 7. *Test results steel bar*

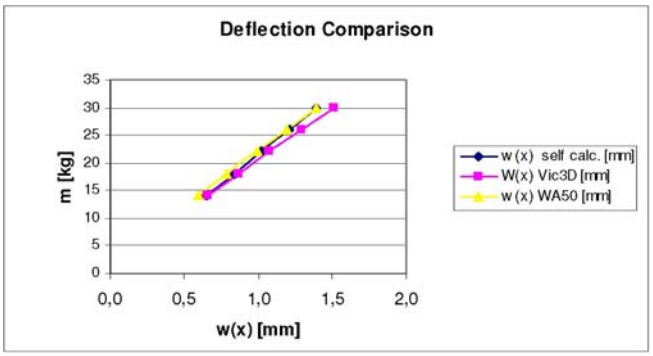

Figure 8. *Test results polypropylene profile*

Therefore displacements and strains from the optical measurement are not directly comparable with the technical strain from the extensometer on the tensile machine.

Because in the uniform part of the curve the percentage strain is independent of the initial measurement length, we suppose:

$$A_{opt} = (U_2-U_1)/(X_2-X_1)$$

if the coordinate system is in plane with the tensile probe. Then $\Delta l_{opt} = A_{opt} \cdot l_{0\_extensometer}$ to convert to the same reference as the extensometer.

4. CONCLUSIONS

These test results are pleasantly surprising.

One can conclude that with the necessary craftsmanship and expertise the DIC technique can help to solve many practical problems in mechanical testing. Nevertheless thorough training and conscientious experts are a necessity for good results.

Figure 9. *Tensile test*

Test results tensile test:

Displacement (mm)			Load cell
Optical	Crossh.	Exten.	Force(N)
0,041	0,081	0,034	903,32
0,076	0,175	0,034	1354,98
0,112	0,262	0,068	1660,15
0,193	0,356	0,170	1843,26
0,278	0,452	0,239	1904,29
0,366	0,532	0,375	1940,92
0,670	0,860	0,683	2160,64
2,676	3,174	2,734	2673,34
4,742	5,507	4,750	3015,13
5,753	6,621	5,776	3161,62
8,724	10,202	8,750	3564,45
10,694	12,698	10,698	3796,38
12,678	14,848	12,680	3967,28
14,686	17,393	14,697	4138,18
16,721	19,716	16,713	4272,46
18,784	21,934	18,730	4382,32
20,879	24,488	20,815	4492,19
23,004	26,446	22,900	4565,43
24,077	27,876	23,925	4614,26
26,270	30,258	26,044	4687,50
28,520	32,581	28,198	4748,53
29,674	33,560	29,326	4772,95
31,993	35,893	31,513	4821,77
34,343	37,765	33,769	4858,40
36,874	40,895	36,025	4907,22
39,580	42,844	38,417	4931,64
44,253	45,081	42,246	4956,05

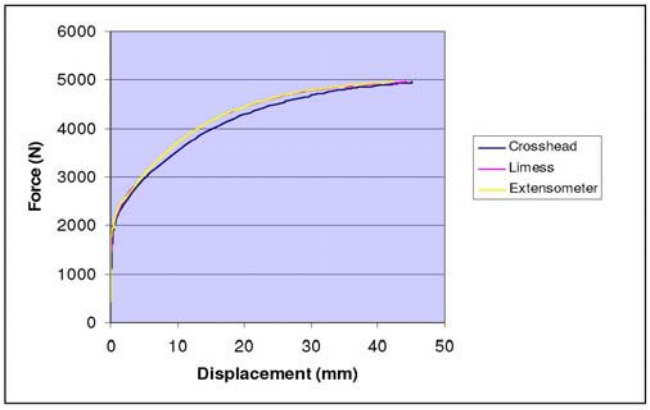

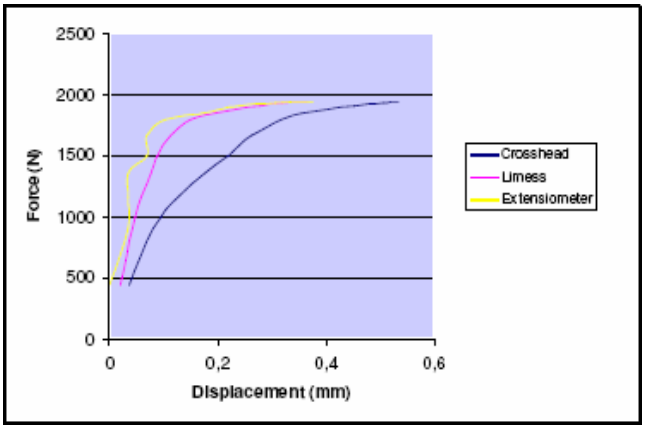

REFERENCES

[1]. **S. Mguil-Touchal, F. Morestin, M. Brunet.** *Various experimental applications of digital image correlation method.* Laboratoire de Mécanique des Solides, INSA de Lyon.

[2]. **D. Lecompte, A. Smits, Sven Bossuyt, H. Sol, J. Vantomme, D Van Hemelrijck, A.M. Habraken.** *Quality assessement of speckle patterns for digital image correlation.* (Available at www.sciencedirect.com since 21 October 2005).

[3]. **David Lecompte.** *Elastic and Elasto-Plastic Material Parameter Identification by Inverse Modeling of Static Tests using Digital Image Correlation.* Phd, March 2007.Vrije Universiteit Brussel and Koninklijke Militaire School.

[4]. **Ralf Pfeiffer**. *Practical semester report on: Strain Gage and Optical Correlation based Measurements.* December 2006. University of Applied Sciences, Hochschule, Merserburg(FH), GERMANY. Preactical semester in KaHo-Sint Liven, Association KULeuven, Ghent, Belgium.

[5]. **Stephen R McNeill.** *Experimental Considerations for 2-D Digital Image Correlation.* Ph.D., P.E. University of South Carolina.

[6]. **Chu, T.C. Ranson, W.F., Sutton, M.A., Peters, W.H.,** *Applications of digitalimage correlation techniques to experimental mechanics.* Experimental Mechanics 25 (3), 1985, p.232-244.

[7]. **Peters, W.H., Ranson, W.F.,** *Digital Image techniques on techniques on experimental stress analysis*. Optical Engineering 21 (3), 1982, p. 427-431.

[8]. **Sutton, M.A., Wolters, W.J., Peters, W.H., Ranson, W.F., McNeil, S.R.,** *Determination of displacements using an improved digital correlation method.* ImageVision Computing 1 (3), 1983, p.133-139.

CAST CLEANING ROBOT FEELS ITS WAY TO LOWER MANUFACTURING COSTS AND HIGHER SURFACE QUALITY

ABB Automation Technologies AB Robotics & Manufacturing, Sweden, www.abb.com

ABSTRACT

*Improved automated grinding and deburring of castings is now possible with the launch of a new robot based system called Force Control Machining. The new dedicated robot based system **Force Control Machining** from ABB removes the bottleneck and greatly increases process efficiency, saving time, raising overall consistency and boosting product quality.*

KEYWORDS: robot, improved automated grinding, deburring, castings, Force Control Machining. process efficiency, product quality.

*Improved automated grinding and deburring of castings is now possible with the launch of a new robot based system called **Force Control Machining**.*

The system provides the user with a ready configured, tested and verified **Function Package Force Control Machining** for different robot-machining applications. In addition ABB developed a ready to produce **Flex Finishing Cell** concept.

At the heart **RobotWare Machining FC** contains two advanced software features. The first, FC Pressure, lets robots grind, polish or buff castings while maintaining a constant pressure between the tool and the work surface.

The second software feature, FC SpeedChange, enables a robot to debur or deflash part line and surfaces of castings at a controlled speed, slowing down when encountering excessive burr.

Traditionally, the foundry finishing process has been extremely labour-intensive with inconsistent end product quality because casts are ground, deburred and polished by hand.

Until now, robots used for this task have been position controlled, moving according to defined positions and speeds. If the robot is struggling to trace the programmed path, the robot's servo will increase power until maximum torque, causing a collision with the excess material along the way. As a result the robot stops; the tool breaks; or the work piece gets damaged. To limit such damage, conventional cast cleaning robots are typically run at a slower pace, limiting productivity.

This conventional approach needs complex and time-consuming programming as the robot path needs to be as exact as possible. The expectation is that the grinding or polishing will give consistent results. But in reality the cast products are all individual with different tolerances and this generates inconsistent process results.

"*The new dedicated robot based system **Force Control Machining** from ABB removes the bottleneck and greatly increases process efficiency, saving time, raising overall consistency and boosting product quality*," says Andreas Eriksson, Product Manager Foundry, ABB Robotics.

"One of the last real barriers to productivity improvement in this sector has been lifted."

The benefits include:

- Improved process results/ product quality
  - Secure controlled contact force in grinding applications gives an improved and consistent product quality
- Reduced programming time
  - 80% faster to program grinding applications by allowing the robot to "feel" the surface
- Shorter cycle time
  - 20% faster deburring applications as the robot adapts to surface defects
- Longer tool life
  - Up to 20% longer tool life as there is consistent wear by avoiding tool and work piece collisions

FC Pressure

FC Pressure software is aimed at processes demanding a high quality surface finish. It allows the robot to effectively "feel" its surroundings and follow the casting surface, changing its position in order to apply a constant pressure on the surface, even if the exact position of the surface is not known.

As there is a consistent contact, debris, such as a burr, is removed to the same depth.

This improved force control accuracy is critical for a good surface finish, where even a 5 Newton force difference can have a huge impact on final quality.

The result is improved surface finish; ability to handle variations in castings; minimum risk of damage to the casting surface; and predictable tool wear.

Constant pressure is obtained by adjusting the robot path. Therefore this function is suitable for polishing, grinding and cleaning, where a surface needs to be even and smooth.

Typical applications in foundry and metal fabrication include:

- Grinding of water taps, turbine/propeller blades and other types of castings
- Polishing of lap tops, mobile phones, electronic parts, water sinks, etc
- Buffing of bumpers, speakers, chromate engine covers, etc.

FC SpeedChange

In processes where path accuracy is important and where the finished result must comply with specific dimensions, FC SpeedChange is recommended. With FC SpeedChange, the robot is position controlled and follows a programmed path that maintains a constant material removal rate.

It operates at maximum process speed and automatically slows down the robot when the machining forces are too high.

When FC SpeedChange is active and if machining forces exceed a certain value, then the path speed will automatically be reduced, thus decreasing forces, minimizing changed dimensions due to deflections of the robot arm and subsequently avoiding damaging the part or tool due to stress and heat.

This results in shorter cycle times; ability to handle variations in castings; minimum risk of damage to the castings; and predictable tool wear.

FC SpeedChange can be used for:

- Grinding unevenly distributed material on cast surfaces
- Milling along the edge of a work piece
- Deburring along the contours of a work piece
- Deflashing unevenly distributed burr along a part line on castings

"*Foundry cleaning operations are now much simpler, enabling finished castings to be produced better, faster and cheaper*," says Eriksson.

Force Control Machining

The new robot-based system provides, for the first time, force control in different machining applications where the robot needs to be sensitive to process forces. It comprises advanced software, described above, instructions for machining applications and a computer adapted for force control.

In addition, for full functionality the system contains standard ABB robots fitted with a force sensor; ABB IRC5 controller housing an interface card linking the sensor to the controller's computer; and cabling between the sensor and the controller.

The force sensor measures the process forces used to adjust the robot's behaviour. For FC Pressure, either a six degree of freedom (6DOF) – that is full force and full torque - or a one degree of freedom (1DOF) force sensor is used.

For FC SpeedChange, either a 6 DOF sensor or an analogue signal representing the machining forces, such as spindle voltage output, will be used.
The choice of sensor input depends on the required flexibility of the application.

"*This ABB solution is fully flexible and can be adopted to almost any machining process or system configuration as required by the customer*," says Eriksson.

"*All the benefits of* ***Force Control Machining*** *open up a huge potential for increased productivity and higher quality using robot automation*."

ABB (*www.abb.com*) is a leader in power and automation technologies that enable utility and industry customers to improve their performance while lowering environmental impact.

The ABB Group of companies operates in around 100 countries and employs about 109,000 people.

ABB is a leading supplier of industrial robots - also providing robot software, peripheral equipment, modular manufacturing cells and service for tasks such as welding, handling, assembly, painting and finishing, picking, packing, palletizing and machine tending. Key markets include automotive, plastics, metal fabrication, foundry, electronics, pharma-ceutical and food and beverage industries.

A strong solutions focus helps manufacturers improve productivity, product quality and worker safety. ABB has installed more than 150,000 robots worldwide.

NOTE: All information given conforms to US GAAP.

Figure 1. Force Control Machining *– robot based system for improved automated grinding and deburring of castings.*

REFERENCES

www.abb.com

For more information please contact:

Reader enquiries:

ABB Automation Technologies AB
Robotics & Manufacturing
Claudia Berg
Hydrovägen 10
SE-721 68 Västerås
Sweden
Tel: +46 21 344 164
claudia.berg@se.abb.com
www.abb.com/robotics

ABB Group

The ABB Group
ABB is a global leader in power and automation technologies that enable utility and industry customers to improve their performance while lowering environmental impact.

Technology
Technology plays a key role for ABB.
We have activities all over the world working to develop unique technologies that make our customers more competitive, while minimizing environmental impact.

Sustainability
Sustainability is integral to all aspects of our business. We strive to balance economic, environmental and social objectives and integrate them into our daily business decisions.

Where to find us
ABB operates in more than 100 countries and has offices in 87 of those countries to give its global and local customers the support they need to develop and conduct their business successfully.

ABB businesses

ABB is a global leader in power and automation technologies that enable utility and industry customers to improve their performance while lowering environmental impact. The ABB Group of companies operates in around 100 countries and employs about 111,000 people.

Power Products
Power Products are the key components to transmit and distribute electricity.
The division incorporates ABB's manufacturing network for transformers, switchgear, circuit breakers, cables and associated equipment.
It also offers all the services needed to ensure products' performance and extend their lifespan.
The division is subdivided into three business units.

Power Systems
Power Systems offers turnkey systems and services for power transmission and distribution grids, and for power plants. Substations and substation automation systems are key areas.
Additional highlights include flexible alternating current transmission systems (FACTS), high-voltage direct current (HVDC) systems and network management systems.
In power generation, Power Systems offers the instrumentation, control and electrification of power plants.
The division is subdivided into four business units.

Automation Products
This ABB business serves customers with energy efficient and reliable products to improve customers' productivity, including drives, motors and generators, low voltage products, instrumentation and analytical, and power electronics.
More than one million products are shipped daily to end customers and channel partners, spanning a wide range of industry and utility operations, plus commercial and residential buildings.

Process Automation
The main focus of this ABB business is to provide customers with integrated solutions for control, plant optimization, and industry-specific application knowledge.
The industries served include oil and gas, power, chemicals and pharmaceuticals, pulp and paper, metals and minerals, marine and turbocharging.
Key customer benefits include improved asset productivity and energy savings.

Robotics
ABB is a leading supplier of industrial robots - also providing robot software, peripheral equipment, modular manufacturing cells and service for tasks such as welding, handling, assembly, painting and finishing, picking, packing, palletizing and machine tending. Key markets include automotive, plastics, metal fabrication, foundry, electronics, pharmaceutical and food and beverage industries. A strong solutions focus helps manufacturers improve productivity, product quality and worker safety. ABB has installed more than 150,000 robots worldwide.

In addition to ABB's automation activities directed at the oil and gas industries, **ABB Lummus Global** continues to design and supply production facilities, refineries and petrochemical plants.

(www.abb.com)

SIMULAREA NUMERICĂ A INTERACȚIUNII FLUIDULUI CU PALETELE CU PROFIL HIDRODINAMIC ALE ROTORULUI MINIHIDROCENTRALEI PENTRU CONVERSIUNEA ENERGIEI CINETICE A APEI

Bostan Ion, Bostan Viorel, Dulgheru Valeriu

Universitatea Tehnică a Moldovei, Chişinău, Republica Moldova, dulgheru@mail.utm.md

REZUMAT: *Minihidrocentralele permit o conversiune eficientă a energiei cinetice a râurilor în energie mecanică şi electrică fără construcția barajelor. Eficiența este asigurată de poziția optimă a paletelor cu profil hidrodinamic. În prezent, stația pilot a minihidrocentralei se află la etapa de execuție şi va fi amplasată pe râul Prut lângă comuna Stoieneşti, r. Cantemir, Republica Moldova.*

ABSTRACT: *Mini – hydro - electric power plants allow an efficient conversion of rivers kinetic energy into mechanical and electric energy, without barrages construction. Efficiency is insured by the optimal position of blades which have a hydrodynamic profile. Now, the pilot station of mini – hydro - electric power plant is its execution stage and it will be installed on Prut river, near Stoienesti village, Cantemir department, Republic of Moldavia.*

CUVINTE CHEIE: Minihidrocentrală, simulare numerică, profil hidrodinamic

KEYWORDS: Mini – hydro - electric power plant, numerical simulation, hydrodynamic profile

1. INTRODUCERE

Cu scopul de a evita construcția barajelor, energia cinetică a râurilor poate fi utilizată prin intermediul turbinelor de curenți de apă.

Acest gen de turbine se instalează uşor, se operează simplu şi costurile de întreținere sunt convenabile. Viteza curentului de 1m/s reprezintă o densitate energetică de 500W/m2 a secțiunii de traversare, însă doar o parte din această energie poate fi extrasă si convertită în energie electrică.

Aceasta depinde de tipul rotorului şi a palelor, care este obiectul de cercetare. Există diverse soluții conceptuale de elaborare a acestui gen de turbine.

În baza cercetărilor efectuate şi multiplelor modelări la calculator a fost elaborată schema conceptuală a minihidrocentralei cu ax vertical cu palete cu profil aerodinamic NACA instalate pe osii verticale.

Paletele sunt orientate sub unghiul de atac α variabil față de linia de acțiune a vectorului vitezei $\vec{V}$ a apei curgătoare (Figura 1).

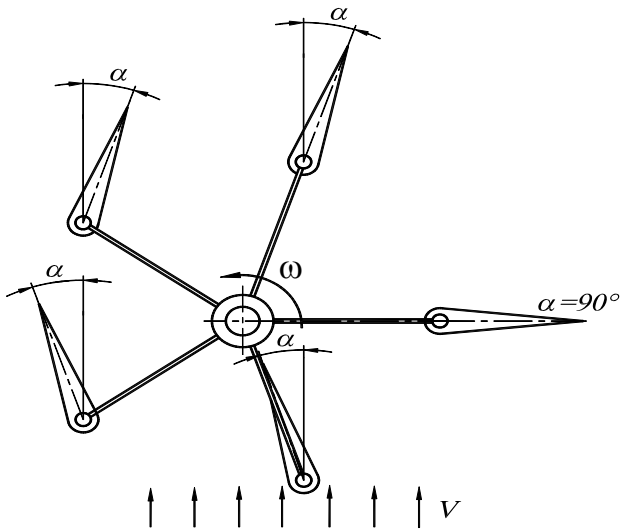

Figura 1. *Diagrama conceptuală a minihidrocetralei cu ax vertical*

2. ACȚIUNEA FLUIDULUI ASUPRA PALETELOR ROTORULUI

Pentru cercetarea teoretică a interacțiunii curentului de fluid cu palele rotorului minihidrocentralei luăm ca bază fragmentul *„grinda rotorului – pală”* schematizat conform figurii 2.

Se consideră profilul simetric al palei, aflat într-un curent de fluid care se mişcă uniform cu viteza $\vec{V}_\infty$ (Figura 2). În punctul de fixare O' a palei simetrice cu braţul OO' considerăm două sisteme de coordonate, şi anume: sistemul $O'xy$ cu axa $O'y$ orientată în direcţia vectorului viteză $\vec{V}_\infty$, iar axa $O'x$ normală la aceasta direcţie; şi sistemul $O'x'y'$ cu axa $O'y'$ orientată în direcţia braţului $O'O$, iar axa $O'x'$ normală la această direcţie. Punctul A corespunde bordului de fugă, iar punctul B corespunde bordului de atac. Unghiul de atac α este unghiul dintre coarda AB a profilului şi direcţia vectorului viteză $\vec{V}_\infty$, iar unghiul de poziţionare φ este unghiul dintre direcţia vectorului viteză şi braţul $O'O$.

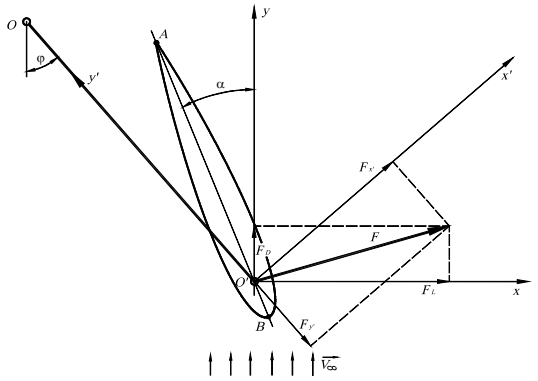

Figura 2. *Paleta cu profil hidrodinamic*

Forţa hidrodinamică $\vec{F}$ are componentele în direcţiile $O'x$ şi $O'y$, numite forţa de portanţă şi forţa de rezistenţă:

$$F_L = \frac{1}{2} C_L \rho_\infty V_\infty^2 S_p, \quad F_D = \frac{1}{2} C_D \rho_\infty V_\infty^2 S_p, \tag{1}$$

unde ρ_∞ este densitatea fluidului, V_∞ este viteza curentului, $S_p = ch$ (c este lungimea corzii AB, h este înălţimea palei) reprezintă aria suprafeţei laterale a palei, iar C_L şi C_D sunt coeficienţii hidrodinamici adimensionali, numiţi coeficientul de portanţă (lift) si coeficientul de rezistenţă (drag). Coeficienţii hidrodinamici C_L şi C_D sunt funcţii de unghiul de atac α, numărul Reynolds Re şi forma aerodinamică a profilului palei. Componentele forţei hidrodinamice în sistemul de coordonate $O'x'y'$ sunt

$$\begin{aligned} F_{x'} &= -F_L \sin\varphi + F_D \cos\varphi, \\ F_{y'} &= F_L \cos\varphi + F_D \sin\varphi. \end{aligned} \tag{3}$$

Momentul de torsiune la axa rotorului OO' dezvoltat de paleta i este

$$T_{r,i} = F_{x'} \cdot |OO'|, \tag{4}$$

iar momentul de torsiune sumar dezvoltat de toate paletele este

$$T_{r\Sigma} = \sum_{i=1}^{Npal} T_{ri}, \tag{5}$$

unde $Npal$ este numărul paletelor rotorului.

Aşa cum forţa hidrodinamică nu are punctul de aplicaţie în originea sistemului de axe ale paletei O', se produce un moment rezultant. Momentul de tangaj, determinat în raport cu punctul situat la distanţa de ¼ de coardă de la bordul de atac B, se calculează după formula

$$M = \frac{1}{2} C_M \rho V_\infty^2 c S_p,$$

unde C_M reprezintă coeficientul de moment al profilului.

3. DETERMINAREA COEFICIENŢILOR C_L, C_M ŞI C_D

Pentru simplitate, coarda profilului se consideră unitară. Iniţial, fluidul este considerat incompresibil şi nevâscos, iar mişcarea sa plană şi potenţială. Astfel, componentele vitezei $\vec{V} = (u, v)$ într-un punct $P(x, y)$ sunt date de relaţiile $u(x,y) = \frac{\partial \Phi}{\partial x}, \quad v(x,y) = \frac{\partial \Phi}{\partial y}$,

unde Φ este potenţialul mişcării, obţinut prin suprapunerea unui curent uniform de viteză $\vec{V}_\infty = (V_\infty \cos\alpha, V_\infty \sin\alpha)$ cu o distribuţie de surse şi o distribuţie de vârtejuri amplasate pe conturul profilului C

$$\Phi(P') = V_\infty x \cos\alpha + V_\infty y \sin\alpha + \iint_C \frac{q(s)}{2\pi} \ln(r) ds - \iint_C \frac{\gamma(s)}{2\pi} \theta ds.$$

Pentru a calcula potenţialul mişcării Φ se foloseşte o metodă de colocaţie: frontiera profilului C este aproximată cu o linie poligonală închisă $\bigcup_{j=1}^{N} E_j$, laturile E_j având vârfurile P_j şi P_{j+1} situate pe C.

Numerotarea vârfurilor începe de la bordul de fugă pe latura inferioară în direcţia bordului de atac, trecând în continuare pe latura superioară.

Se consideră că intensitatea vârtejurilor $\gamma(s)$ distribuite pe profilul C este constantă pe frontieră, având valoarea γ, iar intensitatea surselor $q(s)$ distribuite pe profil este constantă pe fiecare element de frontiera E_j, având valoarea $q_j, j = 1, \ldots, N$.

Cu aceste precizări, avem

$$\Phi = V_\infty x \cos\alpha + V_\infty y \sin\alpha + \sum_{j=1}^{N} \iint_{E_j} \left(\frac{q_j}{2\pi} \ln(r) - \frac{\gamma}{2\pi} \theta \right) ds, \tag{6}$$

Necunoscutele γ şi $q_j, j = 1, \ldots, N$ din relaţia (6), sunt determinate din condiţiile la limită şi condiţia Kutta. Se cere satisfacerea condiţiei la limită în punctele de colocaţie M_j, mijlocurile laturilor E_j.

Componentele vitezei în M_j se notează cu u_j şi v_j. Astfel, condiţia la limită ne furnizează N relaţii algebrice:

$$-u_i \sin\theta_i + v_i \cos\theta_i = 0, \quad i = 1,\ldots,N \tag{7}$$

folosite pentru a determina cele $N+1$ necunoscute..

Condiţia Kutta ne va furniza relaţia finală:

$$u_1 \cos\theta_1 + v_1 \sin\theta_1 = -u_N \cos\theta_N + v_N \sin\theta_N . \tag{8}$$

Componentele vitezei în punctul M_i sunt determinate de contribuţiile vitezelor induse de distribuţia surselor si vârtejurilor de pe fiecare element de frontieră E_j:

$$\begin{aligned} u_i &= V_\infty \cos\alpha + \sum_{j=1}^{N} q_j u_{ij}^s + \gamma \sum_{j=1}^{N} u_{ij}^v, \\ v_i &= V_\infty \sin\alpha + \sum_{j=1}^{N} q_j v_{ij}^s + \gamma \sum_{j=1}^{N} v_{ij}^v, \end{aligned} \tag{9}$$

unde $u_{ij}^s, v_{ij}^s, u_{ij}^v, v_{ij}^v$ sunt coeficienţii de influenţă.

Substituim (9) şi valorile coeficienţilor de influenţă în condiţiile la limită (7) şi condiţia Kutta (8) ca să primim un sistem linear de $N+1$ ecuaţii cu $N+1$ necunoscute: γ şi $q_j, j = 1,\ldots,N$, cu ajutorul cărora, putem calcula componentele tangenţiale ale vitezei $u_{\tau i}$ în punctele de colocaţie M_i (componenta normală a vitezei în punctele de colocaţie este nulă). Coeficientul local de presiune pe conturul discretizat al profilului se poate calcula cu relaţia

$$C_{p,i} = 1 - \left(\frac{u_{\tau i}}{V_\infty} \right)^2 , \tag{10}$$

iar forţele hidrodinamice, care acţionează pe E_j sunt date de relaţiile

$$f_{xj} = C_{p,j} \left(y_{j+1} - y_j \right) \quad \text{şi} \quad f_{yj} = C_{p,j} \left(x_{j+1} - x_j \right).$$

Momentele de tangaj în raport cu punctul de referinţă se calculează prin formulele

$$c_{m,j} = -f_{xj} \left(\frac{y_{j+1} - y_j}{2} \right) + f_{yj} \left(\frac{x_{j+1} - x_j}{2} - \frac{c}{4} \right).$$

Forţa totală este suma contribuţiilor fiecărui element de frontieră

$$F_x = \sum_{j=1}^{N} f_{xj}, \qquad F_y = \sum_{j=1}^{N} f_{yj},$$

iar coeficienţii de portanţă şi de moment se calculează după cum urmează:

$$C_L = -F_x \sin\alpha + F_y \cos\alpha, \quad C_M = \sum_{j=1}^{N} c_{m,j} . \tag{11}$$

Prima etapă a unei metode standard constă în calculul distribuţiei de viteze din mişcarea potenţială în jurul profilului.

Următoarea etapă o reprezintă calculul parametrilor stratului limită corespunzător distribuţiilor de viteze obţinute în prima etapă.

Etapa stratului limită, la rândul său, este divizată în doua subetape: stratul limită laminar şi stratul limită turbulent.

Stratul limită începe în punctul de stagnare (punctul de pe conturul profilului în care viteza este nulă, distribuţia de viteze fiind furnizată de etapa precedentă) şi urmează curentul de-a lungul suprafeţei exterioare sau inferioare în direcţia bordului de fugă. Imediat ce punctul de stagnare este determinat, începem numărătoarea vârfurilor în direcţia bordului de fugă.

Discretizarea profilului se efectuează considerând o partiţie uniformă a suprafeţei exterioare şi inferioare, respectiv.

Calculul parametrilor stratului limită laminar se va efectua utilizând modelul propus de Thwaites. Folosind ecuaţiile Navier-Stokes pentru un fluid incompresibil se derivă ecuaţiile Prandtl a mişcării în stratul limită laminar. Introducem grosimea de deplasare δ^*, grosimea pierderii de impuls θ şi grosimea pierderii de energie θ^* ca să obţinem ecuaţia integro-diferenţială a stratului limită Von Karman:

$$\frac{d\theta}{dx} + \frac{\theta}{V} \left(2 + \frac{\delta^*}{\theta} \right) \frac{dV}{dx} = \frac{1}{2} C_f , \tag{12}$$

unde C_f denotă coeficientul local al forţei de frecare pe suprafaţa profilului. Introducem parametrii de formă $H = \frac{\delta^*}{\theta}$ şi $H^* = \frac{\theta^*}{\theta}$. Din ecuaţia (12) se deduce sistemul de ecuaţii

$$\begin{aligned} &\frac{d\theta}{dx} + \frac{\theta}{V} (2 + H) \frac{dV}{dx} = \frac{1}{2} C_f , \\ &\theta \frac{dH^*}{dx} + \left(H^* (H - 1) \right) \frac{\theta}{V} \frac{dV}{dx} = 2C_d - H^* \frac{C_f}{2}, \end{aligned} \tag{13}$$

unde C_d este coeficientul de disipaţie.

Sistemul de ecuaţii (13) nu este suficient pentru determinarea tuturor necunoscutelor. Relaţiile suplimentare se bazează pe relaţiile semi-empirice Falkner-Skan. Considerînd aceste relaţii, sistemul (13) se rescrie sub forma

$$\begin{aligned} &\frac{V(x)}{2} \frac{d\omega}{dx} + (2 + H) \omega W(x) = f_1(H), \\ &\omega V(x) g(H) \frac{dH}{dx} + (1 - H) \omega W(x) = f_3(H). \end{aligned} \tag{14}$$

Valorile iniţiale sunt determinate astfel încât $\frac{dw}{dx}$ şi $\frac{dH}{dx}$ să ia valoarea 0. $H(0)$ şi $\omega(0)$ se calculează din relaţiile

$\frac{1 - H}{2 + H} = \frac{f_3(H)}{f_1(H)}$, cu rădăcina $H_0 \approx 2.24$ şi

$$\omega_0 = \frac{f_1(H_0)}{W(0)(2 + H_0)} .$$

Pentru rezolvarea sistemului de ecuaţii diferenţiale (14) utilizăm metoda Euler.

Trecerea de la pasul x_i la pasul x_{i+1} se efectuează prin liniarizarea funcțiilor f_1 și f_3 în jurul punctului H_i, iar $g = g_i$. Astfel, se obține un sistem din două ecuații biliniare cu necunoscutele $H = H_{i+1}$ și $\omega = \omega_{i+1}$, care poatet fi rezolvat exact. Aplicăm metoda fie până punctul de tranziție de la stratul limită laminar la stratul limită turbulent x_{tr} este prezis, fie până bordul de fugă A este atins. Tranziția de la curgerea laminară la cea turbulentă este localizată prin criteriul Michel: tranziția are loc atunci când $\mathrm{Re}_\theta > \mathrm{Re}_{\theta\max} = 1.174\left(1+\frac{22.4}{\mathrm{Re}_x}\right)\left(\mathrm{Re}_x\right)^{0.46}$,

unde $\mathrm{Re}_x = \mathrm{Re}\cdot V \cdot x$.

Pentru analiza stratului limită turbulent se vor folosi valorile medii şi fluctuațiile. Similar cu cazul stratului limită laminar se obțin ecuațiile integrale Von Karman.

Calculul parametrilor stratului limită turbulent se va efectua utilizând modelul propus de Head. Consideram volumul fluxului în stratul limită $Q(x)$.

Astfel, pentru grosimea de deplasare avem relația $\delta^* = \delta - \frac{Q}{V}$. Introducem viteza fluxului

$$E = \frac{dQ}{dx} = \frac{d}{dx}\left(V\left(\delta - \delta^*\right)\right) = \frac{d}{dx}\left(V\theta H_1\right),$$

unde $H_1 = \frac{\delta - \delta^*}{\theta}$. Head a presupus că viteza adimensionala E/V este funcție doar de H_1, iar H_1, la rândul său este funcție de H. Cebeci si Bradshaw au considerat relațiile

$$\frac{1}{V}\frac{d}{dx}\left(V\theta H_1\right) = 0.0306(H_1 - 3)^{-0.6169}, \qquad (15)$$

$$H_1 = \begin{cases} 3.3 + 0.8234(H-1.1)^{-1.287}, & H \le 1.6 \\ 3.3 + 1.5501(H-0.6778)^{-3.064}, & H > 1.6 \end{cases} \qquad (16)$$

A patra ecuație folosită pentru determinarea necunoscutelor θ, H, H_1 şi C_f este legea coeficientului local de frecare la perete Ludwieg-Tillman

$$C_f = 0.246\left(10^{-0.678H}\right)\mathrm{Re}_\theta^{-0.268}. \qquad (17)$$

Combinăm ecuația integrală Von Karman, relațiile (15-17) ca să obținem sistemul de ecuații diferențiale:

$$\frac{d}{dx}Y = h(Y,x), \qquad (18)$$

unde $Y = (\theta, H_1)$ şi

$$h(Y,x) = \begin{pmatrix} -\frac{\theta}{V}\left(2+H\right)\frac{dV}{dx} + \frac{1}{2}C_f \\ -H_1\left(\frac{1}{V}\frac{dV}{dx} + \frac{1}{\theta}\frac{d\theta}{dx}\right) + \frac{0.0306}{\theta}\left(H_1 - 3\right)^{-0.6169} \end{pmatrix}.$$

Valorile inițiale sunt valorile finale furnizate de sub-etapa stratului laminar. Integrarea numerica a sistemului (18) se efectuează cu o metoda Runge-Kutta de ordinul 2. Calculul se efectuează fie până este atins bordul de fugă, fie până are loc separarea stratului turbulent.

Pentru calculul coeficientului de rezistență C_D se utilizează formula Squire-Young.

Presupunem că sunt calculate următoarele mărimi: grosimea pierderii de impuls θ, parametrul de formă H şi viteza V în punctul corespunzător bordului de fugă A de pe suprafața superioară şi cea inferioară a conturului C.

Atunci, coeficientul de rezistență este dat de relația

$$C_D = \left(2\theta_A \cdot V_A^\lambda\right)_{C_{\sup}} + \left(2\theta_A \cdot V_A^\lambda\right)_{C_{\inf}}, \qquad (19)$$

unde $\lambda = \frac{H_A + 5}{2}$.

4. MOMENTUL DE TORSIUNE ŞI FORȚELE APLICATE LA ROTOR CU PALETE CU PROFIL HIDRODINAMIC

În cele ce urmează, vom calcula coeficienții hidrodinamici pentru un profil de referință, şi anume profilul NACA 0016 cu coarda $c = 1.3m$.

Aplicăm metodele de calcul descrise anterior pentru a calcula coeficienții corespunzători profilului NACA 0016 cu coarda de lungime $c_{ref} = 1m$: $C_{L,ref}, C_{M,ref}$ şi $C_{D,ref}$ furnizate de formulele (11) şi (19), respectiv.

Coeficienții corespunzători profilului cu coarda de lungime $1.3m$ se calculează din relațiile

$C_L = C_{L,ref}\cdot 1.3$, $C_M = C_{M,ref}\cdot(1.3)^2$ şi $C_D = C_{D,ref}\cdot 1.3$.

Figura 3 reprezintă modulul forței hidrodinamice $\vec{F}$ care acționează asupra unei palete, precum şi componentele sale tangențiale şi normale $F_{x'}, F_{y'}$ în funcție de unghiul de poziționare.

Figura 4 reprezintă momentul T_{ri} dezvoltat de o paletă în funcție de unghiul de poziționare calculat prin formula (4).

Figura 5 reprezintă momentul sumar $T_{r\Sigma}$ în funcție de unghiul de poziționare calculat prin formula (5).

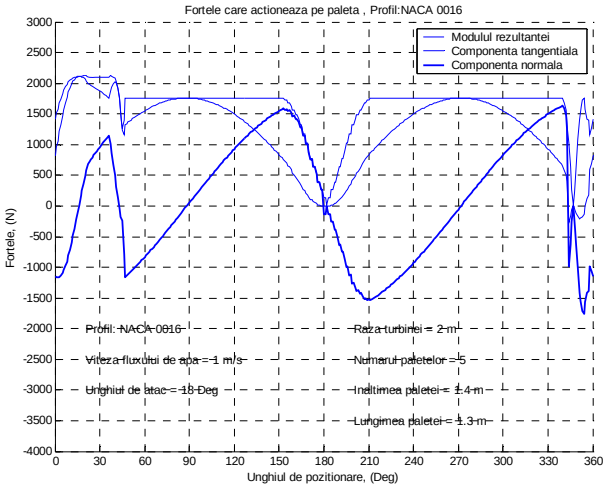

Figura 3. *Forțele care acționează pe paletă*

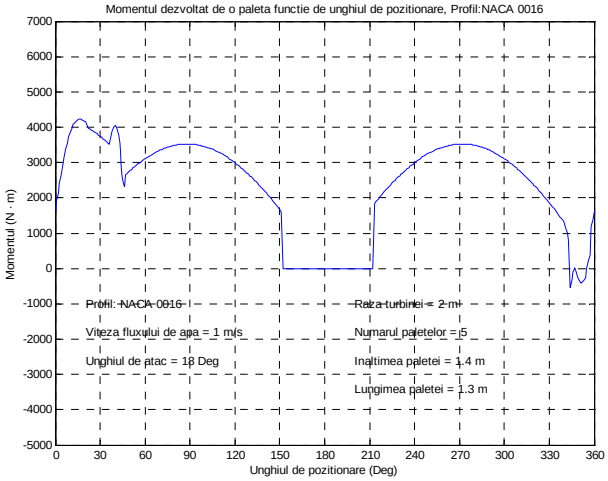

Figura 4. *Momentul dezvoltat de o paletă*

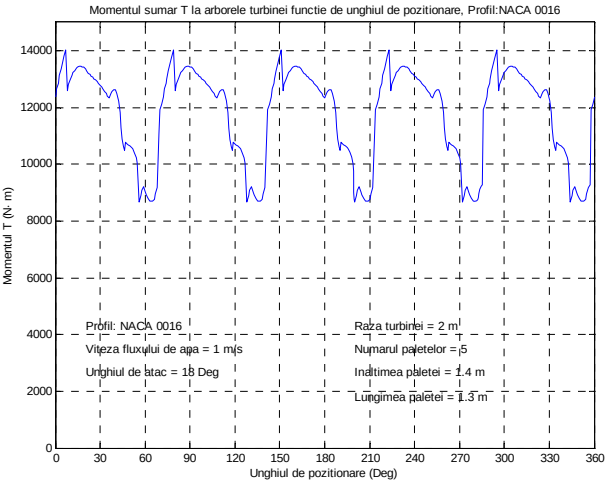

Figura 5. *Momentul sumar la arborele turbinei*

5. CONCLUZII

Folosirea energiei cinetice a râurilor cu ajutorul turbinelor de curenți de apă şi efectuarea de cercetări în domeniu au arătat avantajele acestora – instalare uşoară, operare smplă, costuri de întreținere convenabile.

Minihidrocentralele permit o conversiune eficientă a energiei cinetice a râurilor în energie mecanică şi electrică fără construcția barajelor.

Eficiența este asigurată de poziția optimă a paletelor cu profil hidrodinamic.

În prezent, stația pilot a minihidrocentralei se află la etapa de execuție şi va fi amplasată pe râul Prut lângă comuna Stoieneşti, raion Cantemir, Republica Moldova.

6. BIBLIOGRAFIE

[1] **Drela, M., Xfoil:** *An Analysis and Design System for Low Reynolds Number Aerodynamics*, Springer-Verlag, Lec.Notes in Eng. 54, 1989.

[2] **Katz, T., and Plotkin, A.,** *Low Speed Aerodynamics. Flow Wing Theory to Panel Methods*, Mac-Grow Hill, 1981.

[3] **Mason, W.H.,** *Boundary Layer Analysis methods*, Aerocal, 1981.

[4] **Moran, I.,** *An Introduction to Theoretical and Computational Aerodynamics*, John Wiley and Sons, 1984.

Quick Info

World's 'largest renewable energy city'

A farm of underwater tidally-driven turbines in New York's East River could make the city the world's largest in the renewable energy stakes.

The first set of tidal turbines has been deployed in the Roosevelt Island Tidal Energy (RITE) Project and is under test. The three-bladed units can each generate from 16kW to 32kW of electricity.

The farm will eventually have a capacity of 10MW but the total project, comprising four sites, will have a potential capacity of nearly 40MW. Once developed, it would make New York the world's largest renewable energy city.

The project is led by Verdant Power, which is also conducting a survey of a second tidal energy site in the Buttermilk Channel of the East River, alongside Governor's Island - an area known as New York City's Golden Triangle.

Verdant Power was formed in March 2000 and says it is constantly in a global search for additional locations in areas that need sustainable power generation. It is in the process of examining sites in South America, China, India, and others.

The company says the size of the world kinetic hydropower market is over 250,000MW and the US share is 12,500MW. It quotes the Electric Power Research Institute (EPRI) as believing that free-flow, or kinetic, hydropower systems could be the key answer to distributed generation - putting generation close to consumption.

Verdant Power says by starting its first US project in New York City, conceivably the toughest US regulatory environment, the Company has become the industry's trail blazer in changing the regulatory process and setting its standards.

Verdant Power
(http://www.engineerlive.com/power-engineer/engines-and-turbines)

Tension monitoring fasteners for turbines

Suzlon Energy is now fitting James Walker RotaBolts on all its 1.25 megawatt and 2.1 megawatt wind turbines. The tension monitoring fasteners have now become standard fit on the wind turbine blade connections.

Highly accurate tension at installation and throughout the life of the bolted joint is essential on the turbines, and Germanischer Lloyd certification requires that the turbine blade connections are checked annually. With tension control being the critical factor in the reliability and safety of bolted joints, RotaBolt's ability to deliver tension control at installation and throughout the life of the bolted joint, made it a natural choice.

Suzlon has a subsidiary in Germany for technology development, a research and development facility in the Netherlands for rotor blade design, moulding and tooling, as well as wind turbine and rotor blade manufacturing facilities in India. Subsidiary AE-Rotor in the Netherlands was responsible for the application of RotaBolt systems on the turbine blades.

For more information, visit www.rotabolt.co.uk

Wireless connects servo motors to Ethernet

JVL is introducing a new wireless LAN module for connecting its MAC integrated ac servo motors to an Ethernet network, thereby providing access to set-up and control the motor from anywhere on the network.

Moreover, with appropriate IT-infrastructure, it is possible to access the motors via the internet using fixed IP addresses or via a VPN.

This new module provides completely new opportunities for remote control, monitoring and diagnosis, enabling the motors to be used in distant locations where service would otherwise require considerable transport. For shorter distances or local use, the WLAN module means that cabling can be avoided. Software can be used to connect a PC to the motor as if it were connected via a serial RS-232 cable.

The WLAN module is also useful for applications where the motor is mounted on a moving sub-assembly and is powered via a slip-ring. Another typical application is where control signals are supplied from a handheld, battery-operated unit. It is possible to use a wide range of the most recent encryption standards.

Like the well-known JVL RxP nano-PLC module, the MAC00-EW4 WLAN module is programmable so that small PLC programs can be executed directly in the motor. JVL's Mactalk software with graphical interface (for setting parameters and programming) is identical to that used for the RxP-module, and programs can be directly transferred between the RxP, Bluetooth and WLAN modules, taking the use of I/O signals into account.

Connection of the supply and signals is done via three robust M12 connectors. The Module has a standard antenna connector for connection of the supplied antenna or another antenna of choice.

MAC integrated ac servo motors
(http://staging.engineerlive.com/european-design-engineer)

SOLUȚII CONSTRUCTIVE PENTRU UN TIP DE POMPĂ VOLUMICĂ ROTATIVĂ

Marinescu Adrian, Băran Nicolae

Universitatea POLITEHNICA din Bucureşti, madriandan@yahoo.com

REZUMAT: *Lucrarea prezintă două soluții contructive ale unei maşini de lucru rotative cu două rotoare profilate, care este utilizată pentru vehicularea fluidelor; se stabilesc principalele dimensiuni geometrice ale maşinii şi parametrii de lucru în vederea uitlizării ei ca pompă volumică rotativă.*

ABSTRACT: *The work is introducing two constructive solutions for a two-profiled / figured rotors pivoting machinery used for fluids handling; the main geometrical sizes and the working parameters of the machine are set forth in order to use it as pivoting displacement pump.*

CUVINTE CHEIE: rotor profilat, pompă volumică rotativă

KEYWORDS: profiled/figured rotors, pivoting displacement pump

1. INTRODUCERE. PREZENTAREA SOLUȚIILOR CONSTRUCTIVE

Soluția constructivă prezentată în lucrare se referă la o maşina de lucru care poate fi utilizată ca: pompă, ventilator sau compresor.

Lucrarea prezintă numai varianta în care maşina de lucru este utilizată ca pompă.

În funcție de natura fluidului vehiculat se disting două variante constructive pentru pompa cu rotoare profilate:

I. Dacă pompa vehiculează ape reziduale, fluide polifazice (apă + cenuşe, apă + nisip), fluide reologice, se va adopta soluția constructivă din figura 1; roțile dințate (7), care asigură rotirea sincronă a celor două rotoare, se află în exteriorul pompei, aceasta deorece există pericolul deteriorării acestora.
Ungerea angrenajului este asigurată prin uleiul existent în partea inferioară a cutiei (5).
Maşina de lucru, indiferent de variantă, este compusă în principal din pompa (2) antrenată de un motor electric (1) prin intermediul unui cuplaj (3), montate pe placa (4) (figura 2).

Funcționarea maşinii de lucru, în varianta I, este următoarea: arborele conducător al pompei (figura 1), solidar cu roata dințată şi rotorul profilat cu ajutorul penelor, este antrenat în mişcare de rotație de către un motor electric prin intermediul unui cuplaj.

Arborele condus, primeşte mişcarea de rotație de la o roată dințată care angrenează cu cea de pe arborele conducător.

Fluidul care pătrunde în camera de aspirație este preluat de rotoarele profilate şi trasportat printr-o mişcare de rotație către camera de refulare; fiecare rotor profilat are două pistoane rotative de formă triunghiulară care transportă fluidul de la aspirație către refulare.

II. Dacă pompa vehiculează produse petroliere, roțile dințate (7) se pot monta în interiorul carcasei pompei (figura 3).
Avantajul acestei soluții este că ungerea roților dințate este asigurată de produsele vehiculate, iar construcția pompei este mai compactă.

Ansamblu constituit din pompa volumică (varianta II) şi motorul electric de antrenare se poate observa în figura 4.

În varianta a II-a, funcționarea este similară, cu observația că roțile dințate sunt în interiorul carcasei şi solidare cu rotoarele profilate.

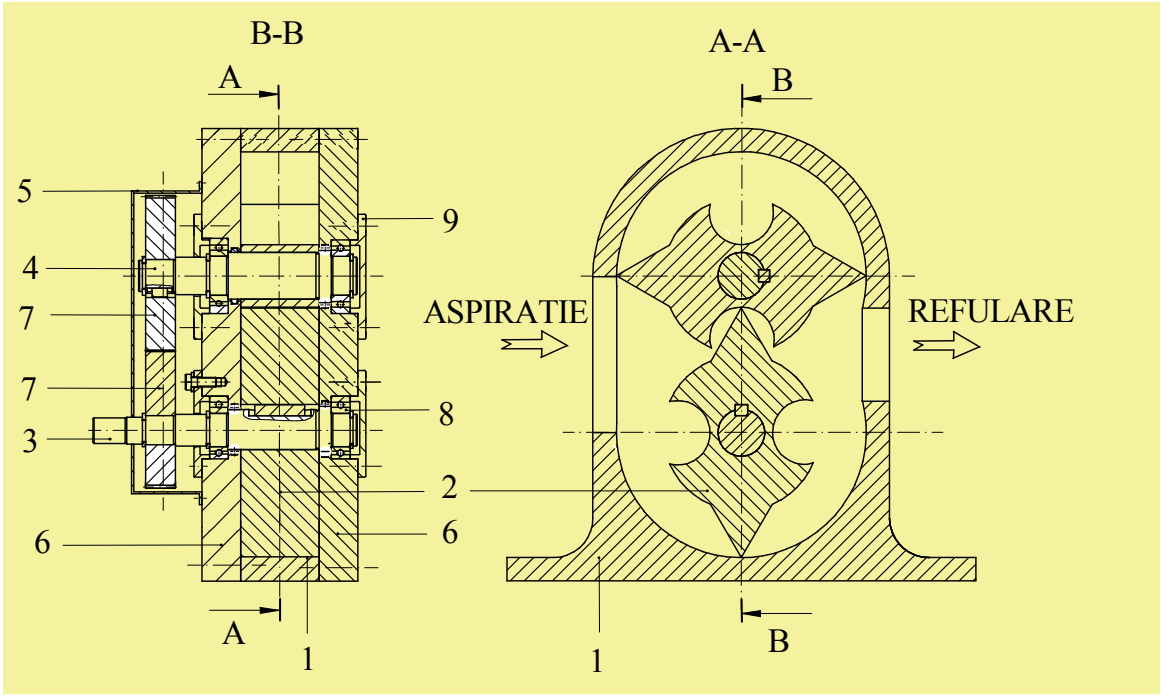

Figura 1. *Pompă volumică rotativă cu rotoare profilate şi roţile dinţate în exteriorul carcasei (varianta I)*
1 – carcasa ovală; 2 – rotor profilat; 3 – arbore conducător; 4 – arbore condus; 5 – cutie cu ulei; 6 – perete lateral; 7 – roată dinţată; 8 – rulment; 9 – capac rulment.

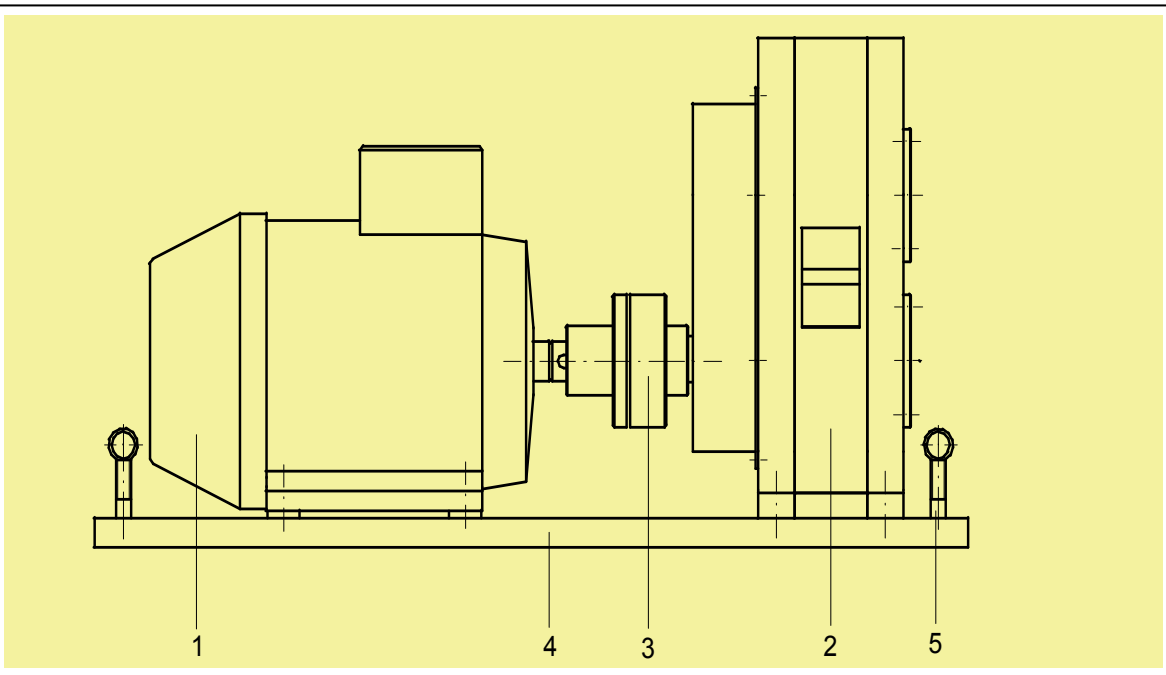

Figura 2. *Ansamblu pompă+motor electric(varianta I)*
1 – motor electric; 2 – pompa volumică rotativă; 3 – cuplaj elastic; 4 – placa suport; 5 – inel de ridicare.

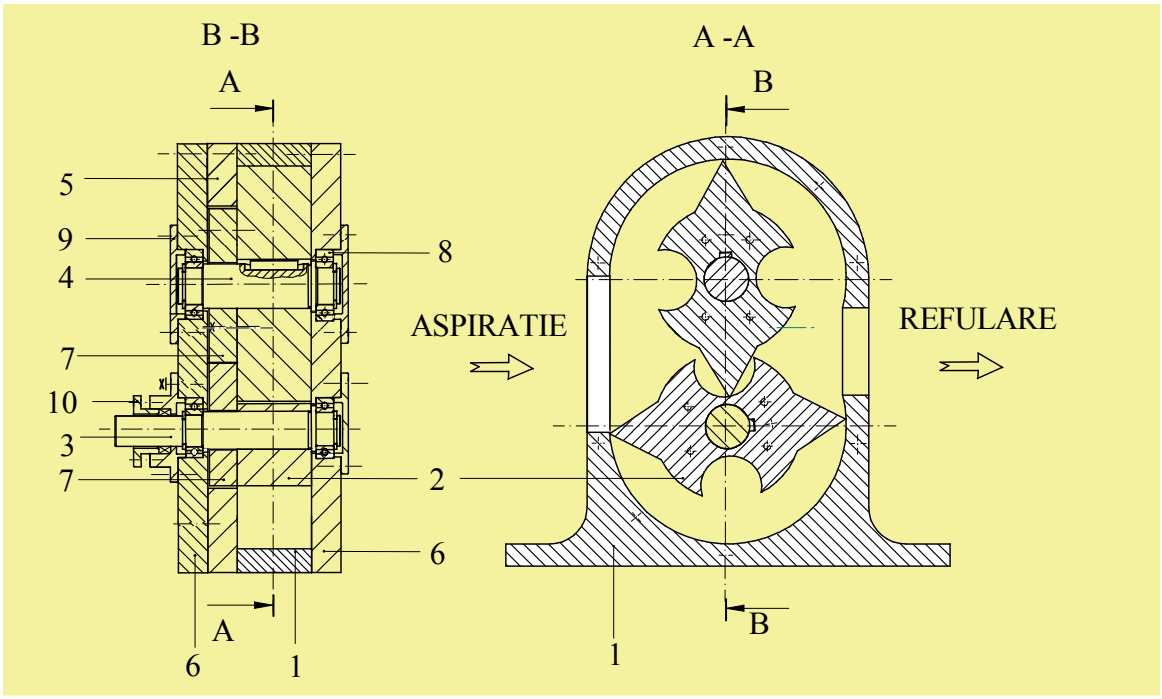

Figura 3. *Pompă volumică rotativă cu rotoare profilate şi roţile dinţate în interiorul carcasei (varianda II)*
1 – carcasa ovală; 2 – rotor profilat; 3 – arbore conducător; 4 – arbore condus; 5 – perete intermediar; 6 – perete lateral; 7 – roată dinţată; 8 – rulment; 9 – capac rulment; 10 – presgarnitură.

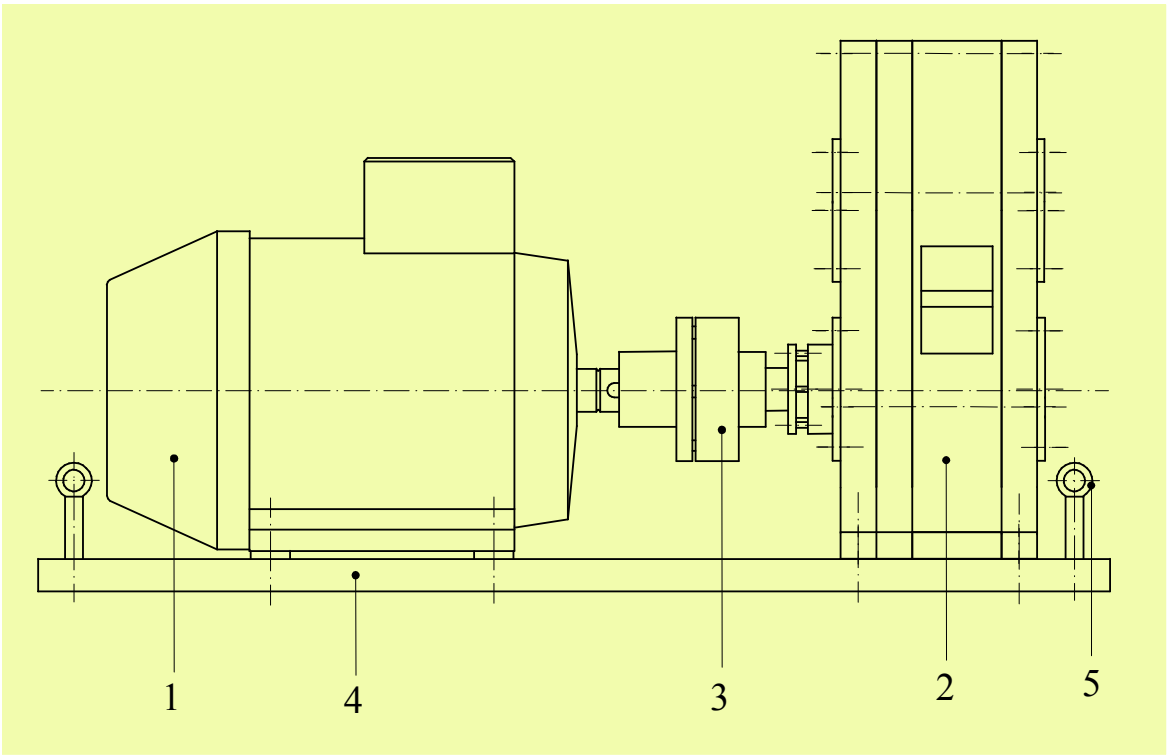

Figura 4. *Ansamblu pompă+motor electric(varianta II)*
1 – motor electric; 2 – pompa volumică rotativă; 3 – cuplaj elastic; 4 – placa suport; 5 – inel de ridicare.

2. ELEMENTE DE CALCUL PRIVIND DIMENSIONAREA MAŞINII ROTATIVE

În lucrările [1]]i, [2] au fost stabilite relaţiile de calcul a debitului volumic ($\dot{V}$) şi a puterii teoretice de antrenare (P) a maşinii de lucru:

$$\dot{V} = \pi \cdot l \cdot z \cdot \left(z + 2 \cdot R_r\right) \cdot \frac{n}{30} \qquad [m^3/s] \qquad (1)$$

$$P = \dot{V} \cdot \Delta p = \dot{V} \cdot \rho_{H_2O} \cdot g \cdot \Delta h \qquad [W] \qquad (2)$$

unde: *l* este lungimea rotorului [m];

z – înălţimea pistonului rotativ [m];

R_r – raza rotorului [m];

n – turaţia maşinii [rot/min];

Δp – creşterea de presiune între aspiraţie şi refulare [N/m^2];

ρ_{H_2O} – densitatea apei[Kg/m^3];

g – acceleraţia gravitaţională [m/s^2];

Δh – creşterea de presiune între aspiraţie şi refulare [m H_2O].

Din relaţia (1) se observă că debitul volumic depinde liniar de parametrii geometrici *l* şi R_r şi de parametrul funcţional n; în funcţie de z, debitul este o funcţie de gradul doi, $\dot{V} = f(z^2)$.

Pentru calculul debitului volumic şi a puterii de antrenare s-a elaborat un program de calcul în care ca date iniţiale s-au considerat mărimi variabile ***l***, R_r, z, iar turaţia n şi creşterea de presiune au fost menţinute constante; datele rezultate din calcul sunt prezentate în tabelul 1.

Nr. varianta	*l* [m]	R_r [m]	z [m]	R_c [m]	n [rot/min]	V [m^3/s]	Δp [N/m^2]	P [W]
1	0,05	0,05	0,03	0,08	750	0,015315264	100000	1531,526417
2	0,05	0,06	0,036	0,096	750	0,022053980	100000	2205,398040
3	0,05	0,07	0,042	0,112	750	0,030017918	100000	3001,791777
4	0,05	0,08	0,048	0,128	750	0,039207076	100000	3920,707627
5	0,05	0,09	0,054	0,144	750	0,049621456	100000	4962,145591
6	0,05	0,10	0,06	0,160	750	0,061261057	100000	6126,105668
7	0,05	0,11	0,066	0,176	750	0,074125879	100000	7412,587858
8	0,05	0,12	0,072	0,192	750	0,088215922	100000	8821,592161
9	0,05	0,13	0,078	0,208	750	0,103531186	100000	10353,11858
10	0,05	0,14	0,084	0,224	750	0,120071671	100000	12007,16711
11	0,05	0,15	0,090	0,240	750	0,137837378	100000	13783,73775
12	0,10	0,05	0,030	0,080	750	0,030630528	100000	3063,052834
13	0,10	0,06	0,036	0,096	750	0,044107961	100000	4410,796081
14	0,10	0,07	0,042	0,112	750	0,060035836	100000	6003,583554
15	0,10	0,08	0,048	0,128	750	0,078414153	100000	7841,415254
16	0,10	0,09	0,054	0,144	750	0,099242912	100000	9924,291181
17	0,10	0,10	0,060	0,160	750	0,122522113	100000	12252,21134

Tabelul 1. *Valorile debitului volumic ($\dot{V}$) şi a puterii teoretice de antrenare (P) a pompei volumice în funcţie de elementele constructive (l, R_r, z) şi funcţionale (n, Δp)*

Pe baza datelor din tabelul 1, a fost reprezentată grafic funcţia: ($\dot{V}$) = f(z) pentru diferite valori ale razei rotorului, menţinându-se constant raportul $\frac{z}{R_r} = 0{,}6$ (figura 5).

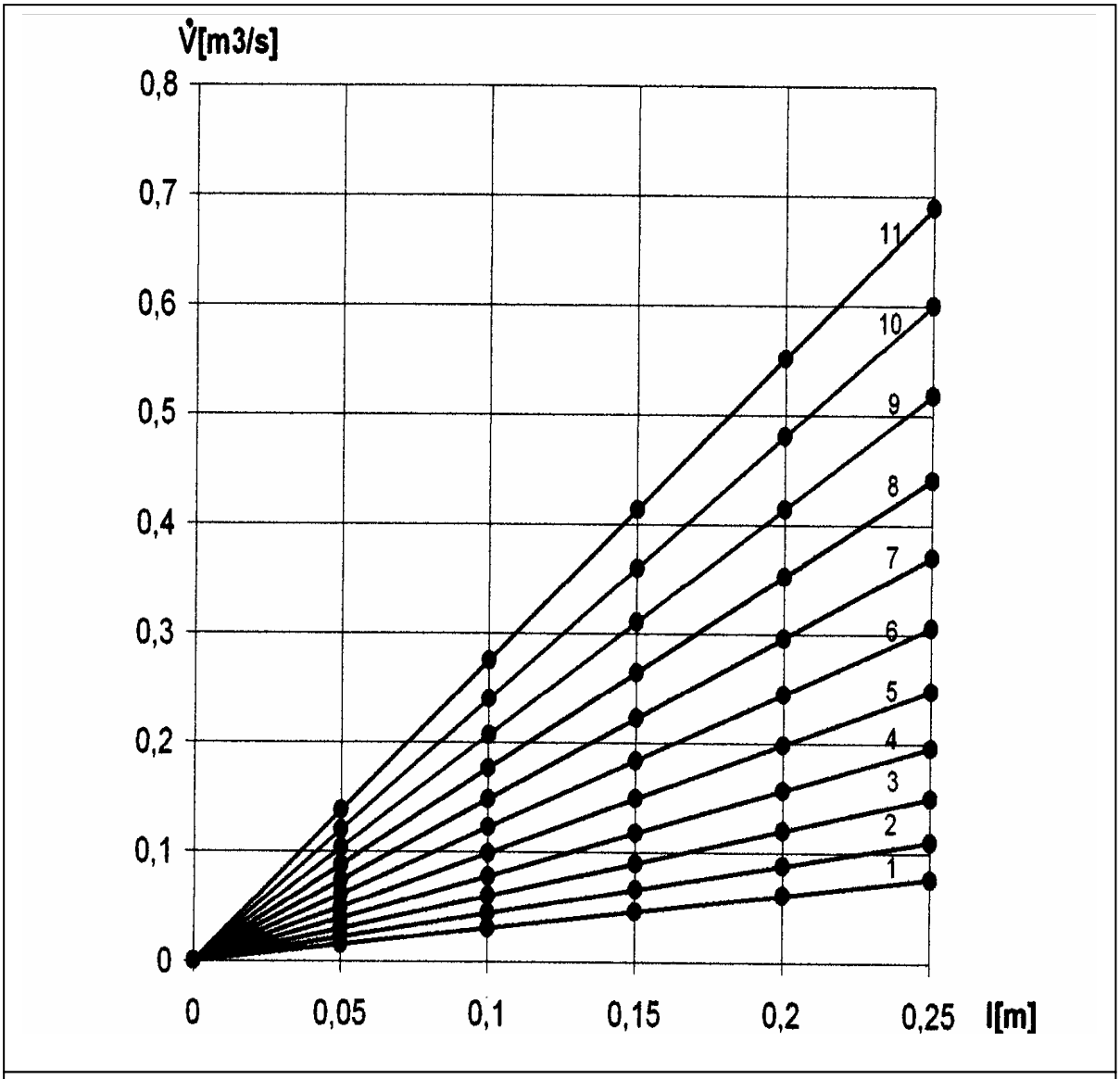

Figura 5. *Variația debitului volumic în funcție de lungimea rotorului*
1 – R_r= 0,05m; z = 0,03m; 2 – R_r= 0,06m; z = 0,036m; 3 – R_r= 0,07m; z = 0,042m;
4 – R_r= 0,08m; z = 0,048m;5 – R_r= 0,09m; z = 0,054m; 6 – R_r= 0,10m; z = 0,06m;
7 – R_r= 0,11m; z = 0,066m; 8 – R_r= 0,12m; z = 0,072m;9 – R_r= 0,13m; z = 0,078m;
10 – R_r= 0,14m; z = 0,084m; 11 – R_r= 0,15m; z = 0,09m;

Au fost reprezentate grafic numai primele 11 variante, deoarece dimensiunile rotorului vor fi din ce în ce mai mari, soluția soluția constructivă va fi, deasemeni, mare şi nu mai prezintă interes, costurile fiind prea mari.

Pentru construcția prototipului maşinii de lucru, care va lucra ca pompă volumică rotativă, a fost aleasă varianta 1 (v. fig. 4): R_r = 0,05m; z = 0,03m; R_c = 0,08m.

Pentru n = 750 rot/min şi $\Delta p = 10^5$ N/m^2 , rezultă $(\dot{V})$ = 0,0153 m^3/s şi P = 1534 W; deoarece pompa va vehicula produse petroliere, roțile dințate vor fi montate în interiorul carcasei maşinii.

4. CONCLUZII

Proiectarea elementelor constructive ale maşinii de lucru, generarea programului de comandă numerică pentru fabricarea pieselor componente şi controlul asistat de computer, prezintă avantajul integrării cu calculatorul a activităților de concepție, fabricație şi control, precum şi obținerea unor precizii ridicate a pieselor componente.

Avantajele acestui tip de maşină de lucru față de alte soluții contructive, sunt prezentate în lucrarea de specialitate [5].

În urma încercărilor efectuate în cadrul laboratoarelor din U.P.B., s-a constatat că soluția propusă este viabilă, prezintă fiabilitate în exploatare şi are performanțe deosebite care conduc către implementarea ei în următoarele domenii:
- vehicularea produselor petroliere;
- vehicularea apelor uzate:
- vehicularea fluidelor reologice:
- vehicularea mediilor polifazice (apă + cenuşă, apă + nisip, petrol + apă sau abur etc.).

BIBLIOGRAFIE

[1]. **Băran, N.,** *Maşini termice rotative – Maşini de lucru, Maşini de forță* – Editura MATRIXROM, Bucurşti, 2001.
[2]. **Băran, N**, *Maşini termice rotative de lucru – Maşini cu rotoare profilate. Maşini cu palete*, Editura MATRIXROM, Bucurşti, 2003.
[3]. **Băran, N., Besnea, D., Duminică, D.,** *Research etablishing the outline of the rotor profile for a new volumetric rotating pump*, Mecatronica nr. 4, 2004, pag. 24 – 27.
[4]. **Băran, N., Besnea, D.**, *Tehnologia de execuție pentru un rotor profilat*, Lucrările Simpozionului: Relansarea şi creşterea competitivității sectoarelor economice din industria prelucrătoare, 23 – 24 septembrie, 2004, pag. 40 – 45.
[5]. **Băran, N., Băran, Gh**., *Studiu comparativ între compresorul Roots şi un nou tip de compresor*, Revista de chimie, Vol 54, 2003, pag. 319.

Quick Info

Pumps can also be used as a motor, drive unit or key element in a variable speed drive

The QX system from Bucher Hydraulics can be used not just as quiet internal gear pumps, but also as powerful motors, high-accuracy flow dividers or as very reliable pumps for low-viscosity fluids.

A QX unit can also be used as a pump in one specified direction and as a motor in the opposite direction (known as two-quadrant mode), as a universal drive unit that can switch between pump and motor function and operate in any direction (four-quadrant mode), or as a key element in a variable-speed drive.

Their straightforward and robust construction makes these units the pumps of choice where quiet running, low pulsation levels and high operational reliability are required.

All six frame sizes are designed for pressure ranges of 100, 160, 210 and 320bar, and for peak pressures up to 400bar. The geometric displacements extend from 5 to 500cm3/rev and their close and systematic spacing gives a range of 72 single pumps and 1764 double pumps. Including triple and quadruple versions, more than 10000 pump combinations are possible.

The principal components of QX internal gear pumps are pinion and internal gear ring, housing, and shaft. There are only three moving parts in each pressure stage, which results in low wear and long service life. The standard components of single pumps can be combined into double and triple pumps with the help of intermediate flanges. Thanks to the special design features of these internal gear pumps, the axial or radial clearances do not require any hydrostatic compensation.

The cutting-edge design delivers its full potential when operating with low-viscosity fluids. Even with viscosities lower than 1mm2/s (cSt), continuous pressures as high as 250bar can be achieved by connecting up to five pump stages in series. QXV pumps are used with diesel fuel, gasoline/ petrol, aviation jet fuel, brake fluids, Pentosin, HFC and HFA hydraulic media, and many other fluids.

The symmetrical design of the QX internal gear pump means that, with only minor modifications, it can be transformed into a drive unit that can be used in two-quadrant or four-quadrant mode. This unit offers numerous possibilities for application in both open- and closed-loop circuits. A current trend, and one that is particularly noticeable in injection moulding machine design, is the growing use of frequency-controlled drives, an application to which QXM internal gear drive units are also ideally suited.

Naturally, QXM units can also be used simply as motors. The special gear tooth geometry creates particularly good inlet behaviour, and motor speeds of more than 10000rpm are attainable.

Bucher Hydraulics GmbH is based in Klettgau, Germany. www.bucherhydraulics.com

EXPERIMENTAL RESEARCH ON MEASURING CUTTING TEMPERATURE AT DEEP HOLES MACHINING

Constantin Minciu[*], *Ioan Tănase*[*], *Sorin Mihai Croitoru**, *Mihai Bălan*[**]

* POLITEHNICA University of Bucharest, minciu@imst.msp.pub.ro
** Romanian Ministry of Internal Affaires

ABSTRACT
For Romanian drills there are few studies and researches regarding the cutting temperature at deep holes machining. In this paperwork the measuring stand, obtained results and their interpretation will be presented. All these aspects are interesting because the cutting temperature influences directly the drill's wear, its durability and the shape of the detached chips.

KEYWORDS: Cutting temperature, Deep hole machining, Experimental stand

1. EXPERIMENTAL STAND

The experimental research was done on SN 400 normal lathe, the drill being fixed into the mobile tail spindle.

In principle, the measurement of the cutting temperature was made using the natural thermocouple method.

The experimental stand for measurement of the temperature is presented in Figure 1.

In Figure 1 the following elements are presented:

1 – deep holes drill;
2 – work piece;
3- insulators;
4 – lathe's holding device;
5 –spindle;
6 – wire conductor for work piece;
7 – insulating plug;
8 – screw of rotary contact;
9 – mercury rotary contact;
10 – fixed wire conductor of the work piece;
11 – electronic mili-voltmeter;
12 – digital multi meter;
13 – wire conductor of the drill;
14 – drill holder contact.

In this case of temperature measurement the problem of insulation of work piece and drill is the most important to be solved.

As Figure 1 shows, the work piece fixed in the lathe's holder and the drill fixed in the mobile tail spindle are insulated from the lathe by use of textolit sheets.

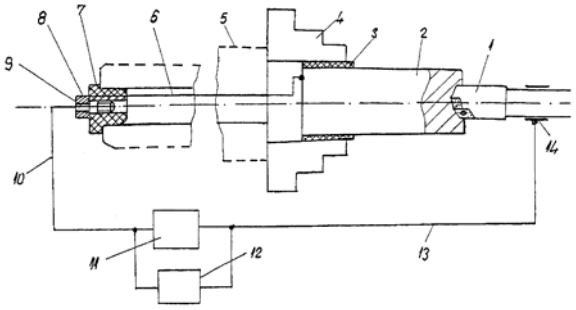

Figure 1. *Experimental stand for measurement of the cutting temperature*

Another problem is the caption of thermo-electric micro currents, because of the rotational movement of the work piece.

This is solved by use of a rotary contact with mercury (see position 9 in Figure 1).

Thermo-electric current between the drill (hot point) and the work piece (cold point) can follow the electric circuit because of the rotary contact with mercury. This rotary contact, in original construction, was assembled at the end of the lathe's spindle.

Reading the electric voltage of thermo-electric currents was made by means of two devices: an electronic mili-voltmeter and a digital multi meter.

The experimental research on the cutting temperature was made using CARMESIN-BOTEK deep holes drills with dismountable inserts. The drills have the diameters d_A=46 mm and d_B=32 mm.

In order to be fixed into the mobile tail spindle a tool holder was made for each drill. In these tool holders the active drilling heads were threaded.

The tool holders end with a conical Morse 2 tail, corresponding to the conical hole of the mobile tail spindle of the lathe.

In the body of each tool holder (see Figure 2) an oval hole was made in order to evacuate the chips during the drilling process.

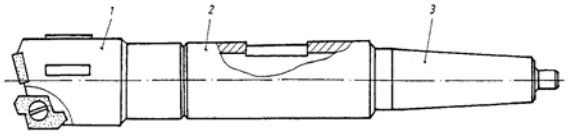

Figure 2. *Drill's supporting system*

It should be underlined the experimental research was done on cylindrical work pieces, made of Romanian carbon steel OLC 45, having the hardness 220 HB in average.

As well, it should be underlined that the deep holes machining was done without coolant.

For any measurement stand, the first problem to solve is the regulation.

In this case, to regulate the thermo-electric currents measurements stand the following principle scheme was used (see Figure 3).

This stand consists of:

1 – deep holes drill;
2 – work piece;
3 – mica-insulating layer;
4 – electric resistor to heat the work piece;
5 – textolit insulating layer;
6 – work piece holder of the lathe;
7 – main spindle;
8 – work piece electric conductor;
9 – screw of the rotary contact;
10 – rotary contact with mercury;
11 – work piece fix electric conductor;
12 – electronic mili-voltmeter;
13 – digital multi meter;
14 – Cromel-Alumel thermocouple;
15 – regulating electric current source.

Natural thermocouple tool-work piece was regulated in conditions that were similar to those during the deep holes machining.

A bar having the diameter of 12 mm, made of work piece material (*OLC 45*) was heated by means of an electric conductor and a regulating electric current source (see Figure 3).

Temperature of hot end of the work piece bar was measured by means of a Cromel-Alumel thermocouple and an electronic mili-voltmeter.

The measurements were conducted in two ways:

a) The work piece bar was heated to 200˚C, this value being considered as minimum cutting temperature. Then the electric contact between the drill's metal carbide edge and hot end of the work piece bar was done. The voltages of both mili-voltmeters corresponding to Cromel-Alumel thermocouple and natural thermocouple tool-work piece were registered. The natural thermocouple tool-work piece was opened and the work piece bar was heated incrementally up to 800˚C. After each step the mentioned voltages were registered.

b) The work piece bar was heated to 800˚C, this value being considered as maximum cutting temperature. Then the electric contact between the drill's metal carbide edge and hot end of the work piece bar was done.

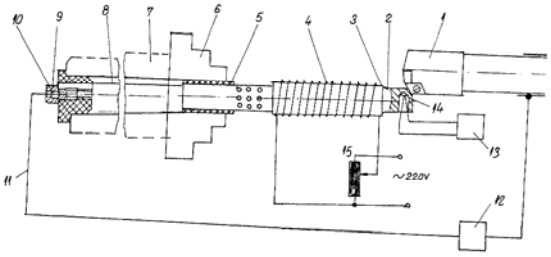

Figure 3. *Stand regulation principle scheme*

The voltages of both mili-voltmeters corresponding to Cromel-Alumel thermocouple and natural thermocouple tool-work piece were registered. The natural thermocouple tool-work piece was opened and the work piece bar was unheated incrementally under 200˚C. After each step the mentioned voltages were registered.

The voltage generated by the natural thermocouple tool-work piece was measured by means of an analogical electronic mili-voltmeter (Figure 1). The measured values were considered to be equal to the effective values of the voltage (RMS). The same voltage was measured simultaneously with a digital mili-voltmeter, the maximum value during the experiment being registered. These voltage values and corresponding temperatures are marked with (*).

The experiments were conducted for drills having the diameters d_A=46 mm and d_B=32 mm.

Based on the measurements done for the regulation of the stand, considering the correspondence between the temperature and the voltage, the formula to transform the voltage into temperature was calculated. The formula is valid for the case the drill has inserts of P20 sort of metal carbides and the work piece is made of OLC 45 carbon steel.

$$\Theta = 89{,}27 \cdot U_{tm} + 20° \, [°\mathrm{C}] \qquad (1)$$

2. EXPERIMENTAL RESULTS

The measurements results are presented in tables 1 and 2. These results will show the influence of the cutting regime parameters on the cutting temperature.

With the data in tables 1 and 2 some graphics were done to show the influence of the cutting speed and feed on the cutting temperature.

Even if in practice these data have small applicability, based on tables 1 and 2 the exponential function of cutting temperature during deep holes machining were determined (Table 3).

Table 1. *Experimental results, case d_A=46 mm*

s [mm/rot]	v [m/min]	Θ [ºC]
0,06	33,23	288
	44	448
	55	448
0,1	33,23	332
	44	448
	55	484
0,16	33,23	431
	44	495
	55	511
0,2	33,23	440
	44	502
	55	538

Table 2. *Experimental results, case d_B=32 mm*

s [mm/rot]	v [m/min]	Θ [ºC]
0,06	30,67	341
	38,2	359
	46,25	395
0,1	30,67	359
	38,2	359
	46,25	448
0,16	30,67	332
	38,2	359
	46,25	468
0,2	30,67	305
	38,2	395
	46,25	484

Table 3. *Exponential function of cutting temperature*

a) d_A=46 mm, tool P20, work piece material OLC 45	
v=33,23 m/min	$\Theta=773\cdot s^{0,35}$
v=44 m/min	$\Theta=590\cdot s^{0,1}$
v=55 m/min	$\Theta=685\cdot s^{0,15}$
s=0,06 mm/rev	$\Theta=13,17\cdot v^{0,88}$
s=0,1 mm/rev	$\Theta=24\cdot v^{0,75}$
s=0,16 mm/rev	$\Theta=131\cdot v^{0,34}$
s=0,2 mm/rev	$\Theta=92,3\cdot v^{0,44}$
a) d_B=32 mm, tool P20, work piece material OLC 45	
v=30,67 m/min	-
v=38,3 m/min	$\Theta=450\cdot s^{0,08}$
v=46,25 m/min	$\Theta=636\cdot s^{0,17}$
s=0,06 mm/rev	$\Theta=100\cdot v^{0,36}$
s=0,1 mm/rev	$\Theta=56,5\cdot v^{0,54}$
s=0,16 mm/rev	$\Theta=20\cdot v^{0,82}$
s=0,2 mm/rev	-

3. CONCLUSIONS

Based on the experimental results the following concluding remarks are underlined:

- for the chosen cutting regime parameters the temperature varied between 300ºC … 600ºC
- cutting temperature rises significantly with the rise of the feed, but even more with the rise of the cutting speed;
- the cutting temperature rises approximately linearly, both with the rise of the cutting speed and feed;
- experimental research on the cutting temperature is justified by the fact that it is one of the most important factor to influence the durability and wear of the cutting tools. The variation laws of the cutting temperature are the same with the variation laws of the cutting tools durability.

As expected, the cutting temperature is more influenced by the cutting speed than the feed.
This is shown by the values of the exponents in the exponential functions of the cutting temperature in Table 3.
For example, in case of the drill having its diameter d_A=46 mm, the exponent of the cutting speed varies between 0,88 … 0,44 and the exponent of feed varies between 0,35 … 0,15.

Consequently, from the point of view of the cutting temperature and also the tool's durability, it should be better to increase productivity by increasing the feed (extensive cutting regimes) than by increasing the cutting speed (intensive cutting regimes).

Still, great feeds should be carefully used because of some aspects, as following.

Firstly, great feeds mean great cutting forces, because for the same productivity the increase of the cutting forces with the increase of feed is ,uch greater than the increase of the cutting forces with the increase of cutting speed.
In some cases, the increase of the cutting speed leads to the decrease of the cutting forces.

Secondly, the increase of the feed leads to the decrease of the machine surface quality.

Thirdly, the chip formation and detachment should be considered. Starting with a specific value of the feed, the danger of articulated chip instead of fragmented chips could appear. This will block the chip evacuation channels of the tool.

In case of CARMESIN-BOTEK drills, was observed that in the central zone, of the triangular insert, because of the large width of the chip there is a risk these chips will block the evacuation channel of the deep holes drill.

REFERENCES

[1]. **Brîndaşu, D. P., Cernuşca, D.**, *„Burghie pentru găuri adânci. Indrumar de proiectare."* Univ. "Lucian Blaga", Sibiu, 1993
[2]. **Constantinescu C.,** *„Cercetări privind optimizarea constructivă şi geometrică a burghielor pentru prelucrarea alezajelor lungi"* PhD Thesis, Technical University"Gh. Asachi", Iaşi, 1993
[3]. **Cozmîncă M., Constantinescu C.,** *„On the Geometry of Deep-Hole Drills"*, Bul. I.P.Iaşi, tom XXIX, 1983.
[4]. **Cozmîncă M., Constantinescu C, Romanescu I.,** *„Cercetări privind forţele de frecare la prelucrarea prin aschiere a găurilor adânci"*, 1986, Sesiunea de tribologie I.P.Iaşi.
[5]. **Elekes C.,** *„Scule pentru găurirea alezajelor lungi"*, Ed. Scrisul Românesc, Craiova, 1985.
[6]. **Greuner, B.** *„Beitrag zur Frage der Krafte an Schneide und Fuhrungsleistern an einschneidigen hartmetallbestuckten Tiefbohrwerkzeugen"*. Dissertation TU Hannover, 1970
[7]. **Greuner B.,** *„Tiefbohren aus der Sicht einer versuchs und Entwicklung sabteilung"*, TZ Metallbearbeit, no 8, 1984.
[8]. **Minciu, C., Aurite, T., David, A.** *„Determinarea analitică a sistemului de forţe la prelucrarea găurilor lungi",* Buletinul IPB, Bucureşti, tom XLV, 1983.
[9]. **Mironeasa, C., Cozmâncă M.** *„Stabilirea ecuaţiilor de echilibru ale burghiului la aşchierea alezajelor lungi"*. A-IX-a Conferinţă TEHNOMUS. Suceava, 1997.
[10]. **Mironeasa C.,** *„Cercetări privind optimizarea autoghidării burghielor utilizate la aşchierea alezajelor lungi",* PhD Thesis, Technical University "Gh. Asachi", Iaşi, 1997.
[11]. **Sakuma K., Katsuki A.,** *„Study of the BTA drilling process"*, Kusushu Daygakou Sukho. Technl. Repts, Kyushu University, no 3, 1983 .
[12]. **Sauer L., Ionescu C.,** *„Găurirea adâncă"*, Ed. Tehnică, Bucureşti, 1982.

Quick Info

Photo-to-measurement software

Eos Systems is releasing the latest version of its Photomodeler software. Photomodeler 6 is the result of three years of development to enhance the already well-acclaimed version 5.

Photomodeler automates the science of 'photogrammetry' – measurement from photographs.

The PC-based application enables objects to be measured accurately and photorealistic 3D computer models to be generated.

The versatile tool has been adopted across a wide variety of industries, including engineering, scientific, accident reconstruction and architecture, as well as film and game production.

In PM6, Eos Systems has added a powerful new 'Shapes' function for working with geometric solids and it provides a new, flexible means to export results into other software. The KMZ export format allows users to upload textured building models into the popular 3D globe application Google Earth, or utilise the Google Earth's 3D environment as a background for presenting a Photomodeler analysis of real-world scenes. Automatic processing of reference points now occurs in the background, which greatly speeds 3D model generation. PM6 also offers new printing and output options, an automated camera library, and Idealize, a module that removes lens distortion from photographs for high-end film and animation projects.

For more information, visit www.photomodeler.com

A family of high-specification SLS materials

CRP Technologies has developed a number of high-performance SLS materials and is now in a position to offer customers a choice of materials with properties and prices to suit different types of application.

Windform GF is a light grey composite based on polyamide with added aluminium and glass. It benefits from an improved heat deflection temperature (HDT) and superior stiffness, excellent surface finish, wear resistance and first-rate detail reproduction.

Windform GF absorbs slightly less liquid than the other Windform products and is particularly suitable for applications that require a superior surface finish. It is typically used for wind tunnel models and functional components.

Windform Pro offers higher stiffness than Windform GF. It is a light grey polyamide-based composite with added aluminium and glass. Windform GF has a high heat deflection temperature (HDT), superior stiffness, excellent surface finish, wear resistance and first-rate detail reproduction.

WindformPro B is similar to WindformPro but it has an opaque black appearance. In addition it has superior elasticity compared to the other Windform materials.

(http://staging.engineerlive.com/european-design-engineer/time-compression)

STRUCTURED SURFACES. A NEW PERSPECTIVE FOR TRIBOLOGICAL BEHAVIOR OF LUBRICATION CONTACTS

Gabriel Arin Mihalcea, Leonard Mihăescu, Ecaterina Camelia Pocriş

SC ICTCM SA Bucharest, l.mihaescu@ictcm.ro

ABSTRACT

Structured surfaces means the achievement of a rate, or controlled micro–geometry for one or both friction surfaces. These surface profiles are used to guarantee lubrication functions of transport, hoarding and spread of the oil and to collect the wear products for maintaining the uprightness of the friction couple surfaces.
The first textured surfaces where obtained by plateau–honing.
Effectively structured or textured surfaces are done by processing dimples and channels forms on the active surfaces of the friction couples.
In these micro–geometry forms the lubrication oil is guarded in starvation times, during the transition periods.

KEYWORDS: tribology, structured surfaces, friction couples, lubrication

1. INTRODUCTION

A new concept in the field of tribology has been the development of contact surfaces which are designed for improved lubrication capability.
This can vary from simple control of the surface roughness of two mating surfaces, to the more complex formation of regular structures which serve the double purpose of retaining lubricant and trapping debris particles.
For increasing efficiency, trying not to have a random character of the micro–geometry, after the 60's people began the texturing of the surfaces, [1,8,9].

The first forerunners of textured surfaces where obtained by plateau–honing.

Structured surfaces are done by processing dimple and channels forms on the active surfaces of the friction couples. In these micro–geometry forms the lubrication oil is guarded in starvation times, for example in the transition periods.

In the present article will be presented the advantages of these surfaces, the technological processes used to accomplish these surfaces and the main machine elements fields where these are used.

Structured surfaces create a lubrication film, which produces a load carrying capacity when there is no condition for the wedge effect.

This kind of surface engineering produce:

- continuous and discrete textures, for friction control;
- thin and soft lubrication films;
- thin hard films for durability of fluid lubrication;
- surfaces chemistry protecting films, for reliability.

The general motivation is the same: to reduce friction and increase durability and energy transmission components and engines, [1,8,9].

Texture and topography of surfaces has a very strong influence on the tribological properties. In many experiments and real application it has been shown that the friction can be dramatically reduced if the contacting surfaces are given a texture comprising a pattern of small recesses. It is generally believed that the beneficial effect of these recesses in boundary lubricated conditions is twofold; they act as a local containers of lubricants capable of feeding the lubricant directly between the two contacting surfaces and they can bury wear debris and contaminants, thereby keeping the interface flat and clean which minimizes the amount of deformation in the sliding process and this reduces the friction.

For a number of years, textured surfaces have been used in applications ranging
from cylinder bores to rolls for steel sheet rolling. However, the adopted texturing tech-niques do not allow high definition and micron scale of the areas of real contacts. New tex-turing techniques are introduced for improving mechanisms of textured surfaces.

2. STRUCTURED SURFACES PROPERTIES

The applications of structured surfaces are connected with large area flat – surfaces contacts as sliding bearings and seals.

The main function of the structure procedure is on one way the transport and the spread of the lubricant into the contact area and on the other way to remove and collect the wear products obtained in the tribological processes.

These functions defined above can be obtained by three kinds of structured surfaces:

- stochastic surfaces structures, represented in Figure 1,[5]; in this structure the micro-channels spread the lubricant all over the surface, without discriminated senses; these stochastic structures warrant the remove of the wear products from the contact area; but they have also the drawback spreading and ousting the lubricant from the contact area too, so the couple goes into lubrication starvation process;
- deterministic surfaces structures, with lubrication closed pockets, represented in Figure 2, [5]; these kind of structures assure the presence of the lubricant in the contact area, unconnected with the feed pressure; the spread of the lubricant out of these pockets is possible only by the increment of hydrostatical pressure; as drawback is the fact that the lubricant affects by his physical and chemical properties the behavior of the friction couple;

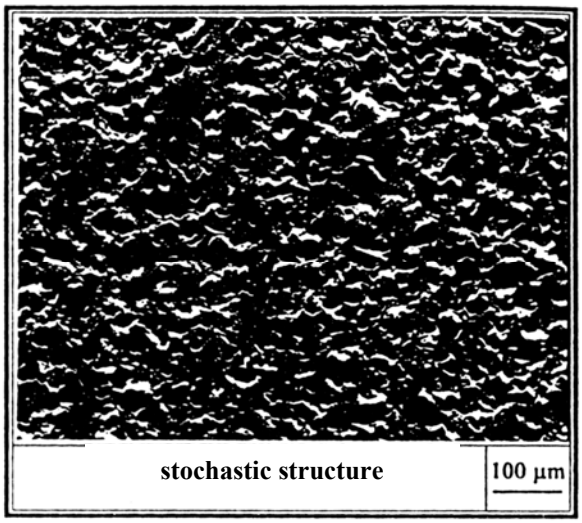

Figure 1. *Stochastic structure obtained by electron – microscopy*

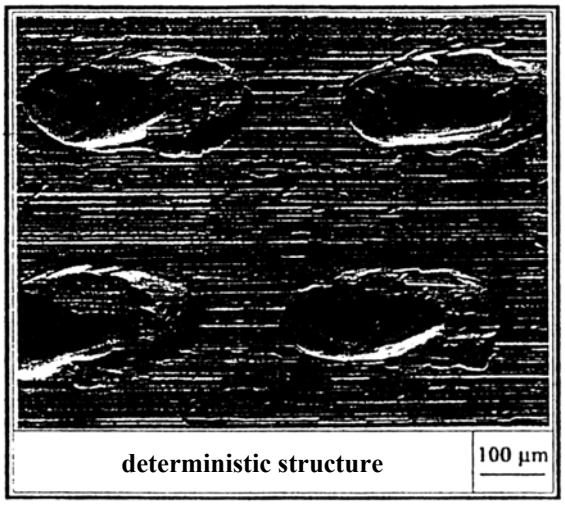

Figure 2. *Deterministic structure obtained by electron – microscopy*

- mixed surfaces structures, or determinist – stochastic surfaces structures, represented in Figures 3, 4, 5, [5]; they join the advantage of deterministic structures referring to the use of the effects of lubrication pockets, that means the permanent presence of the lubricant in the contact area, with the undertake of the transportation and remove of the wear products out of the contact area, from the stochastic structures.

3. USED TECHNOLOGIES TO ACHIEVE STRUCTURED SURFACES

There are many technologies to obtain structured surfaces:

• the process of plateau–honing; in conditions of optimal manufacture, the honing using super–abrasives for hard steel processing leads to uniform textures with well outlined asperities; these asperities assure surfaces formation type plateau; Figure 6, [7], presents a plateau surface processed by horning technologie;

• surface chemical pickling, by photogravure, like in Figure 5, [5];

• surface laser processing (LBM) of micro–dimples all over the active area of the friction couples; the process is presented in Figure 7b, [5];

• surface abrasive–jet processing (AJM) of micro–dimples all over the active area of the friction couples; the process is presented in Figure 7a, [5].

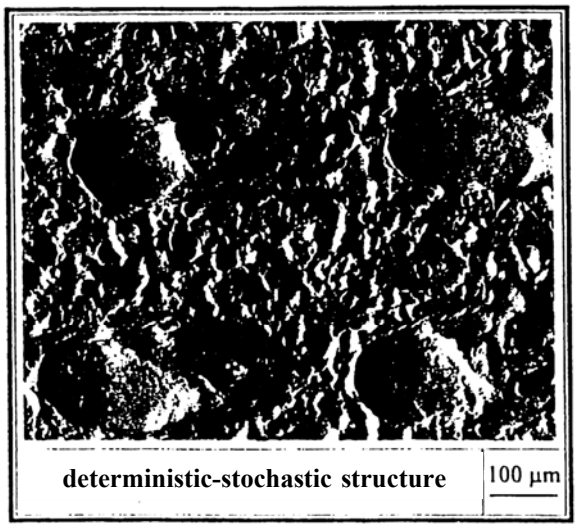

Figure 3. *Deterministic - stochastic structure obtained by electron – microscopy*

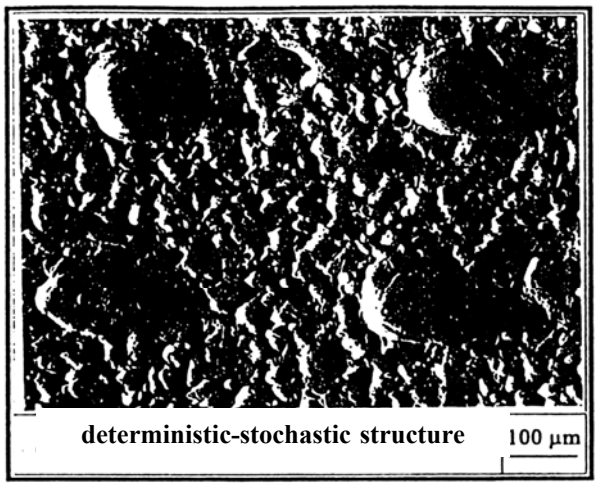

Figure 4. *Deterministic - stochastic structure of a fine structure surface without bourne asperities*

Technological aspects for the processes of manufacture of structured surfaces:

- the manufacture procedures are used for different kind of surface dimples geometries, as shown in Figure 9, [3];
- some technologies to create dimpled surfaces can produce bourne asperities around the dimples performed into the manufactured surface, as it is shown in Figure 10, [3]; these asperities have a negative impact on the lubrication of the active surfaces lubrication; it can be used a process of polishing or lapping to remove these asperities;
- the profile of dimples differs in connection of the technological process used to produce these structured surfaces; Figure 8a, [6] shows that the AJM process let to obtain dimples with soft tapered form, in opposition with the cillindrical one, Figure 8b, [6] obtained by the LBM process;

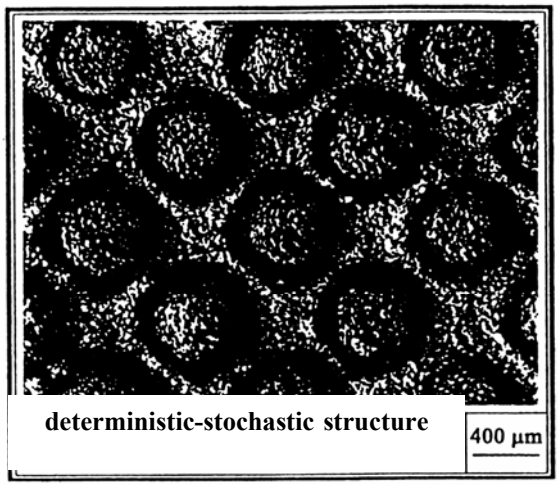

Figure 5. *Deterministic - stochastic structure obtained by surface chemical pickling*

Figure 6. *Plateau–honing structured surface*

Figure 7. *Micro–dimples surface manufacture:*
a. abrasive–jet machining (AJM),
b. laser–beam machining (LBM)

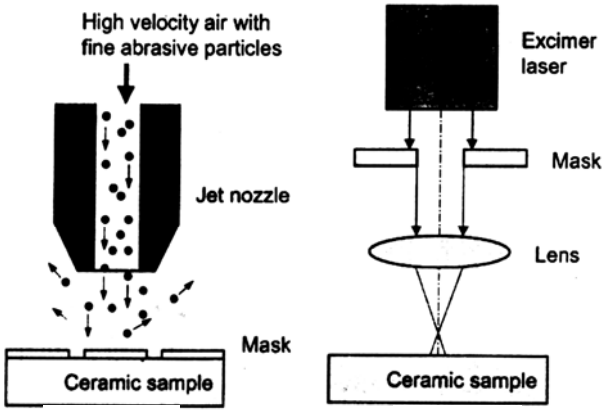

a. AJM b. LBM

Figure 8.
Geometry of micro–dimples manufactured by:
a. jet abraziv–jet (AJM), b. laser–beam (LBM)

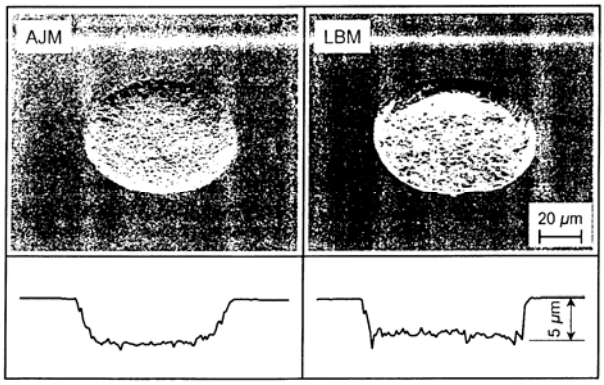

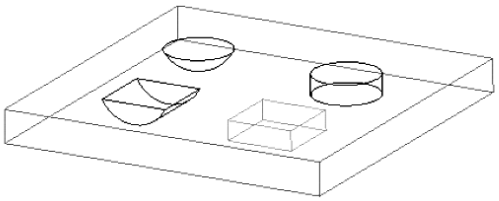

Figure 9. *Different forms for the geometry of dimples*

Some papers presents optimization for structural manufacture of the surface using the deterministic–stochastic procedure, in three steps, [5]:

- the first step can be obtained by superposition of the two procedure, the deterministic and the stochastic technologies;
- the second step is to remove the asperities produced in the process of manufacturing of deterministic dimples on the surfaces;
- the third step is to realize and improve the stochastic structure in order to spread it on the entire processed surface; this can be obtained by deforming procedures.

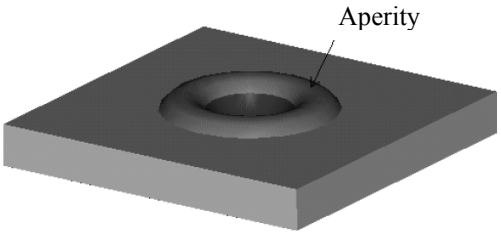

Figure 10. *Asperity obtained by manufacturing dimpled surfaces*

4. MACHINE ELEMENTS USING STRUCTURED SURFACES

Structured or textured surfaces are used for different kind of machine elements:

- mechanical seals; scientific studies and articles show the impact that the using of structured surfaces can produce to improve tribological properties of these machine elements; the presence of this structured geometries leads to assure a lubrication film, and avoids premature wear of the of the active surfaces; Figure 11, [3] presents a seal textured ring; the surface structure is a cheapper mean to realize carrying capacity, comparatively with other procedures for manufacture the surfaces: channels, buckles, skewed areas;
- thrust sliding bearings, where only one part of the bearing is structured, in order to obtain a joint effect of the dimpled zones, like the one obtained in the step thrust bearing; Figure 12, [3] shows the principle of this bearing; the gain of carrying capacity is less then the one obtained in a step bearing, but the friction is smaller as the friction of the pure step bearing, and they have the advantage of a smaller required precision in the manufacture process;
- contact between piston ring–cylinder layer in combustion engines, where the friction forces are in direct relation with the amount of fuel used by the engine and the performances of the car; Figure 13, [3,4] presents a textured ring, because this the part of the friction couple with structured surface; the use of these structured surfaces has positive followers: reducing the friction coefficient and good working in starvation conditions;
- big roller bearings; for these machine elements it can be used for the roller cage, in order to avoid the bearing failure in case of cage miss alignment; Figure 14 presents the use of textured surfaces for roller bearings;

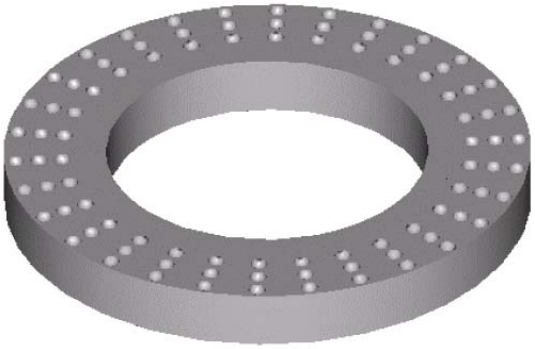

Figure 11.
Mechanical seal ring with structured surface

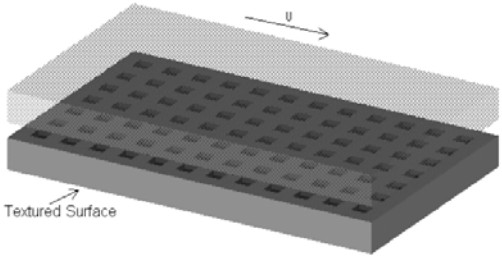

Figure 12.
Textured segment of a thrust slide bearing

Figure 13.
Piston ring with textured surface

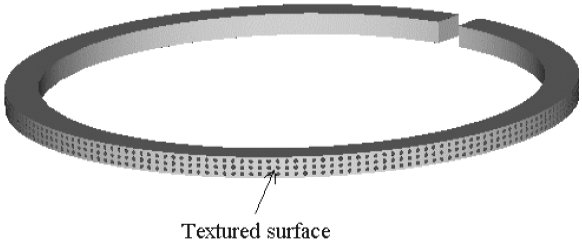

of plast
reduce

Figure 14.
Roller bearing with textured surface cage

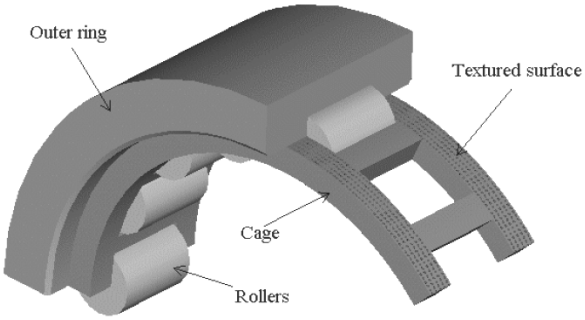

problem in the 60's. But only in the 90's the subject of structured surfaces was carefully studied by the tribology specialist researchers.

Probably there will be a growth of the area of machine elements using structured surfaces. The main problem remains in computing the boundary lubrication regime using this kind of surfaces. Another problem is the tribological research and detect the most important friction characteristics for many variants of surface geometry and establishing some optimum variants.

REFERENCES

[1]. **Iancu, C.,** *„Contributions to dimensional optimization of mechanical presses in dynamic regime"*, Ph.D. Thesis, University of Pitesti, Romania, 2001.

[1]. **Iliuc, I**. – *Tribology of thin layers,* Editura Academiei R.S.R. şi Elsevier, Amsterdam–Oxford–New York– Tokyo, 1980*;*

[2]. **Marian, V**.- *Contribuţii privind lubrificaţia cuplelor de frecare cu suprafeţe texturate*, rezumatul Tezei de Doctorat, Bucureşti, 2006, Universitatea Politehnica din Bucureşti, Romania

[3]. **Marian, V.** – *Lubrication of the textured surfaces*, Depart. Of Machine Elements and Tribology, University Politehnica of Bucharest, Romania

[4]. **Pettersson, U.** – *Surfaces Designed for High and Low Friction*, Acta Universitatis Upsaliensis, Uppsala, 2005

[5]. **Steinhoff E., Rasp W.,Pawelsky O.** – *Entwicklung von tribologisch optimierten Oberflächenstrukturen für die Blech–und Massivumformung*, The XIIth International Coloqium Tribology 2000+, January 11 – 13, 2000, Technische Akademie Esslingen, Germany

[6]. **Wakuda M., Yamauchi Y., Kanzaki S., Yasuda Y.** – *Effect of surface texturing on friction reduction between ceramic and steel materials under lubricated sliding contact*, Wear, Volume 254, 2003, Elsevier Science S.A.

[7].**Bardac D.** – *Contribuţii privind creşterea preciziei şi îmbunătăţirii calităţii alezajelor utilizate în industria motoarelor cu reacţie prelucrate prin superfinisare* – Teza de Doctorat, Universitatea Politehnica Bucureşti – Facultatea Inginerie Aeronautică, Bucureşti,1996

[8]. **Pavelescu D., Muşat M.,Tudor A.** – *Tribologie, frecare, uzare, ungere (Tribotehnică)* – Editura Didactică şi Pedagogică, Bucureşti, 1977

[9]. **Pavelescu, D.,** – *Tribotehnica*, Ed. Tehnica, Bucuresti, 1983.

Quick Info

New version of materials selection software

Granta Design is releasing a new version of CES Selector, the company's PC-based software for the selection of engineering materials and manufacturing processes.

CES Selector helps product designers and manufacturers to innovate, avoid undue costs and meet environmental and other regulations. The new CES Selector 2007 version adds capabilities for applications including cost analysis, medical devices, plastics and elastomers, eco-design, and guiding and communicating materials decisions.

CES Selector combines data on the mechanical, physical, economic, and eco-properties of materials with powerful graphical software for analysis and selection developed at Cambridge University and Granta. The 2007 version features new price estimate data for over 3000 materials, generated using an improved and updated price model. Together with new software features enabling materials to be easily ranked based on 'cost per unit of function', this allows users to quickly identify and compare optimal materials for complex combinations of properties. For example, cost per unit stiffness could be assessed to help choose an appropriate material for a light, cheap panel. CES Selector is useful for identifying substitute materials - such as a lower-cost grade of plastic, or an alloy with lower nickel content.

New specialist data is also available for medical plastics, thermoplastic elastomers (TPEs), and the eco-properties of materials. These enable the CES Selector to find the best materials for a medical device or food-contact application, to navigate the fast-moving and commercially important field of TPEs, and to estimate more accurately the environmental impact of product designs.

New communication, usability, and documentation features make CES Selector easier to use and improve even further its outstanding graphical presentation of analysis results. These graphical capabilities help materials teams or designers wishing to present or discuss selection decisions, as well as materials producers wishing to position products against competitive offerings.

Professor Mike Ashby of Cambridge University and Granta says: "Manufacturers must make the right choices when selecting or substituting materials. Materials producers need help in positioning their products. With its extensive new data and improved analysis, presentation, and usability, CES Selector offers more help than ever in tackling such commercially significant problems."

(from http://staging.engineerlive.com/news)

USB key resistant to industrial environments

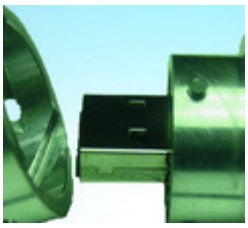

USB keys are a tool used more and more frequently for downloading data from measuring equipment or automation systems. Amphenol-Socapex, a leader in reinforced RJ45, RJ11, USB connectors now offers a new sealed (IP67) USB key, one that is shock and vibration resistant.

This key comes with a metal casing. It is available with various surface coatings to match the application: nickel, olive green and black.

This way, critical operating data can be carried around just as reliably and simply as when using a conventional USB key.

The capacities offered are 256 Mbytes, 512 Mbytes, 1024 Mbytes, 2 Gbytes and 4 Gbytes.

This key also can be proposed with a coupling nut (as a derivative from MIL-DTL-38999 series III) to have a sealed and secure connection with a USBF TV receptacle.

Its applications are numerous: process control, machine-tool, military, oil and gas, aeronautics, entertainment consoles, event recorders.

Amphenol-Socapex

(from http://www.engineerlive.com/european-process-engineer/instrumentation)

INDUSTRY OR SERVICES ?
INDUSTRY AND SERVICES' INTEGRATION IN GLOBAL KNOWLEDGE ECONOMY

Radu Popescu, Irina Sandu*, Emilia Stănescu**, Raluca Pop***

* The Romanian Academy, The National Institute for Economic Research, The Centre of Industry and Services Economics,
** The National Institute for Small and Medium Enterprises, radupopescuceis@yahoo.com

REZUMAT

Afirmarea Economiei Globale a Cunoaşterii (G.K.E.) determină schimbări în structura economiei ţărilor dezvoltate, în natura activităţilor din interiorul industriilor precum şi între relaţiile dintre industrii. Cele mai notabile dintre acestea sunt: creşterea importanţei serviciilor, odată cu sporirea complexităţii şi mai ales a integrării sistemelor de producţie şi distribuţie.

ABSTRACT

The assertion of Global Knowledge Economy (G.K.E.) has determined the changes in the structure of the developed countries' economy, in the nature of the inside industries' activities, as well as in the relationship between these industries. The most notable of them are the increase of the importance of services together with the growth of complexity and especially of production and distribution systems' integration.

KEYWORDS: Investment, innovation, industry, services, globalization, synergy, trend, productivity, efficiency, knowledge economy

CUVINTE CHEIE: investiţie, inovare, industrie, servicii, globalizare, sinergie, trend, productivitate, eficienţă, economia cunoaşterii

1. INTRODUCTION

According to a **traditional point of view,** the analists show that there is observed an increase in services extension and a decrease in fabrication amount. Consequently there has been asserted that we are entering a new Economic Era (Bell 1976, P. Drucker 1969 etc.).

Many researchers see this increase as a natural economic progress, the development starting from agriculture towards fabrication and then towards services. The Services Economy represents for these the development climax. In therefore the G.K.E. a new post-industrial Services economy?

The traditional modality of approach for the industrial classification sees the economy as consisting of a hierarchy of sectors, industries, firms, so : the primary sector: agriculture, farming, fishing, mining, the secondary sector: processing industry, the tertiary sector: the services industry.

In every sector, the industries are seen as being more or less independent, grouping firms that are interested in obtaining similar products/services, on the grounds of similar production processes. From this point of view, the recent structural changes in the developed economies seem to confirm the fact that E.G.C. is a services-focused post-industrial economy. This feature is valid if we regard the economy as a simple sum of some more or less independent industrial sectors and firms.

We acknowledge the evidence of the increase of services and the decrease in production, but we will show that the reality is more complex and different. We shall remind that the agricultural and mining activities were not **replaced** by production/processing activities during the industrial revolution, but were incorporated by it. It is thus unnatural to expect that production will be replaced by services as part of the informational revolution.

2. PRODUCTION – SERVICES RELATION

In 1987 Cohen and Zysman showed in „Manufacturing Matters" that services and property over these depend on the production-processing duo because the **processing industries are large consumers of services and without processing activities the demand of such services is extremely low or doens't even exist.**

More recently there is evidence of an even complex interrelationship between production and services, which interrelationship reaches a level where the traditional differences between services and production become extremely dim.

In „Made by Hong Kong", Berger and Lester characterize the convergence of production and services as follows:

''From the point of view of the input, the activities traditionally regarded as services (the logistical ones) are considered key-input, determining factors for the production processes, while the processing industries are the source of numerous and important inovations in the production of services.

The convergence is even more evident when talking about the outputs. On one hand, for today's consumers the value of the processed products is evaluated on the grounds of intangible atributes (design, the capacity to provide confort, durability, inovation, fashion, on-time delivery, flexibility regarding client's preferences etc) When these are not incorporated by the product, they are considered as being services.

On the other hand, the traditional characteristic of services (these cannot be neither stored nor transported and thus need to be produced at the place where they are consumed) is gradually changing.

Today, many services can be electronically stored, transported over great distances by using telecommunication technology and delivered on demand. These atributes transform the services and causes them to seem more and more to the processed products.

The process of production of goods and services is every time more convergent.

Peter Drucker noticed that the software production, that is usually classified as a service industry, is clearly a **production activity.** Truly, the idea of software factories has been a subject for a long time now. We can call it service, but the manipulation of thousands of credit cards is clearly a process of production. The same applies to the clearing of checks, as well as to the numerous insurance applications. Even the consultancy services seem to be more and more like a flexible factory with a generic product or its subparts being continously produced, ready for personalized assembly for a client with some specific demands.

Peter Drucker (1998) showed that: „As services are increasingly organised more similarly with a systematic production process and they adopt more characteristics of the production processes, their productivity will consequently grow and they will be successfull. In fact, the simple misleading view of the decreasing of production in favor of services, that is presented by the traditional statistics, hides more than it reveals. It overlooks the increasing complexity of ties between goods production and services and conceals the central and permanent importance of processing in the economies of developed countries."

Services become more and more important for the existing change of the consumer expenditure model. As the real income of the population increases, so do the expenditures made on services. Changes in the employment offers in favor of the services field are mainly due to a high level of work productivity when it comes to goods, as well as for services.

Services become more complex and intensive, when they are about goods, as well as when they concern production and distribution processes. Still, this does not mean the end of production.

The processing industry becomes more intensive regarding the services, both in the increasing of input services (semifinished products, resources) and in terms of increase of the employment level (work-places in the service field). There was an increase of services by 29%-33% in the field of the processing industry in areas such as: distribution, new sources for materials, testings, marketing, design, C-D, transport, commerce, finance and design or for the head-quartes of corporations.

Thus, meanwhile the production activity is reducing, the internally related services activity of it and the manufacturing one are more and flourishing.

3. THE KNOWLEDGE ECONOMY

The Knowledge Economy is the key to the increase of the complex integration between processing activities and services. The creation, production and distribution of goods and services is a characteristic of the rising E.G.C. The economical prosperity is more and more based on the complex body of processing activities and services, taken as a whole.

In 1992, Peter Drucker said: „The systemic activity incorporates the physical process of doing things, the manufacturing in the economical process of business, meaning the activty of value-creation. As soon as we define manufacturing as being the process that converts things in economical gratifications, it becomes clear that production doesn't stop when the product leaves the factory**.**

The physical distribution of the good and service attached to the product are still parts of the production process and they should be integrated under there coordonates managed together with it."

This integration suggested by the New production is ever more evident in the developed countries' economy. There are producers asserting that: **beyond their production lines new business is developed correlated with services in the view of creating value for the costumers.** Thus, the machine-building producers (I.C.M.) are not selling simple hardware products any more (equipment and outfits) but are also delivering integrated systems consisting of: the equipment itself, electronic control elements, informational system, software packs, durability warranty, operation and maintenance support (systems).

It is not unusual for these to send their employees at the client factories for months or even years to help or even schooling (providing training services) to operate and keep functioning, repairing their equipments (is the case of the Romanian firm, T.M.G., - 3).

In the aircraft and aerodynamic industry, marketing continues after selling in order to offer modern and efficient maintenance and operation solutions.

Bending the balance towards the client, the fabrication must be able to satisfy bigger and bigger expectances. This means the products and services personalization in order to satisfy the specific local requirements and to get really close to the client.

4. COMPLEX INTEGRATION OF PRODUCTION AND SERVICES

Nowadays, an engineer being at the client's headquarters stays in front of a PC to accomplish the product's online configuration and can immediately verify if errors have been interjected; he transmits the order to the delivery department of the firm. The price structure is already programmed. A provider within the firm fills in the order with some data.

Thus, instead of soliciting the Firm, to give the order, the client with an adequate authorization, may access information from the firm's web. Over 80% from the clients receive online filled in orders and 50% of the orders pass through the system without being touched by someone.

The producers of aero spatial equipments adapt their products: flexible automation, chairs positioning, luggage hoarding, maintenance systems, in order to correspond to any airship configuration and development of the desired planes, to serve the clients online.

It becomes more and more **usual for the big producers to work in partnership with the clients to identify their requirements, to anticipate the needs and to offer more and more value from the customer's point of view**.

The leaders from the market rely on technology, on INTERNET, in order to realize business in real time, in the processing area, directly with the providers and clients, to improve the services provided to the clients, to increase the feed-back and delivery capacity.

The Otis elevators firm uses service technologies and interconnection coalitions between industry and services in order to heighten the market position.

The market leaders concentrate themselves on innovation. They try to become more quickly and efficient in the products development cycle.

Over 50% of them are using CAD / CAM to integrate the design, the development and the fabrication. Nowadays all the implied parties in projecting new vehicles: designers, provider engineers and fabrication and assembling personnel work as a team contributing to the process from the beginning up to the end.

As a result of computerization, steps that were lasting weeks or months are now made in a few days. By using: CAD / CAM / CAE (computer aided design / manufacturing / engineering) the whole team can study the dossiers and folders and use 3D (tridimensional), modelling techniques to project vehicles and notice how to harmonize and assemble the parts without realizing the prototype.

When the final drawing in made, CAM data are charged in machines (M.U.C.N.) that are building the SDV-s and parts of the prototype. This reduces the time necessary to concept and build a new vehicle from 6 years to 2 years.

The integration of the delivery chain is decisive. Nowadays the fabricants performances went up to: 68% of the fabricants, integration with the client and 73% integration wit the provider.

The fabricants are step by step diminishing the providers number and extent their supplying chains. They use IT as a key help.

Technological platforms as: E.D.I. (electronic document interchange) and E.R.P. (enterprise resource planning) integrate providers, fabricants and en-detail sellers in an uninterrupted logistics chain, CREATION – PRODUCTION – DISTRIBUTION.

These practices demonstrate that: **fabrication and services are now interconnected and mutually supportive**. The success belongs to those who use efficiently **the potential of both type of activities and are looking for capitalization and amplification of the synergies** resulted from their combination.

Peter Drucker notices (1998): "The essence is not that of making goods, but to provide services that allow the client to obtain the complete benefit from the goods. To make goods is a costs centre, to offer services is a profit centre."

The examples demonstrate **the more and more complex integration of production and services as production system activities**. This emergent system slips to the observation when we use the traditional classification, but it is in the centre of new E.G.C.

The technology integrated in equipments and machinery is determined by:

- new cutting methods (laser cutting)
- tool machines with numeric command (MUCN)
- weaving machines with numeric command, etc.

The production modalities may be changed and there may be introduced new design possibilities and therefore new types of requirements for the fabricants. The specialists are designed to establish partnerships with the equipment providers, to ensure that: the communication line is opened and the modernization is accomplished systematically and the introduction of new technologies develops according to the strategy. Any derogation from this implies a discontinuity in strategy and it may lead to bankruptcy.

The innovating materials providers constitute also an important source of new production processes.

The existent settlements or their changes have an important role in innovation: influence the products, safety standards, sometimes determine the development of the products through the system: from en-detail seller – fabricant – materials provider.

5. CONCLUSIONS

The traditional industries are activitated by the providers and industrial services which are **available** for them. The services extension mode which characterizes the New Fabrication is important to understand the traditional industries.

More and more the integration of C-P-D activities orientate the economic activity in the emergent E.G.C. Focusing on the new fabrication allows us to notice the intensity of the knowledge volume increase, as it characterizes the E.G.C., showing how the intensive knowledge goods interfere in the services (fashion, design) within a C-P-D system which is the base of E.C.

These have profound implications on economic development.

Fabrication is more and more integrated with activities relied on services, it becomes difficult to geographically separate the high value fabrication by the services correlated with.

The low value fabrication (gross production) can be located to take profit from the low wage advantages and other location costs. But the high level fabrication (flexible, extended and supported by services) so the New Fabrication, **is made only where it can be integrated in the suitable services**.

Thus it is more probable to be **located there where are strongly developed service industries, close to the client and where more developed T.I.C. transportation and distribution systems are capable to connect them uninterruptedly in a global C-P-D chain**.

To realize **investments** as a producer relying on **low costs** may determine constraints and condemn a country or a region to a reduced-value mass production and therefore to a more and more small coverage of the world economic activity. The investment in knowledge allows us to avoid this situation.

Romania can concentrate the correlated services around the existing manufacturing industrial areas and industrial platforms: electronics, the machine construction industry, the textile industry, by developing the necessary T.I.C. for the transport and distribution systems, as well as the necessary competences of the specialists to make correlations and obtain positive synergies.

REFERENCES

[1]. **Luban, F. Vasilescu, I.,** *"Investments and the economical relaunching"*, A.S.E., 1998.

[2]. **Pițurescu, I.,** *"Business incubators centres"*, Ed. Giuleştino, Bucharest, 2002

[3]. **Popescu, R.,** *"The road to excellence for industrial factory units",* Chiminform Data, Bucharest, 2005.

[4]. **Popescu, R.**, *"Management of industrial property"*, Chiminform Data, Bucharest, 2006.

[5]. **Stoica, M., Ivănel, D.,Popescu, R. Doval, E., Jors, C.,** *"Evaluation and administration of the financial-banking risk"*, Tipart, 2004, Bucharest.

[6]. **Vasilescu, I.,** *"Preparing the evaluation and audit of projects"*, EfiCon Press, Bucharest, 2006.

ECOLOGICAL MANAGEMENT IMPLICATIONS CONCERNING THE PRODUCT LIFE CYCLE

Irina Rădulescu

S.C. ICTCM S.A. Bucureşti, irena_sandu@yahoo.com

ABSTRACT

The paper presents an interdisciplinary study concerning ecologic management for product life cycle, in order to integrate durable concepts and actual demands about projection - development - implementation. Worldwide, it is established the long life development problem, the achievement actions for quality products and services are in correlation with promotion of reliable and clean environment preservation to next generations, using technological continuous innovations, research and development actions.
Ecologic products activities is based on the development of economic factors and also, of environmental and social factors, which must be company standards in decisions process.

KEYWORDS: Ecological management, Product Life Cycle, Product Life Cycle Management

1. INTRODUCTION. PRODUCT LIFE CYCLE

Every activity that a business performs has an impact - on a social, economic and environmental level. Often these impacts are not obvious or immediate, there are many that are hidden or indirect, that only appear when you take a more holistic view - essentially, when you take a step back and examine the complete life cycle of your products and services**.**

A life cycle is made up of all the activities that go into making, selling, using, transporting and disposing of a product or service - from initial design, right through the supply chain. [1].

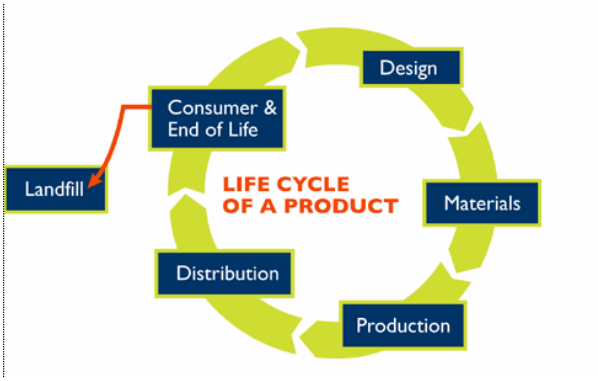

Figure 1. *Life Cycle of a Product*

Every product or service must, almost by definition, have a life cycle. It is about a process which develops in time, from the first stage to the final one. The *Product Life Cycle* refers to the succession of stages a product goes through [3].

Typical Product Life Cycle is exposed in figure 1.

Products tend to go through five stages, each one has its proper characteristics:

1. New product development stage
   - very expensive, no sales revenue, losses;
2. Market introduction stage
   - cost high, sales volume low, no/little competition – competitive manufacturers watch for acceptance/segment growth, losses;
3. Growth stage
   - costs reduced due to economies of scale, sales volume increases significantly, profitability, public awareness, competition begins to increase with a few new players in establishing market, prices to maximize market share;
4. Mature stage
   - costs are very low as you are well established in market & no need for publicity, sales volume peaks, increase in competitive offerings, prices tend to drop due to the proliferation of competing products, brand differentiation, feature diversification, as each

player seeks to differentiate from competition with "how much product" is offered, very profitable;

5. Decline or Stability stage
   - costs become counter-optimal, sales volume decline or stabilize, prices, profitability diminish, profit becomes more a challenge of production /distribution efficiency than increased sales.

Actual society modified Typical Product Life Cycle and pointed new aspects regarding the product (figure 3), [4]:

- the research & development period, which refers to the emission and examination of ideas, the detailed analyse of ideas and their development – as an introduction stage;
- existance of revivaled products, which have a second new life, after their decline period, by improving their characteristics;
- re-arrange the product over new market share;
- redesign the product having same performances and different materials with lower costs;
- the final stage, after the decline, which involves the recycling of the product [5].

2. PRODUCT LIFE CYCLE MANAGEMENT

Product Life Cycle Management is the process of managing the entire life cycle of a product from its conception, through design and manufacture, to service and disposal.

It is one of the four cornerstones of a corporation's information technology structure. All companies need to manage communications and information with their customers (CRM-Customer Relationship Management) and their suppliers (SCM-Supply Chain Management) and the resources within the enterprise (ERP-Enterprise Resource Planning).

In addition, manufacturing engineering companies must also develop, describe, manage and communicate information about their products (PLM). There are important documented benefits as: reduced time to market, improved product quality, reduced prototyping costs, savings through the re-use of original data, a framework for product optimization, reduced waste, savings through the complete integration of engineering workflows.

Product Life Cycle Management is the succession of strategies used by management as a product goes through its life cycle.The PLC goes though many phases and involves many professional disciplines and requires many skills, tools and processes.

Product life cycle management, sometimes "product life cycle management", represents an all-encompassing vision for managing all data relating to the design, production, support and ultimate disposal of manufactured goods**.**

PLM concepts were first introduced where safety and control have been extremely important, notably the aerospace, medical device, military and nuclear industries.

These industries originated the discipline of configuration management (CM), which evolved into electronic data management systems (EDMS), which then further evolved to product data management (PDM).

In the last 5 years, manufacturers of instrumentation, industrial machinery, consumer electronics, packaged goods and other complex engineered products have discovered the benefits of PLM solutions and are adopting efficient PLM software in increasing numbers [6].

The core of PLM is in the creation and central management of all product data and the technology used to access this information and knowledge. PLM as a discipline emerged from tools such as CAD/CAM and PDM (Product Data Management), but can be viewed as the integration of these tools with methods, people and the processes through all stages of a product's life.[6]

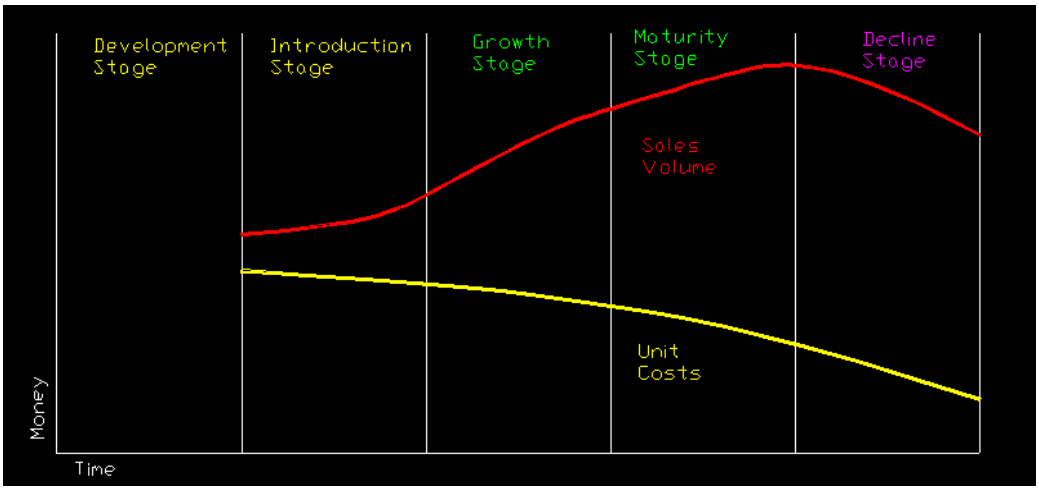

Figure 2. *Typical Product Life Cycle*

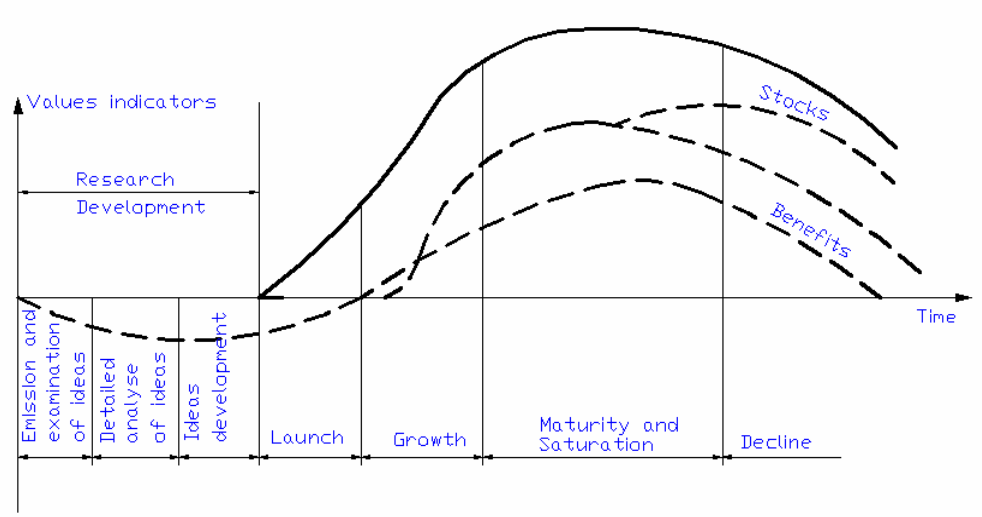

Figure 3. *New Product Life Cycle*

It is not just about software technology, but is also a business strategy [8].

Figure 4 shows the simplified stages in a traditional sequential engineering workflow.

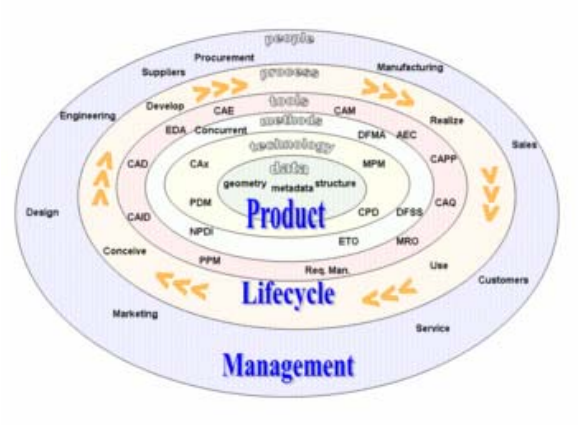

Figure 4. *Stages in a traditional sequential engineering workflow*

The exact order of event and tasks will vary according to the product and industry in question but the main processes are, [8]:

- Conceive – Specification, Concept design
- Design - Detailed design, Validation and analysis (simulation), Tool design
- Realize - Manufacturing Planning, Manufacture, Build/Assemble, Test (quality check)
- Service - Sale and Deliver, Use, Maintain and Support, Dispose.

The major key point events are: Order, Idea, Kick-off, Design freeze, Launch.

The reality is however more complex, people and departments cannot perform their tasks in isolation, they intergrowth and one activity cannot simply finish and the next activity start, there are joint times for activities.

As an example - design is an iterative process, often designs need to be modified due to manufacturing constraints or conflicting requirements.

3. THE " ENVIRONMENTALLY FRIENDLY" PRODUCTS DEVELOPMENT

Our actual society is more and more preocupied in ecological management implications concerning the product life cycle.

It is a serious concentration on the "environmentally friendly" products development, which are named green products.

About the development it is important to say that it is not only a growth of economic factors importance, but also of the environmental and social factors, they became company standards for the decisions taking and a real basis for the "environmentally friendly "ecological production activities.

The enterprise must operate an ecologic management system, according to international standards (ISO14001).

A new concept was developed – LCA (Life cycle assessment) and due to it - the enterprise must recognize and quantisize polluting emissions, for different product development stages.

This policy is addopted in order to find improvements of those processes and to come down the polluting transmissions.

Another policy is to implement the development in steps of products, in harmony with environment, in order to assess the type and the wastes quantities, from the beginning stage of design. The environment protection became also a priority in the refills case.

There are different areas (electronic products), where the quantity increase of wastes generates the shortening of life cycle products and that became an interest problem. It is necessary to adopt an active atitude for reducing resulted wastes from the producing process, still beginning with the projection stage and following implementation of DfE (Design for Environment) [8].

Choosing ecologic materials from development stage it is possible to reduce at any stage the wastes sources. There are opened recycling centers, in other countries and also in Romania, to lower the wastes which are generated by the products with life cycle out of stock.

„Clean technologies" are the target and the actual instrument against the pollution.

There are many firms as Alternative Fuel Systems Inc., Vancouver-based Westport Innovations Inc. (Canada), which are committed to providing practical clean air solutions. They offer today's high performance options, while continually developing new innovative environmental technologies.

Combining specialized, proprietary hardware and software technologies, they has developed systems that enable diesel and gasoline base engines to produce fewer harmful emissions without sacrificing performance [11].

Another example is LG Electronics, which makes all efforts to offer the best servicies for clients and also has as purpose a clean and safe environment for next generations, using continuous technological innovations, Research and Development [9].

A study of a reseach team which incorporates a Research Institution and University's Excelence Centers proposes the accomplishment of a new integrated informatics instrument for the modeling and simulation of the wear behavior and lubricant's durability [7].

These researches are made pursuant to the actual necessity of fast designed and adaptable in industry, using instruments for modeling, simulation and integrated products.

The importance of this project consists in available information the wear behavior and durability of the oils. It was developed a fast diagnose method for the liquid lubricants, with minimal investments and a high precision level, easy to use.

The small quantity of lubricant needed for a determination, the low time of measurement and the adaptability character of this method present some essential advantages of this project.

These aspects give a strong economical and ecological impact and are according to the reglementations and corresponding standards requests at European and international level (quality, medium, risk).

4. CONCLUSIONS

Life Cycle Management is a business decision-making approach that considers benefits, costs and risks over the full life cycle of a product or service. Life cycle and DfE principles consider local as well as global impacts.

LCM applies approaches to product design and development that minimize environmental impacts of products throughout all life stages of a product, starting with the extraction of resources for raw material inputs, and continuing through processing and manufacturing of all feedstocks and final products, distribution, use, and disposal.

It is important to access all the tools in order to work at entreprise business [10]:

- Life cycle analysis (LCA) is a tool used for Life Cycle Management (LCM), to quantify the life cycle impacts of a product;
- Design for the Environment (DfE) is a tool used in applying life cycle design principles in all life phases of a product or process;
- Another tool consists in Incorporating Life Cycle Analysis and consideration in entreprise environmental and procurement policies;
- It is a necessity to involve, educate, and empower suppliers to use life cycle designs and practices;
- Enterprise ecologic products activities are based on the development of economic factors and also, of environmental and social factors, which must be company standards in decisions process. Enterprise must operate an ecologic management system, according international standards (ISO14001).

REFERENCES

[1] *http://www.epa.vic.gov.au/Lifecycle/*

[2] **BOX, J.** *Extending product lifetime: Prospects and opportunities,* European Journal of Marketing, vol 17, 1983.

[3] **DAY, G.** *The product life cycle: Analysis and applications issues,* Journal of Marketing, vol.45, '81.

[4] **LEVITT, T.***Exploit the product life cycle,* Harvard Business Review, vol 43, Nov.-Dec.1965.

[5] **POPESCU, R.** *Management şi creativitate în dezvoltarea industrială,* Institutul Român de Management, Bucureşti, 1980.

[6] **STEINHARDT, G.** *Extending Product Life Cycle Stages*, 1985.

[7] *Proiect CEEX nr. 39 /2005 – "Cercetări privind realizarea unui instrument informatic integrat pentru modelarea şi simularea comportării la uzură şi a durabilităţii lubrifianţilor".*

[8] **DHALLA, N. K. and YUSPEH, S.,** *Forget the product life cycle concept,* 'Harvard Business Review' (January-February 1976)

[9] *http://ro.lge.com/experience/social_commiment/enviroment.jsp*

[10] *http://www.life-cycle.org/*

[11] **J.D. MELINE and G.A. DAVIS,** *Cleaner Technologies Substitutes Assessment: A Methodology & Resource Guide.* U.S. Environmental Protection Agency, Washington DC, Kincaid, 1995.

MADICO LAUNCHES INDUSTRY'S MOST HEAT RESISTANT LABEL

Madico Graphic Films Limited, Maidenhead Berkshire, United Kingdom, www.madico.co.uk

ABSTRACT
Madico Graphic Films is a leading solutions supplier for durable label applications. It has expanded its wide range of heat resistant labels with the launch of a revolutionary heatproof tag that offers the highest level of heat-resistance and durability available on the marketplace.
Enabling product identification in extreme temperatures up to 1080°C, the new HP-L80 thermal transfer printable barcode tag is set to offer unique benefits over current methods of applying barcoded labels and plates in hot metal applications.

KEYWORDS: durable label applications, heat resistant labels, thermal transfer printable barcode tag

New Total Barcoding Solution Delivers Unmatched Performance to 1080°C

Madico Graphic Films, a leading solutions supplier for durable label applications, has expanded its wide range of heat resistant labels with the launch of a revolutionary heatproof tag that offers the highest level of heat-resistance and durability available on the marketplace.
Enabling product identification in extreme temperatures up to 1080°C, the new HP-L80 thermal transfer printable barcode tag is set to offer unique benefits over current methods of applying barcoded labels and plates in hot metal applications.

The exclusive attributes of the HP-L80 make it perfectly suited to fulfil product identification needs within the steel industry, including slabs, booms and bars; hot coils; and billets and wires.
Additionally, the HP-L80 meets similar requirements for aluminium products, including sows and pigs; hot and cold coils; ingots; homogenising billets; and other aluminium reheating processes.

Thanks to its application by fully automated or mechanical systems, the HP-L80 tag delivers a multitude of cost-saving and safety benefits compared to alternative methods of applying information, which can still entail writing directly to hot metals using chalk.

The advantages afforded by Madico's HP-L80 include eliminating reading or writing mistakes, which would otherwise impact upon both the lead-time and financial cost to customers through shipping errors, inaccurate inventory management, and re-ordering of lost metal.

In addition, the health and safety of personnel is increased over more traditional means involving chalk-scribing spray-paint, or other manual methods.

The HP-L80 heatproof tag also enables automatic tracking of work in progress via barcode identification, and the elimination of identification post-cooling, as well as the ability to track and manage materials throughout the supply chain.
"*The HP-L80 is set to revolutionise product identification in the aluminium and steel industries*", says Andy Voss, Managing Director, Madico Graphic Films. "*Quite simply its tolerance for high performance and durability at 1000°C differentiates it from any other tag currently available, which typically only operate to 600°C. As a result it affords manufacturers a new level of benefits that will significantly improve workflow by eliminating human error, as well as meeting increasingly strict health and safety legislation*."

Michael Alekseev, of Power Service, a Russia-based engineering solutions company, adds, "*For steel producers, HP-L80 is set to make a world of difference, simply by the fact that it delivers a safe, secure and accurate means of product identification in steel applications up to 1080°C.*

"*Current methods fail to provide these benefits and as a result, misidentification resulting in 'unidentifiable' product is still commonplace. Given that steel is tailor-made to suit individual applications, it is only usable if manufactured to specific requirements of the respective purpose. Incorrect or illegible product labelling could easily make 15 tonnes of steel slab redundant, resulting*

in possible wastage, huge costs and missed-delivery deadlines for the steel manufacturer."

Continues Alekseev, "*We are currently trialling HP-L80 with one of our steel producing clients, who have naturally been overwhelmed by its performance benefits. The tag is attached to steel billets at temperatures of around 750C. As far as product identification is concerned, they now have a solution that virtually eliminates the possibility of lost earnings, time and even customers, all of which could have a potentially disastrous effect on their business operations.*"

Madico's range of heat resistant label products also includes the HP-700 heatproof tag, designed for application on steel slabs or blooms.
Thanks to its ability to perform at temperatures up to 815°C, the HP-700 is still greatly superior to that of other available products.

In addition to the extreme heat resistant HP-L80 and HP-700 tags, Madico offers a series of high performance heat resistant products, capable of withstanding temperatures up to 600°C. These comprise the HP-600 for direct application to hot metals such as aluminium sows or steel billets; the HP-350 for hot direct applications such as high temperature ingots and steel coils; and the HP-300, designed to survive aluminium homogenizing and annealing processes.

All of Madico's heatproof labels are engineered to withstand harsh environments, which as well as extreme temperatures, include chemical exposure and adverse outdoor weather conditions.

About Madico Graphic Films

Established in 1994, UK-based Madico Graphic Films is one of the foremost suppliers of specialist pressure sensitive film products for durable label applications and screen/digital solutions. Madico's range of films includes durable products developed to withstand extreme climatic, chemical and mechanical exposure; as well as variants offering tamper-indicating qualities. These products serve a diverse number of applications across a range of sectors; including automotive and product security labelling, to window films used within the wide-format digital printing arena.

The company reaches an extensive client base via eight agent offices located throughout Europe, all of which receive full back-up and support from a dedicated European conversion and R&D facility in Maidenhead, where the company is continually involved in delivering innovative new products to the marketplace.

REFERENCES

www.heatproof.eu

www.madico.co.uk

For more information, please contact:

Andy Voss
Managing Director, Madico Graphic Films
T: +44 (0) 1628 777766
F: +44 (0) 1628 776666
AVoss@madico.co.uk

ABOUT HEATPROOF

The total barcoding solution for applications up to 1000°C

High Temperature Product Identification
Revolutionary HEATPROOF labels are designed to withstand harsh environments including extreme temperatures, chemical exposure and outdoor weather conditions.

Inventory Control Systems
Guidance provided in choosing inventory management software, hardware and barcoding solutions.

Customised Label Applicators

RP and SD series are fully automated systems designed to apply variable product identification and barcoding directly to hot metals. MC and MS series applicators are designed for manual application.

- **ELIMINATE reading and writing errors**
- **IMPROVE safety**
- **IMPROVE productivity**
- **IMPROVE inventory management**
- **ELIMINATE shipping errors**
- **REDUCE the cost of lost metal**

Features

- Automatically track work in progress via barcode identification
- Eliminate the requirement to identify after cooling
- Eliminate human mistakes and improve safety
- Track and manage materials throughout the supply chain
- Unique heat activated adhesives
- Suitable for outdoor storage and transportation
- Can be applied with manual or automatic applicators

Site Test and Customer Service

- **On-site technical evaluation plan**
- **Design and Install automatic applicator**
- **On-going support and maintenance programmes offered**

HEATPROOF PRODUCTS

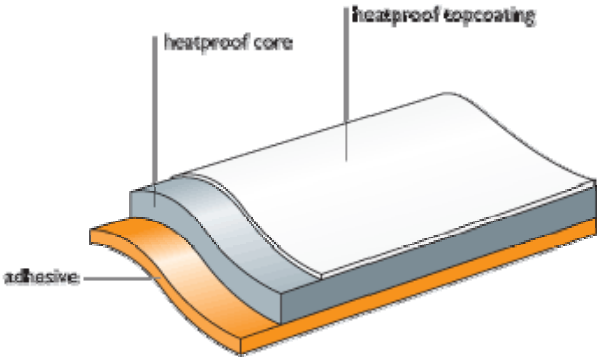

Label Specifications

	HP-PET	HP-300	HP-350	HP-600	HP-700	HP-L80
Face Material	White polyester	White HP coating	White HP Smudge-Proof coating	White HP coating	White HP coating	White HP coating
Ink Ribbon	TT Ribbon PET	TT Ribbon YS 540	TT Ribbon YS 350	TT Ribbon YS 540	TT Ribbon YS 540	TT Ribbon YS 540
Heat Resistance	200°C	600°C	600°C	600°C	815°C	1000°C
Characteristics	Strong, durable adhesive and excellent outdoor weather resistance	Designed to survive aluminum homogenizing and annealing processes	Ideal for hot direct applications such as high temperature ingot and steel coil	Hot direct application including aluminum sow or steel billet	Ultra high heat resistance for application on steel slab or bloom	Thermal transfer printable barcode tag with highest heat resistance and durability

Heat Resistance Index

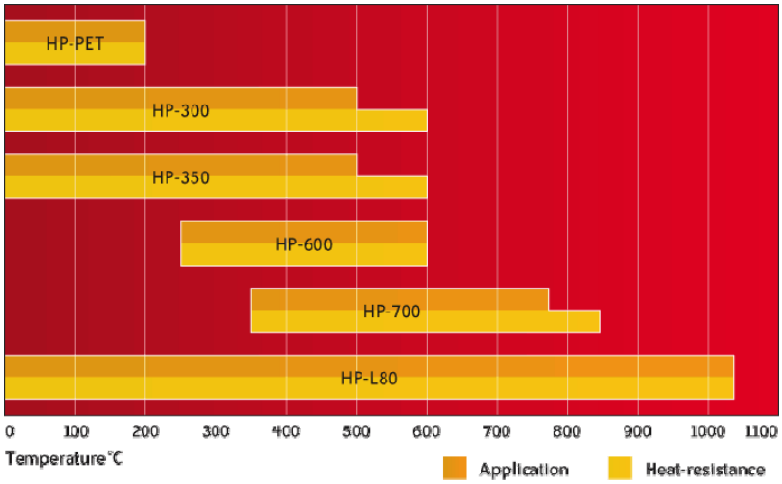

HEATPROOF APPLICATIONS

Steel Products

- **Slabs, Blooms and Bars**
- **Coils (Hot)**
- **Billets**
- **Wires**

Aluminium Products

- **Sows & Pigs**
- **Coils (Hot & Cold)**
- **Ingots**
- **Billets (Homogenising)**
- **Other Aluminium Reheating Processes**

Both room and extreme temperature applications

(www.heatproof.eu)

COMPOZITE ELECTROCHIMICE
PARTEA I

R. Stancu[*]*, C. A. Boose*[**]*, A. Nicolae*[*]

* S. C. ICTCM Institutul de Cercetare si Proiectare Tehnologică pentru Construcţii Maşini S. A.
das@ictcm.ro
** ECA CORRINT Olanda

REZUMAT

Cele mai cunoscute metode de obţinere a materialelor compozite sunt: turnarea, metalurgia pulberilor, vaporizarea în vid, oxidarea internă, pulverizarea în vid, pulverizarea în plasmă, depunerea chimică prin evaporare, spraierea. Mai puţin utilizată este obţinerea acestor materiale prin procesul de electrodepunere. Materialele obţinute prin această tehnică au devenit cunoscute ca "electrocompozite". În ciuda avantajelor, metoda electrochimică nu este atât de mult utillizată ca celelalte metode. Deşi s-a realizat o bogată cercetare a procesului electrochimic de depunere a compozitelor, mecanismul procesului este parţial înţeles. Datorită avantajelor procesului de obţinere electrochimică a materialelor compozite, studiul acestei tehnici a câştigat mai multă atenţie în ultimul timp.

ABSTRACT

The most known obtaining methods of composite materials are: fount, powder metallurgy, vacuum vaporization, internal oxidising, vacuum pulverization, plasma pulverization, chemical deposition through vaporization. Less used is obtaining of this materials through the electrodeposition process. The materials obtained through this technique have become known as "electrocomposites". Despite the advantages, electrochemical method is not that much used like the others methods. Although it has been realised an abundant research of the process of electrochemical composite deposition, the process mechanism is partially understood. Thanks to all advantages of the process of composite materials electrochemical obtainig, the study of this technique has lately won more attention.

CUVINTE CHEIE: Compozite cu matrice metalică, Electrodepunere.

KEYWORDS: Composites with metallic matrix, Electrodeposition.

1. INTRODUCERE

Este bine cunoscut că substanţele prezente într-o baie de galvanizare se depun în acelaşi timp cu ionii metalici. Proprietăţile metalelor sunt puternic afectate de includerea diferitelor substanţe în depunere. În băile convenţionale de galvanizare aceste substanţe sunt un dezavantaj şi de aceea pentru evitarea lor se impune filtrarea continuă a băilor şi utilizarea sacilor anodici.

În cazul compozitelor electrochimice particule inerte sunt adăugate în mod intenţionat în electrolit pentru obţinerea compozitelor cu matrice metalică având proprietăţi îmbunătăţite comparativ cu metalul pur.

Metoda electrochimică de obţinere a materialelor compozite este cunoscută încă din 1838. Cu toate acestea cu apoximativ 30 de ani în urmă puţine cercetări au fost făcute în acest domeniu. Încă de la începutul anilor 1960 au început primele investigaţii, şi curând după aceasta au fost realizate şi primele aplicaţii industriale.

Prezenţa particulelor fine de oxizi, carburi, sulfuri, polimeri, grafit, etc., dispersate într-o matrice metalică îmbunătăţesc proprietăţile mecanice şi

chimice, extinzând astfel domeniul de aplicaţie al acoperirilor metalice.

Deşi mult mai scumpe decât acoperirile clasice, acoperirile compozite au performanţe caracteristice care depăşesc preţul lor de cost.

Trei domenii majore de aplicaţii se pot distinge în cazul materialelor compozite: durificarea acoperirilor, rezistenţa la uzură şi/sau la coroziune a compozitelor, autolubrifierea stratului.

2. CLASIFICAREA COMPOZITELOR ELECTROCHIMICE

Compozitele electrochimice vor fi clasificate în cele ce urmează în funcţie de matricea lor şi faza dispersă. Astfel se disting următoarele *tipuri de acoperiri compozite:*

a) Acoperiri *compozite cu matrice metalică.* Din această categorie fac parte:

-*compozite metal/ceramice* – în materialul metalic sunt înglobate materiale ceramice, cele mai cunoscute fiind oxidul de aluminiu, oxidul de siliciu, carbura de siliciu, carbura de crom ş.a.;

-*compozite metal/metal* – în materialul metalic sunt înglobate particule metalice cum ar fi Ni, Cr, Co ş.a.;

-*compozite metal/lichid* - în matricea metalică sunt înglobate microcapsule. Microcapsulele sunt formate dintr-un perete solid numit membrană care înconjoară un miez lichid; [1]

-*compozite metal/organice* - în matricea metalică sunt înglobate particule organice de teflon (PTFE), polistiren şi diferite tipuri de fibre organice.

b) Acoperiri *compozite cu matrice organică*. Din această categorie fac parte:

-*compozitele polimer/metal* - filme ultra fine de polimeri pot fi depuse pe electrod prin polimerizare electrochimică cu complecşi ai diferitelor metale cum ar fi nichelul, cobaltul, cuprul, rutheniul etc.;

-*compozitele polimer/oxid* - electrodepunerea unor oxizi (oxidul de wolfram, dioxidul de titan) într-o matrice polimerică de anilină, pyrol, acetonitril. [2]

3. INFLUENŢA PARAMETRILOR EXPERIMENTALI

Concentraţia particulelor, tipul, forma şi dimensiunea lor

Concentraţia particulelor depuse depinde de parametrii depunerii electrochimice.

În lucrările [2-6] s-a arătat că volumul particulelor codepuse depinde de concentraţia acestora în electrolit.

În condiţiile unei viteze constante de agitare şi a unei curgeri staţionare a electrolitului în jurul catodului, codepunerea depinde de numărul coliziunilor particulelor cu suprafaţa catodului, deci de concentraţia particulelor în baia de electrodepunere. [7]

S-a constatat că, volumul particulelor incluse în depunere creşte odată cu creşterea concentraţiei lor în electrolit până la o anumită valoare. Dacă concentraţia particulelor în electrolit depăşeşte această valoare, volumul ocupat de acestea în depunere rămâne constant. Această comportare a fost confirmată de mai mulţi cercetători pentru diferite tipuri de sisteme compozite (metal-particule). [3, 5, 7- 9]

Valoarea absolută a concentraţiei particulelor în depunere poate varia în funcţie de sistemul compozit.

De exemplu, Velerst ş.a. [4] au observat că particulele de alumină incluse într-o matrice de nichel nu depăşesc 5% procente de volum, în timp ce particulele de Cr_2O_3 pot fi incluse până la o concentraţie de 23% procente de volum.

Exceptând compoziţia lor chimică, aceste particule au proprietăţi fizice diferite. Este foarte important să se ia în considerare diferenţa de mărime şi densitate a granulei (d_{Cr2O3}=5,2; d_{Al2O3}=4).

Energia cinetică a particulelor care se ciocnesc cu suprafaţa catodică este mai mare pentru oxidul de crom, care se îndepartează de suprafaţă, conducând astfel la o scădere a cantităţii de Cr_2O_3 codepus odată cu creşterea vitezei de agitare a electrolitului.

Figura 1 arată creşterea cantităţii particulelor codepuse odată cu creşterea concentraţiei acestora în electrolit.

Dimensiunea şi suprafaţa specifică a particulelor de alumină codepuse în matricea de nichel nu au nici un efect asupra parametrilor morfologici, chiar şi în cazul creşterii cantităţii codepuse. Un comportament electrochimic diferit s-a observat în cazul pudrei submicronice şi supermicronice de Cr_2O_3 (Fig. 2a).

În ciuda diferenţelor dintre procesele de prelucrare ale fiecărei şarje de pudră, nu este posibilă explicarea variaţiei concentraţiei particulelor codepuse numai în funcţie de suprafaţa specifică şi dimensiunea particulelor.

Pentru confirmarea acestui fapt, s-au caracterizat două şarje de pudră (A) şi (B) cu diferenţe mari in aptitudinile de codepunere. Utilizând spectrometria de masă (figura 3) se observă că pudra (A) are conţinutul de crom mai mare pe suprafaţa particulelor decât în interiorul lor, pe când acest fenomen nu apare la pudra (B).

Aceste observaţii au fost verificate de analiza termogravimetrică. În figura 4, creşterea cantităţii de crom pe suprafaţă observată la o temperatură mai mare de 600 °C pentru pudra (A) a confirmat prezenţa fazei suboxidate pe suprafaţa particulelor.

Aceasta explică proprietăţile specifice ale pudrei respective. Excesul de Cr pe suprafaţa particulelor este oxidat într-o baie electrolitică pâna la Cr^{3+}. Ionii de Cr^{3+} sunt reduşi in vecinătatea suprafeţei catodice la Cr^{2+}. Aceştia, foarte instabili,

pot reduce ionii de Ni^{2+} prin reacție chimică. Astfel, se poate spune că în timpul codepunerii Cr_2O_3 a intervenit un proces chimic simultan cu reacția electrochimică.Celis [3] a arătat că există diferențe majore în cantitatea de α-alumină şi γ-alumină inclusă într-o matrice de cupru.

S-a observat că există o strânsă compatibilitate chimică şi electrochimică între *tipul de particule* codepuse şi matricea metalică.

De exemplu, în timp ce particule de MoS_2 şi WC se pot codepune cu nichelul [5] ele nu se codepun cu aliajul Ni-Sn, ba chiar împiedică depunerea aliajului. [7]

Compoziția chimică a particulelor, reflectată în proprietățile fizice diferite ale acestora, influențează energia cinetică de coliziune a particulelor cu suprafața catodică, implicit procentul de particule incluse în matrice.

Un tip tip mai nou de particule codepuse sunt microcapsulele. Compozitele cu microcapsule conțin până la 50% lichid. [10]

Figurile 5 şi 6 prezintă micrografiile acoperirilor de metal-lichid obținute dintr-o baie de formiat de cupru şi sulfat de cupru. Diferențele pe scara in nuanțe de gri între diferitele microcapsule reflectă diferitele lor stadii de înglobare.

Pentru ca microcapsulele să poată fi codepuse trebuie ca peretele lor să fie rezistent la temperatură, pH şi la condițiile chimice ale băilor de depunere. Materialul membranei poate:

- controla (de exemplu scădea sau elimina) dizolvarea şi/sau reacțiile miezului capsulelor;
- să îmbunătățească codepunerea particulelor în matricea metalică;
- să îmbunătățească sau să extindă activitatea anticorozivă a stratului depus;
- să fie mai puțin solubil decât materialul miezului în electrolit;
- avea proprietăți anticorozive şi lubrifiante care să suplimenteze activitatea miezului.[11]

S-a observat că microcapsulele se pot codepune într-un mod similar ca şi particulele de SiC şi alumină. [12]

Nici o influență asupra *formei particulelor* nu a fost arătată până în prezent. Totuşi, forma particulelor influențează adsorbția lor pe catod, adsorbția ionilor pe suprafața particulelor şi stabillitatea suspensiei - factori ce influențează codepunerea. [13]

În ceea ce priveşte *influența dimensiunii particulelor* codepuse, diferite rezultate au fost prezentate în literatură.

Studiindu-se influența dimensiunii particulelor s-a găsit că există un maxim al transferului de masă când diametrul particulelor este egal cu grosimea stratului de difuzie. [14]

În lucrarea [8] s-a arătat că nu există particule cu anumite dimensiuni care se codepun preferențial. Aceasta este în contradicție cu observațiile altor cercetători care au studiat influența dimensiunii pulberilor încorporate într-o matrice metalică. [7, 14] Aceasta poate fi cauza unui domeniu prea îngust de dimensiuni de particule utilizate pentru codepunere, de aceea nu a fost observată nici o diferență în codepunere.

În figura 7 este prezentată distribuția mărimii particulelor in pudra de SiC şi sunt comparate 3 specii de pudră: (A) cea neprocesată; (B) cea dispersată în baia de electrolit, (un volum de 50 ml a fost extras din electrolit conținând 10g/dm^3 de SiC, la 50 mm de la suprafața soluției); (C) cea încorporata în matricea de NiSn (un strat compozit de 50 μm grosime a fost electrodepus dintr-o solutie de depunere conținând 10g/dm^3 SiC la 1,25Adm^{-2} şi 70ºC, aliajul a fost dizolvat în pudra colectată).

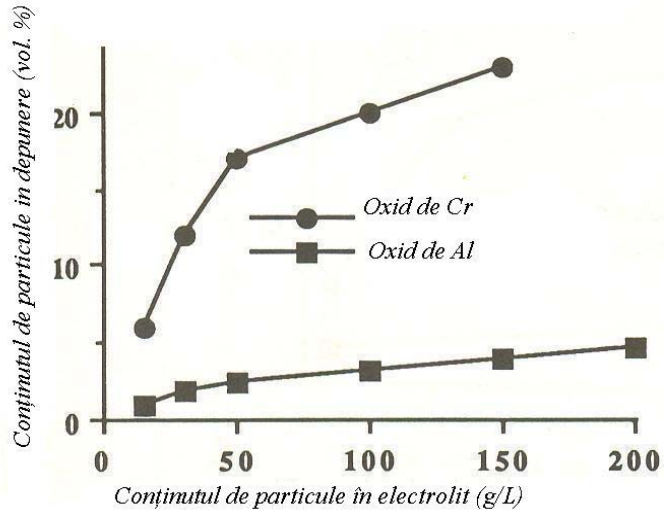

Figura 1. *Volumul particulelor de Cr_2O_3 şi Al_2O_3 incluse în matricea metalică de Ni, în funcție de concentrația acestora în baie.*

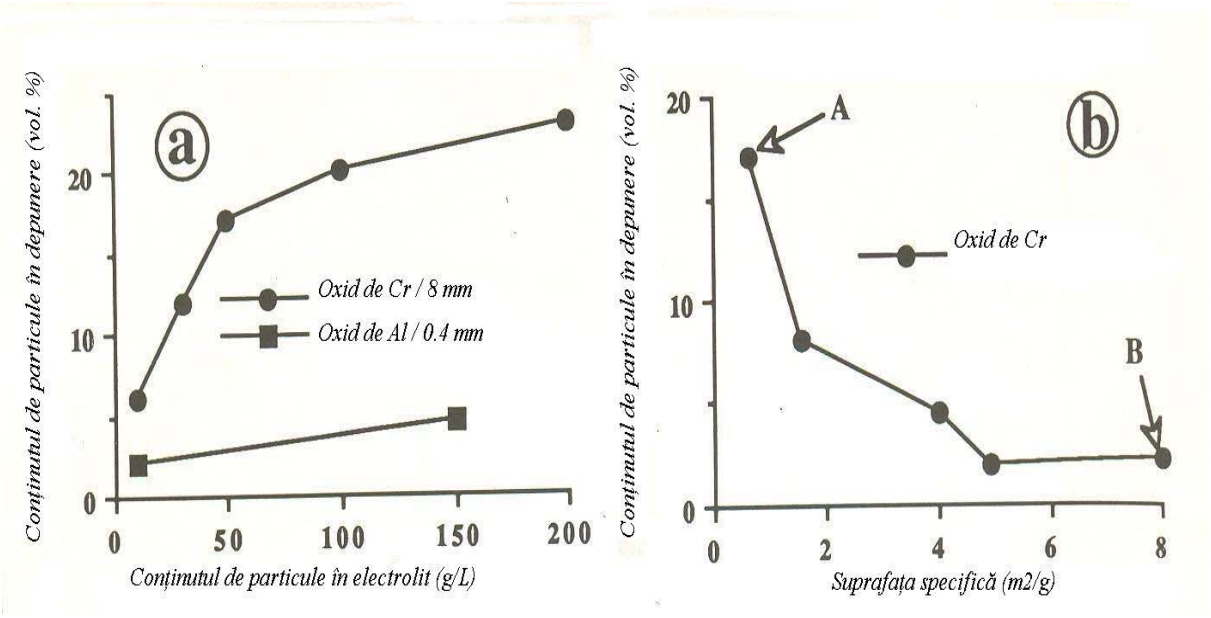

Figura 2. *Efectele a) Mărimii granulei şi b) Suprafeţei specifice asupra procentului în volume a particulelor de oxid de crom, (A) Cr_2O_3 cu mărimea granulei de 8µm şi (B) Cr_2O_3 cu mărimea granulei de 0,4µm.*

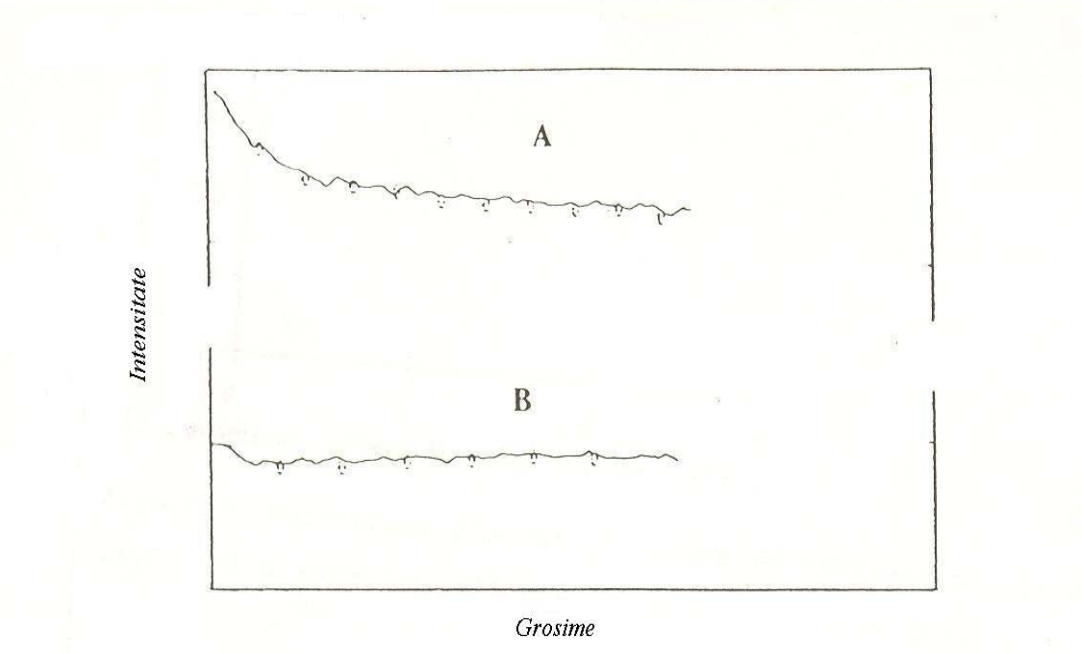

Figura 3. *Profilul concentraţiei superficiale a cromului in particulele de Cr_2O_3 obţinute prin analizele de Spectrometrie de Masă a (A) Cr_2O_3 cu mărimea granulei de 8µm şi a (B) Cr_2O_3 cu mărimea granulei de 0,4µm.*

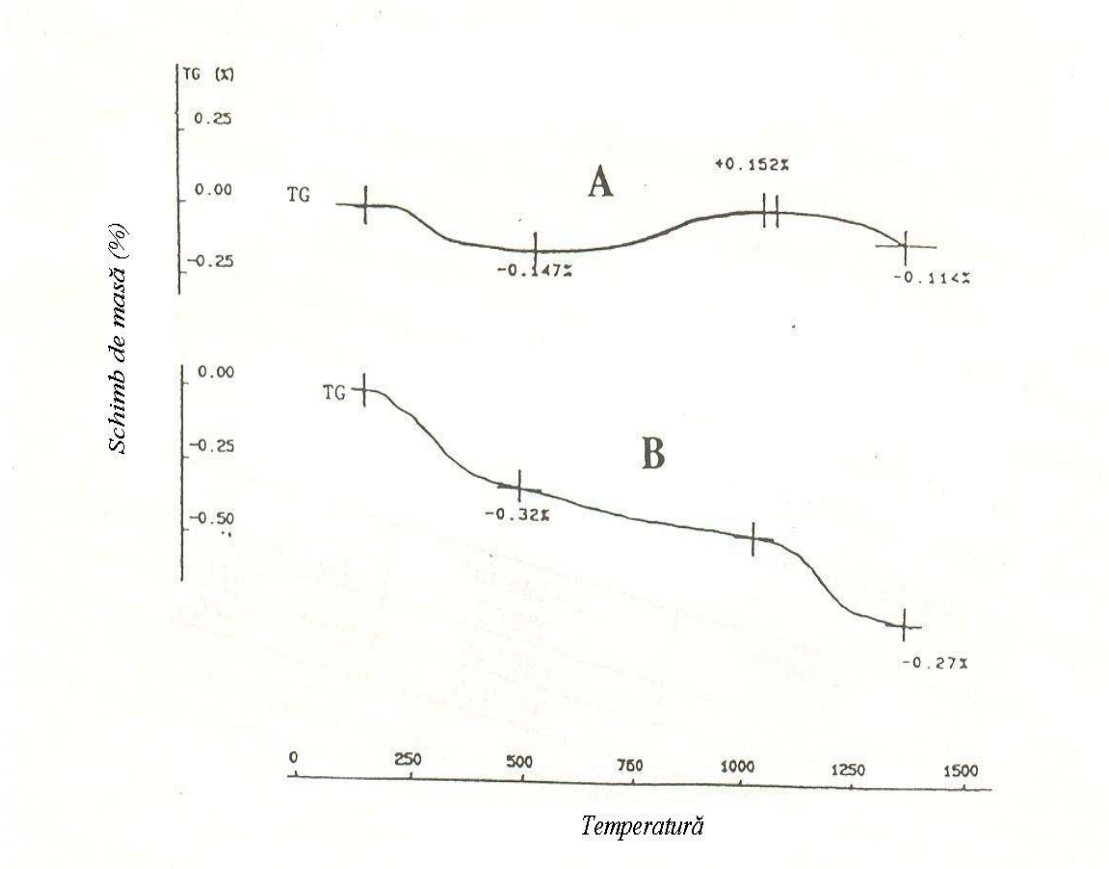

Figura 4. *Analiza termogravimetrică a (A) Cr_2O_3 cu mărimea granulei de 8μm şi a (B) Cr_2O_3 cu mărimea granulei de 0,4μm.*

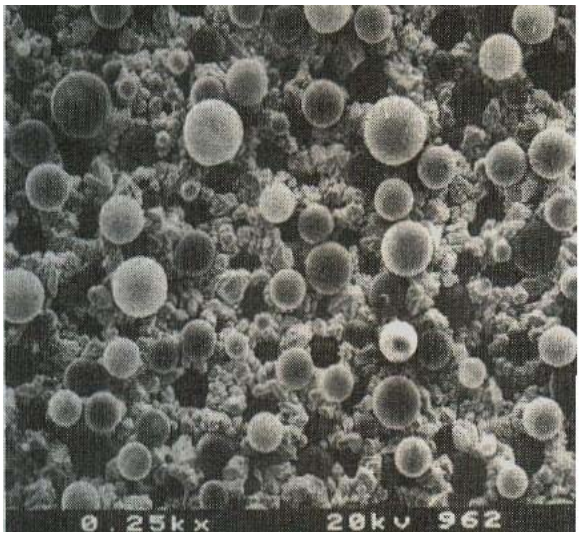

Figura 5. *Micrografia suprafeței compozite de cupru obținute din baia de formiat de cupru cu microcapsule.*

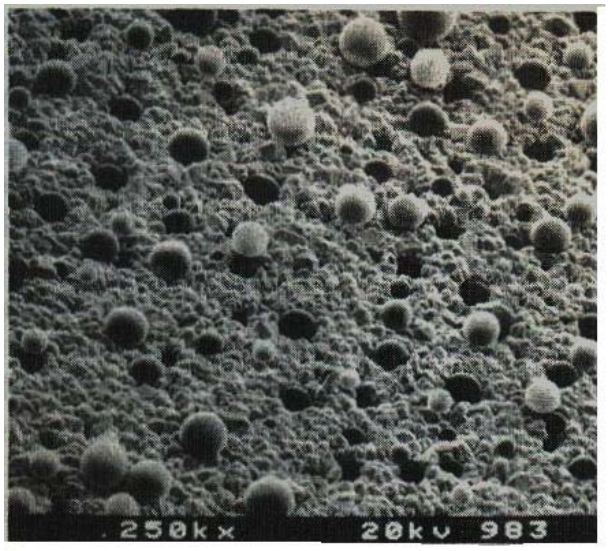

Figura 6. *Micrografia suprafeței compozite de cupru obținute din baia de sulfat de cupru cu microcapsule*

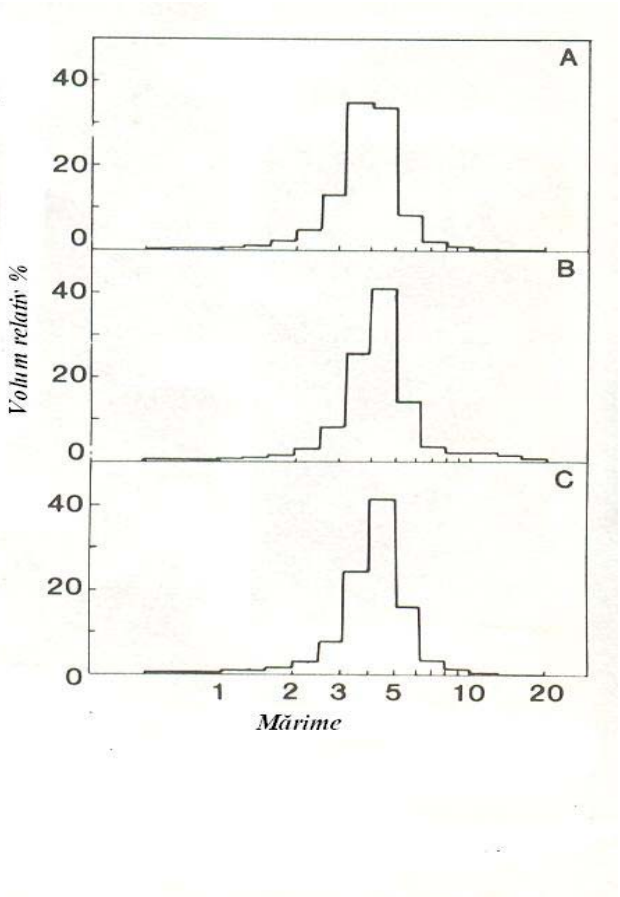

Figura 7. *Distribuția mărimii particulelor de pudră de SiC:*
(A) neprocesate (B) în suspensia electrolitului (C) codepusă.

S-a observat că toate dimensiunile de particule de SiC din domeniul studiat s-au inclus în stratul depus. Acest lucru este contrar observațiilor altor cercetatori care au studiat efectul mărimii particulelor asupra încorporării în matricea metalică. Această comportare poate fi cauza domeniului îngust de dimensiune de particule de SiC folosite în electrolit.

În consecință o fracțiune din particule, care depinde de condițiile de depunere, nu se codepun.

Lucrarea prezintă o sinteză a literaturii de specialitate, cuprinzând date legate de clasificarea sistemelor compozite electrochimice şi de influența diferiților parametrii experimentali asupra procesului electrochimic de obținere a materialelor compozite.

BIBLIOGRAFIE

[1]. **J.Fransaer, , J.P.Celis şi J.R.Roos,** *Metal Finishing, 87 (1989) 107.*

[2]. **L.Benea,** „*Electrodepuneri compozite în teorie şi practică"*,Ed.Porto-Franco, Galați, 1998, 23, 64.

[3]. **J.P.Celis. J.R.Roos, C.Buelens şi J.Fransaer;** *Trans.IMF*., **69** (1991) 133.

[4]. **M.Verelst, I.P.Bonino şi A.Rousset;** Proceedings *„INTERFINISH",* (1992) 410

[5]. **G.N.K.Ramesh Bapu**; *Metal Finishing*, **92** (1994) 37.

[6]. **G.N.K.Ramesh Bapu**; *Plating and Surface Finishing*, **82** (1995) 70.

[7]. **J.Sadowska-Mazur, M.E.Warwick şi R.Walker***; Trans.IMF*., **64** (1986) 142.

[8]. **Y.Z.Wan, Y.L.Wang, H.M.Tao, G.X.Cheng şi X.H.Dong;** *Trans.IMF*., **77** (1999) 52.

[9]. **R.Narayana şi B.H.Narayana***; J.Electrochem.Soc*., **128** (1981) 1704.

[10]. **J.P.Roos, J.P.Celis, J.Fransaer şi C.Bulens**; *J.Metals* **42** (1990) 60.

[11]. Brevet 0323756A1 (1989) Japonia.

[12]. **J.P.Celis, J.R.Roos şi J.Fransaer;** Proceedings *„INTERFINISH",* (1992) 442.

[13]. **A.Hovestad**; Phd-thesis, TU Eindhoven, (1997).

[14]. **P.J.Sonneveld, W.Visscher şi E.Barendrecht**; *J.Appl.Electrochem*., **20** (1990) 563.

Quick Info

Solid-state light-emitting plastics

Light Beam Industries has developed a new solid-state light emitting plastic. The LEC (light emitting converter) material is based on patents by inventor Daniel Naum.

This new substance uses fluorescent laser dyes and solid-state light sources in conjunction with optical waveguides to generate multicoloured or white light.

The light is generated by wavelength shifting through a photoptic process of absorption and emission in the plastic material, which is a cross-linked polymer. The shorter wavelengths of light from the solid-state emitting source are absorbed completely - or partially, if preferred - and re-emitted as light at longer wavelengths.

LEC material has a wide range of potential applications, as well as offering the opportunity to save energy. Other uses include architectural lighting, instrument panels and switches, as well as, solid-state laser dye rods.

Future research and development will focus on nano-crystalline lasing structures incorporated in a plastic matrix (paint-on nano lasers) with further potential applications in lighting, solar collection and visual displays, as well as search and rescue.

(www.engineerlive.com)

Quick Info

Undersea advances, from ropes to deep-water repair robots

Allseas Group, a Swiss offshore pipelaying company, has collaborated with DSM Dyneema to improve the safety and speed of underwater pipe-laying using next-generation rope technology. The two companies have worked to replace traditional steel wire rope used to adjust pipelay stingers with a new product from BEXCOropes that is made with ultra-strong, lightweight polyethylene Dyneema fibre. The new rope, which has been installed on Allseas' pipe-laying vessel Audacia, enables faster, easier and safer operations.

"Adjusting the stinger is a critical part of the pipe-laying process because it determines the precise curvature of the pipe as it enters the water," explained André Steenhuis, Allseas Innovation Manager. "The heavy, rough steel wire rope hampered our crews, slowing down our operations. With the rope's high strength and low weight provided by Dyneema fibre, we can achieve the precision we need more quickly and easily. Our partnership with DSM Dyneema has led to a major advance in pipe-laying efficiency and safety." Because of the heavy weight of the 150-metre steel wire rope, Allseas' crews experienced difficult handling, and higher risk of damage and injury. Also, corrosion shortened the rope's useful life. In contrast, the new stinger adjustment rope is easy to lift and manoeuvre, is exceptionally durable, and can help avoid injuries.

The high strength-to-weight ratio of the polyethylene fibre enables use of thinner ropes that are easier to deploy, recover and store. For example, the rope made with Dyneema fibre only weighs 9.8 kg/metre; steel wire rope of equivalent strength weighs about 65 kg/metre.

BEXCOropes created the load-bearing portion of the adjustment rope from 100percent Dyneema fibre. The core of the 136mm diameter rope is protected against abrasion by a Deltaflex cover, which is BEXCOropes' proprietary technology. Adjustment ropes, which are kept on a winch, can be subjected to as much as 250 tonnes of force.

Rigo Bosman, Market Segment Manager Offshore at DSM Dyneema said: "We have closely collaborated with Allseas Group and BEXCOropes to perfect new rope technology based on Dyneema fibre, which will help pipelaying companies improve the efficiency and safety of day-to-day operations. Although this is the first use of Dyneema fibre in this industry, its strength, light weight and durability have proven their value in many other marine applications, and we see great potential for it in new offshore applications such as abandonment and recovery ropes."

Robot for pipeline repairs

Meanwhile Statoil is building on its leading role in underwater technology development with a new pipeline repair robot capable of working at depths down to 1000 metres.

The new remotely operated welding machine will undergo testing and final adjustments before being deployed in an emergency response role during the year.

"We're getting a lot of enquiries from international oil and gas companies," says Kjell Edvard Apeland, who is heading the development job. "They're interested in using our robot for pipeline repair and field operations in such areas as the Gulf of Mexico."

Work on the new device is taking place in Haugesund north of Stavanger, where Statoil's pipeline repair system (PRS) pool is located. The robot will join a number of other remotely operated tools used in deepwater operations, including tie-in of new pipelines in water depths beyond the reach of divers.

Measuring about four metres long by two metres high, the new welding machine has been developed by Statoil and built in cooperation with external suppliers. The robot cuts out the damaged pipe section before welding in a new piece inside an enclosed habitat. Systems are provided for preheating and controlling the habitat atmosphere.

A submarine pipeline can be damaged by a shipwreck, for instance, or by having a trawl or anchor dragged over it. "Many technological experts say that developing such technology and carrying out operations of this kind are more difficult than a moon landing," says Asbjørn Erdal. He is manager of the pipeline operation sector, which maintains 8000 km of pipeline and will probably be the biggest customer for the new robot.

The Norwegian government requires that oil and gas distributors have such equipment available. Regulations restrict diving to a maximum water depth of 180 metres.

Statoil currently has a deepwater emergency response system based on remotely operated vehicles that can seal leaks. With the new robot, the group will also be able to weld pipes.

(www.engineerlive.com)